Interactions between Cognitive and Automatic Components of Biological, Artificial, and Hybrid Sensory-Motor Systems

Dissertation zur Erlangung der naturwissenschaftlichen Doktorwürde

(Dr. sc. nat.)

vorgelegt der

Mathematisch-naturwissenschaftlichen Fakultät

der

Universität Zürich

von

Timoleon Moraitis

aus

Griechenland

Promotionskommission

Prof. Dr. Kevan Martin (Vorsitz)

Prof. Dr. Giacomo Indiveri

Dr. Arko Ghosh

Dr. Matthew Cook

Zürich 2017

Acknowledgments

This thesis would have been impossible without the invaluable support I received from many people. First and foremost, my advisors Kevan Martin, Arko Ghosh, Matthew Cook, and Giacomo Indiveri have supported me not only with direct scientific contributions, suggestions, and funding, but most importantly each by contributing to different aspects of my development as a person, thinker, and academic. Furthermore, I would like to specially thank Fabio Stefanini and Federico Corradi, as the effort needed to complete the neuromorphic part of the thesis would have been many times larger if they didn't bequeath to me their theoretical and practical expertise. Additionally, I am grateful for having been a member of the Institute of Neuroinformatics. Working in this environment, discussing, collaborating, and being friends with this impressive concentration of highly intelligent, lively, and well-rounded personalities has made my stay at INI an inspiring and exciting all-round life experience, additional to the impressively broad academic exposure offered by the institute's interdisciplinary culture. Furthermore, I would like to thank Richard George for translating the thesis abstract in German, and Gina Paolini, Magali Chytiris, and Myriam Balerna for the precious help with much of the experimental work. Finally, I am especially grateful to my closest circle, including my parents, my close friends, and Fabiola for supporting me emotionally, and coping with me during the ups and downs of this experience.

Abstract

Sensory-motor systems control the movements of a body according to sensations from the environment and from the body itself. These systems, be they biological, such as in animal nervous systems, artificial, such as in robots, or hybrid such as in brain-machine interfaces that integrate biological nervous systems with artificial body parts, often comprise multiple controllers that undertake different sensory-motor roles, such as controlling movements of different body parts, or abstracting movements at different levels ranging from strategizing motor plans to interfacing with muscles or motors. Understanding biological systems, designing artificial ones, and interfacing biological with artificial systems necessitates the study of how controllers equipped with cognitive functions such as learning, volition, working memory, and context-based decision-making interact with automatic controllers that lack cognitive features. This thesis is concerned with the theoretical, experimental, and applied study and design of four different interactions between cognitive and automatic controllers in biological, artificial, and hybrid sensory-motor systems.

Firstly, a mechanism is proposed, through which developmentally early spontaneous and reflexive automatic movements generated by the spinal cord may influence motor control and learning by the cerebral cortex. In a simulated sensory-motor system capturing aspects of the spinal cord, the cortex, and the body, this mechanism emerged from the system's and its components' properties. The simulated system benefited from and was strongly influenced by the mechanism, suggesting that biology may be taking advantage of such a mechanism, and that robotic systems could exploit it too. Secondly, an experiment designed to uncover how voluntary inhibition acts on spontaneous eye-blinks is described. The experiment involved recording neuromuscular activity around the eyes of human subjects who were occasionally instructed to stop blinking and subsequently to relax. The timing of blinks after periods of voluntary inhibition revealed mainly that the voluntary inhibition and its release stop and reset the automatic blink controller, as opposed to alternative hypotheses of volition either (a) acting peripherally through opposite contractions of

the eye muscles, or (b) negating the output of the blink generator while the generator itself continues outputting motor commands, or (c) pausing the blink controller in its pre-inhibition state. Thirdly, an experiment is presented, which examined whether a voluntary reaction task such as clicking a computer mouse in response to mechanical stimulation of the fingertip can influence whether and when an automatic movement such as an eye-blink is generated. The distributions of stimulus, mouse press and release, and eye-blink timings reveal that the voluntary reaction introduces a trigger to an individual eye-blink, and that eye-blinks are likely triggered separately and not as a part of a single plan to "click and blink". Finally, a spiking neural network on a neuromorphic mixed digital-analog electronic chip was configured to learn to decode the activity recorded in an anesthetized rat's motor cortex, into forces acting on a movable object. The object's position was encoded through electrical microstimulation into the rat's somatosensory cortex, evoking the recorded motocortical activity, thus forming a closed-loop bidirectional brain-machine interface. The network on the chip made use of the variability among silicon neurons and synapses, as well as of the chip's neurons' "stop learning" feature. After training, the chip enabled the bidirectional set-up to successfully guide the controlled object to a pre-defined target. These results propose possible design strategies for artificial and hybrid systems, while suggesting that automatic controllers could furnish future reductionistic experimental paradigms revealing of general principles of biological sensory-motor function.

Zusammenfassung

Sensorimotorische Systeme steuern die Bewegung eines Körpers entsprechend der Wahrnehmung der Umgebung des Körpers und seiner Eigenwahrnehmung. Diese Systeme können sowohl biologische wie in etwa Nervensysteme, als auch künstliche wie in etwa Roboter, als auch hybride Systeme wie Brain-Machine-Interfaces darstellen, welche biologische Nervensysteme mit künstlichen Körperteilen integrieren. Ein solches System besteht oft aus mehreren Steuerelementen welche unterschiedliche sensorimotorische Aufgaben wie die Kontrolle unterschiedlicher Körperteile oder die Abstraktion von Bewegungen auf verschiedenen Ebenen von Bewegungsplanung bis zum Ansprechen der Muskulatur übernehmen. Um biologische Systeme zu verstehen, künstliche zu entwickeln und biologische Systeme mit künstlichen zu verbinden ist es notwendig zu verstehen wie Steuerelemente die mit kognitiven Funktionen wie Lernfähigkeit, Willensbildung, einem Arbeitsgedächtnis und kontext-basierter Entscheidungsführung ausgestattet sind mit Steuerelementen interagieren welchen diese Fähigkeiten fehlen. Die vorliegende Thesis behandelt die theoretische, experimentelle und angewandte Forschung und Entwicklung von vier unterschiedlichen Interaktionen zwischen kognitiven und automatischen Steuerelementen in biologischen, künstlichen und hybriden sensorimotorischen Systemen.

Zunächst wird ein Mechanismus vorgestellt durch welchen die in der Entwicklung frühen, spontanen und reflexiven automatischen Bewegungen, welche im Rückenmark generiert werden, generiert werden lernen und Bewegungsregelung im zerebralen Kortex beeinflussen können. In einem simulierten sensorimotorischen System welches die Aspekte von Rückenmark, Kortex und Körper, entspringt dieser Mechanismus aus dem System und den Eigenschaften seiner Komponenten. Das simulierte System profitierte von- und wurde stark beeinflusst durch den beschriebenen Mechanismus, was die Vermutung nahe legt, dass auch in der Biologie ein ähnlicher Mechanismus verwendet werden könnte und dass robotische Systeme diesen genauso verwenden könnten. Weiterhin wird ein System beschrieben welches entwickelt wurde um aufzudecken wie bewusste Inhibition spontanes blinzeln des Auges

beeinflusst. Dieses Experiment beinhaltete die Erfassung neuromuskulärer Aktivität in nähe des Auges an menschlichen Probanden, welche ab- und an aufgefordert wurden aufzuhören zu blinzeln und ab-und an zu entspannen. Die Zeitliche Abfolge des Blinzelns nach Phasen der bewussten Inhibition zeigten dass bewusste Inhibition und ihr Fehlen das automatische Steuerelement des Blinzelns stoppen und einen Reset durchführen. Dies steht im Kontrast zu alternativen Hypothesen der Willensbildung, welche a) auf periphärer Aktion, der Kontraktion von antagonistischen Muskeln, basiert, oder b) der Negation des Ausgangssignals des Blinzel-Generators während dieser Generator weiterhin ein Ausgangssignal generiert, oder c) das Pausieren des Blinzel-Steuerelements in seinem Pre-Inhibition Zustand. Des weiteren wird ein Experiment präsentiert, welches untersucht ob eine bewusste Reaktionsaufgabe, wie in etwa das Klicken einer Computermaus in Reaktion auf eine mechanische Stimulation der Fingerspitze beeinflussen kann, ob und wann eine automatische Bewegung wie ein Augenblinzeln generiert wird. Die Verteilung von Stimulus-, Mausklick- und Augenblinzeln- Zeit zeigen dass die bewusste Reaktion eine Auslösung eines individuellen Augenblinzelns induzieren und dass Augenblinzeln wahrscheinlich separat ausgelöst werden und nicht im Rahmen eines Plans des "Klickens und Blinzelns". Weiterhin wurde ein Spikendes Neuronales Netzwerk auf einem neuromorphen mixed digital-analog Chip konfiguriert um zu lernen, die Aktivität in einem anästhesierten Ratten-Motorkortex in Kräfte welche auf ein bewegliches Objekt einwirken zu dekodieren. Die Position des Objektes wurde weiterhin durch elektrische Mikrostimulation des somatosensorischen Kortex der Ratte kodiert, was motokortikale Aktivität hervorrief, welche wiederum erfasst wurde und somit einen vollen Regelkreis eines bidirektionalen Brain-Machine-Interfaces darstellt. Das Netzwerk verwendete Neuronen und ihre Synapsen auf dem Chip sowie das "Stop-Learning" Feature der Neuronen des Chips. Nach der Lernphase erlaubte der Chip dem bidirektionalen Setup das erfolgreiche Steuern des Objektes auf an vordefiniertes Ziel. Diese Resultate zeigen mögliche Entwicklungsstrategien für künstliche und hybride Systeme auf. Des weiteren wird veranschaulicht wie zukünftige reduktionistische Experiment-Paradigmen automatische Steuerelemente heranziehen können um grundlegende Prinzipien biologischer sensorimotorischer Funktion zu erklären.

Disclaimer

I hereby declare that the work in this thesis is that of the candidate alone, except where otherwise indicated in the text, and as described below.

Chapter 3 is a modified version of [Moraitis and Ghosh, 2014]. Raw data in chapter 4 were acquired by Myriam Balerna and Magali Chytiris. In chapter 5, the neurosurgical procedures and related data acquisition, as well as the integration of our neuromorphic decoder in the complete brain-machine interface were performed by Fabio Boi, Vito De Feo, Francesco Diotalevi, Chiara Bartolozzi, and Alessandro Vato from the Italian Institute of Technology.

Contents

Chapter 1

Introduction

1.1 Multiple controllers in sensory-motor systems

Motor control, the study of sensory-motor systems, i.e. of systems that sense the environment and the body, and move the body accordingly, is a scientific field of fundamental interest to both animal biology and robotics, and with crucial implications for medicine, psychology, computer science, and other disciplines.

In its most basic sense a sensory-motor system is a system that receives sensory input and produces motor output that may depend on the sensory input. Sensory input may drive motor output in reactive movement scenarios, or, alternatively, motor output may be triggered independently. The physical consequences of the motor output on the environment and on the body are reflected in the subsequent sensory input that is fed back, thus completing a sensory-motor loop. Often, sensory-motor systems make use of the sensory feedback to produce subsequent re-adapted motor outputs accordingly, resulting in a closed sensory-motor loop. On the other hand, in some aspects of motor control, the motor output does not re-adapt itself based on continuous sensory feedback. Such open-loop motor movements are the result of fully pre-computed motor commands, often when the delays characterizing a complete closed loop are longer than the duration of the movement itself, such as in ballistic movements.

Sensory-motor systems, be they biological, artificial, or hybrid, are rarely monolithic or centralized. Rather, they commonly consist of multiple interacting components that undertake different elements of motor control [Pearson, 1993, Houk and Wise, 1995, Wolpert and Kawato, 1998, Wolpert and Ghahramani, 2000, Ghahramani et al., 1997, Mussa-Ivaldi, 1999, Ahmadzadeh and Masehian, 2015, Rizzolatti et al., 1998, Jacobs et al., 1991].

In a physical sensory-motor system, the separation of these controllers may be defined according to their physical location. The sensory-motor system of animals is

physically distributed across their nervous system. For example, mammals employ for motor control a long chain of anatomically defined neural structures with sensory-motor functions, including the spinal cord, the brainstem, the cerebellum, the basal ganglia, the thalamus, and the cerebral cortex.

A sensory-motor system can alternatively be segmented in conceptual controllers defined by the sensory-motor functionality that each of them undertakes. For instance, they may be responsible for the control of different movements, or of different parts of a complex movement, or they may be concerned with different levels of abstraction of motor control, ranging from strategizing and motor planning at the high level, to direct activation of a muscle or an electrical motor at the low level.

Under this functional definition, in biological motor systems, certain controllers may also be physically localized so as to match anatomically defined structures. For example, spinal reflexes are controlled by the spinal cord [Creed et al., 1932], while voluntary motor commands originate in the cortex [Hallett, 2007]. Nevertheless, this definition does not preclude conceptual controllers that may either be themselves distributed across a network of anatomical structures, or be of unclear anatomical location [Kaminer et al., 2011, Lerner et al., 2009, De Havas et al., 2016]. This definition is well-suited for the study of a motor system's function rather than its anatomy. As such, contrary to the anatomy-based definition, this definition is also applicable to the analysis of sensory-motor systems that are controlled by immaterial processes such as computer software. Furthermore, it facilitates the translation of functional components of biological sensory-motor systems to biologically inspired robotic components, notwithstanding potential differences between the biological and artificial physical architectures.

1.2 Cognitive vs automatic controllers

1.2.1 Cognitive

In a sensory-motor system certain controllers may be able to self-modulate through cognitive functions such as acquiring memories by learning [Wolpert et al., 2001]; holding and manipulating information in working memory [Baddeley, 2012]; selectively concentrating on certain aspects of sensory input through attention [Arnsten and Rubia, 2012]; voluntarily initiating or inhibiting movements [Haggard, 2008]; and making context-based decisions [Gold and Shadlen, 2007, Neftci et al., 2013]. In this dissertation, a controller in a sensory-motor system that can demonstrate any such cognitive function is termed a *"cognitive controller"*.

1.2.2 Automatic

Other components of a sensory-motor system may not have the ability to self-modulate, but may rather only generate motor output either in a fixed dependence on sensory input and on input they receive from other components, or in an input-independent fashion that is fixed or random. In biology, this class of controllers comprises reflexes, central pattern generators and other generators of involuntary motor output. In this dissertation, these controllers are referred to as *"automatic controllers"*.

Types of automatic controllers

An automatic controller may be hard-wired, for instance due to genetics in biology [Thelen et al., 1981, Eibl-Eibesfeldt, 1973, Desmurget et al., 2014], or engineered to be so in an artificial system. Alternatively, a controller that is capable of learning may consolidate into an automatic one through development and learning [Robertson et al., 2004].

Sensory-motor automaticity in the literature

In the literature, the meaning of the term "automatic" has often been used without an explicit definition, and cases that do provide a definition can be crucially different from each other. For instance, the term has been used as synonymous to involuntary [Bisio et al., 2010, Sathian et al., 2011]; to describe processes that do not require attention [Norman and Shallice, 1986, Uleman and Bargh, 1989]; or even as a category of movements that is separate from both "voluntary" and "involuntary" movements [Shibasaki, 2012]. These definitions and uses of the term include different sets of movements which are even contradicting. In this dissertation, the term "automatic" is used with a strong meaning that contrasts automatic sensory-motor components with those equipped with *any* cognitive function including learning, attention, and volition. Thus, a controller characterized as automatic according to this definition would be in agreement with most usages in the literature.

1.3 Fresh approaches are needed

Both automatic and cognitive controllers in a modular sensory-motor system function in the context of one another. So, understanding or engineering such a system necessitates the study not only of the system as a whole or of each component individually, but also of potential interactions between the components. Characteristics of complex sensory-motor systems such hierarchy, sharing of common resources, learning, differential development, structural links are some characteristics that enable

the system's individual components to interact in a variety of ways.

The first steps in designing the scientific approach to understanding a sensory-motor system involve making two decisions. Firstly, which aspects of the system to address, and, secondly, how to address them. Intuition suggests that to maximize the scientific gain from a research effort, the focus should be on those aspects of the system and of its components that the present understanding describes as core elements, i.e. the elements with the most direct roles in shaping behavioural output. In turn, intuitively, the experimental approach of maximum gain should address the core functions by measuring their most direct expressions.

While focusing on the core of a studied system makes intuitive sense as a first approach, it does not suffice to cover the complete picture of a sensory-motor system's function. The combination of a large number of controllers with a variety of functional mechanisms in a complex sensory-motor system can enable a wide array of secondary interactive phenomena between controllers that influence the system's core aspects. For instance, in one pair of controllers, there may be a direction of influence between the two that is thought of as dominant. However, a potential effect of opposite direction may conceivably have effects significant enough to reshape the output of the former dominant mechanism, thus indirectly influencing a core aspect of behavioural output. In a variation of such a set-up, a temporary mechanism of influence between the two controllers may have persistent effects on the outputs that later govern the opposite, dominant direction of influence. Understanding such secondary or temporary mechanisms would be crucial for the understanding of the core and persistent behaviour of the system.

Regarding the choice of the experimental approach, understanding the mechanism that underlies a behavioural phenomenon through directly targeting the phenomenon in question may not always be feasible. In this case, indirect approaches may provide valuable insights. For instance, the variety of interacting pairs in a motor system may include paradigms of interactions in simple pairs of controllers that bear generalizable analogies to more complex paradigms. Similarly, analogies between different systems can be used to facilitate the study of one type of system such as the mammalian nervous system indirectly through another such as an artificial simulation built to this purpose. Furthermore, even when approaching in situ the mechanism underlying a phenomenon of interaction in a pair of controllers, observing corollary phenomena such as after-effects of the interaction can potentially provide direct insights into the core of the mechanism, even when the core phenomenon itself may not.

In this dissertation, we seek for a resource of fresh approaches, models and experiments that have been neglected by the literature. We focus on inter-controller interactions that may be viewed as secondary or temporary but may have significant and persistent effects on core sensory-motor functions. Additionally, in following

indirect experimental approaches we find an efficient strategy in filling many of the existing gaps in understanding of sensory-motor systems. In the next we provide a review of the types of inter-controller interactions that have been studied previously and we provide arguments as to why the interactions between cognitive and automatic controllers are a particularly interesting class of interactions that were not in the main focus of traditional sensory-motor literature.

1.4 Cognitive-cognitive controller interactions

Resource sharing between controllers

Many studies of how controllers within the human motor system interact have been concerned with interactions between concurrent voluntary tasks [Sala et al., 1995]. These studies of dual-task paradigms have revealed that concurrently operating controllers do interfere with each other in various degrees, either diminishing each other's performance, or increasing reaction times [Welford, 1952, Pashler, 1994, Fischer and Plessow, 2015, Marti et al., 2015]. A large number of studies support the view that this between-task interference is due to central bottlenecks in the availability or accessibility of cognitive resources [Pashler and Johnston, 1989, Sigman and Dehaene, 2005, Kahneman, 1973, Tombu and Jolicœur, 2003]. The focus of these studies has generally been on pairs of motor tasks that both involve cognition, as they are performed according to the experimenter's instructions.

Hierarchy and voluntary inhibition in sensory-motor systems

Modularity in biological sensory-motor systems is accompanied by links that enable the components to directly communicate. These links may be asymmetric, resulting in hierarchies within the system, whereby hierarchically higher motor controllers directly excite, inhibit, or modulate lower ones [de C. Hamilton and Grafton, 2007, Flash and Hochner, 2005, Kühn et al., 2009, Stein and Capaday, 1988]. In a particular class of the concurrent voluntary task paradigm, the controllers of the two studied tasks are in a hierarchical relationship such that one controller's task is to inhibit the other voluntary task. This type of hierarchical link is essential at the behavioural level in exerting self-control over one's actions, and has been proposed as one of possible cognitive strategies in balancing conflicting long- and short-term motives guiding behaviour [Fujita, 2011]. In addition, empirical evidence from intentional action paradigms supports a model according to which voluntary action control involves three decisions made by the sensory-motor system, namely, what action to perform, when to do it, and whether to actually execute it [Brass and Haggard, 2008, Zapparoli et al., 2017]. The latter component is fundamentally linked to voluntary inhibition

[Brass and Haggard, 2007]. A large body of literature has found the neural correlates of voluntary inhibition in parietal, frontal and prefrontal cortical areas [Filevich et al., 2012a, Swick et al., 2011, Brass and Haggard, 2007, Kühn et al., 2009, Zapparoli et al., 2017, Schel et al., 2014]. While it appears that in at least some cases inhibition is a top-down signal on premotor areas [Kühn et al., 2009], it is still unclear how exactly the controllers of voluntary inhibition interface with the inhibited controller. Experimental paradigms wherein the inhibited controller produces automatic, simple, predictable outputs may be able to shed light on the operation of voluntary inhibition.

1.5 Cognitive-automatic controller interactions

1.5.1 Cognitive-automatic interactions in biology

In biological sensory-motor systems, the properties of the system and the differences between automatic and cognitive controllers make interactions between cognitive and automatic controllers particularly interesting in terms of their potential effects on behaviour, and suitable for simple models and experimental approaches that can be efficient in advancing the understanding of the sensory-motor system.

Cognitive-automatic hierarchy

Cognition has likely been added by evolution to sensory-motor systems to guide more elaborate than automatic reactive behaviour [Cruse, 2003], and as a result cognitive controllers are able to exert control over automatic ones through direct hierarchical links, that are expressed functionally, but are supported by anatomical connections. As a prominent case in point, the spinal cord generates automatic motor outputs such as reflexes, but supra-spinal circuits such as the cortex can directly access sensory-motor circuits in the spinal cord to trigger, modulate and inhibit the spinal output [Lemon, 2008]. Prominent examples of such control of the spinal cord by superior structures are those essential for locomotion, such as swimming, walking, and flying in vertebrates.

Firstly, reflexes autonomously controlled by the spinal cord such as the stretch reflex and the H-reflex are deeply modulated in amplitude by commands of higher origin during locomotion [Akazawa et al., 1982, Capaday and Stein, 1986, Zehr and Stein, 1999, Rossignol et al., 2006]. Furthermore, the rhythmic patterns of motor output that control locomotive movements are generated by spinal sensory-motor circuits known as central pattern generators (CPGs) [Cohen et al., 1988, Calancie et al., 1994]. While CPGs can generate the rhythmic outputs autonomously with the integration of sensory inputs, they receive executive commands that control them from higher structures such as the brainstem, the cerebellum, and the cortex [Proc-

hazka and Yakovenko, 2007]. Breathing and swallowing similarly involve CPGs, that are supraspinally located in the brainstem and the medulla [Smith et al., 1991, Dick et al., 1993]. The understanding of neural networks composing CPGs and their interface with higher commands during locomotion is not only interesting as a basic research topic but also essential to restoration of mobility in paraplegic patients. Due to this these controllers have been studied and modeled extensively [Stein, 1978, Mushahwar et al., 2000, Yakovenko et al., 2002, Stein, 2005, Ijspeert, 2008, Mazurek et al., 2012], and even replaced by artificial, silicon neurons [Vogelstein et al., 2008].

Apart from hierarchical interactions underpinning locomotion and other rhythmic movements, measurements of neural connectivity define multiple anatomical hierarchical links between structures in the nervous system [Van Essen and Maunsell, 1983, Markov et al., 2014], and support a view of a functionally hierarchical nervous system. The fact that evolution placed cognitive components high in the functional hierarchy, as evidenced and mediated by the directionality of direct anatomical links, suggests that additional mechanisms may have evolved to reinforce this functional hierarchy.

Isolation of automatic controllers

On the other hand, the fact that certain controllers have been capable of functioning automatically and autonomously throughout evolution and development, may have caused them to be partially insulated from certain between-controller interactions that may necessitate stronger functional interdependence. Because of this, certain links that exist between cognitive controllers may be different in the case of cognitive-automatic pairs.

Simplicity, and differential evolution and development of automatic controllers

Additional characteristics that distinguish automatic controllers lend particular interest to potential interactions between cognitive and automatic controllers. The relative simplicity of some automatic movements in animals results in largely stereotypical repetitive movements. Additionally, automatic controllers are functional earlier than cognitive ones in both evolutionary and developmental terms. These distinguishing features of automatic controllers may have caused idiosyncratic interactions between cognitive and automatic controllers.

Developmentalists have long theorized that the early automatic movements of infants contain hereditary information that helps prepare the sensory-motor system [Piaget and Cook, 1952, Thelen et al., 1981, Blumberg, 2015]. In support of this, evidence suggests that automatic controllers within the spinal cord, capable

of producing spontaneous movements, enable the spinal cord to learn its reflexes by associating sensory inputs with self-generated motor outputs, through structural self-organization [Blumberg, 2015]. The mismatch in developmental and evolutionary timelines of automatic and cognitive controllers in biological sensory-motor systems may have enabled additional mechanisms of interaction between the two classes of controllers.

Reductionistic approach

Moreover, the lack of cognitive features allows automatic controllers to lend themselves to reductionistic experimental paradigms that could more effectively isolate certain principles of interaction within the sensory-motor system.

Known interactions

While cognitive controllers can excite, inhibit and modulate automatic ones, and spinal reflexes are learned through spontaneous spinal motor outputs, our understanding of the underlying mechanisms of these cognitive-automatic interactions is incomplete. Furthermore, we know little about what additional kinds of interactions between automatic and cognitive controllers take place in the biological sensory-motor system.

The additional instances of such interactions that have been reported fall in the category of interference between concurrently operating automatic and cognitive motor controllers. Specifically, voluntary rhythmic tapping of the finger entrains the rhythm of spontaneous eye-blinks [Cong et al., 2010]; voluntary saccades towards target visual stimuli and automatic saccades to distractors influence each other with effects on saccade landing point, latency, and trajectory [Eggert et al., 2002, van Zoest et al., 2004, Doyle and Walker, 2001]; and direction of walking with the eyes closed is influenced by involuntary post-contraction activity (Kohnstamm phenomenon) of the pelvis [Ivanenko et al., 2006].

1.5.2 Cognitive-automatic interactions in artificial systems

The study of cognitive-automatic controller interactions is highly relevant to artificial systems as well. Artificial motor systems often comprise multiple components which are characterized by varying degrees of cognitive function. While certain aspects of a robot's function may be pre-programmed and hard-wired, others may be designed to demonstrate learning, attention, action planning etc. which are features associated with cognition [Clark and Grush, 1999]. Implementing such a system necessitates the design of mechanisms through which the system's cognitive components best cooperate with the automatic ones.

Importantly, most robotic systems in commercial or industrial use today are designed to only perform very specific tasks in well-defined environments [Pfeifer et al., 2007, Shi et al., 2015, Iida and Ijspeert, 2016], therefore the design of robotic applications for uncertain or variable environments can benefit from the translation of biological mechanisms that permit biological systems to excel in these kinds of environments [Iida and Ijspeert, 2016]. In fact, considerable progress in this direction has been made over the last 30 years, at all levels [Bar-cohen and Breazeal, 2003, Shi et al., 2015, Iida and Ijspeert, 2016] ranging from biologically inspired materials and mechanics [Cham et al., 2002, Spagna et al., 2007], to brain-inspired sensory-motor controllers [Konolige et al., 2008, Cully et al., 2015, Kober et al., 2013, Cowan et al., 2005], to biologically inspired behavioral robustness and diversity [Saranli et al., 2001, Cully et al., 2015], to social cooperation [Rubenstein et al., 2014], but challenges still remain as evidenced by the domination of industrial robotics by conventional robots [Pfeifer et al., 2007, Shi et al., 2015, Iida and Ijspeert, 2016].

Furthermore, apart from being a means to improve aspects of robotic implementations, biologically-inspired artificial motor systems can be designed to test the plausibility of theoretical biological mechanisms and generally further our understanding of biological systems [Iida and Ijspeert, 2016].

1.5.3 Cognitive-automatic interactions in hybrid systems

A third class of sensory-motor systems, of not purely biological or artificial sensory-motor systems but of hybrid ones, has been under development in the last 20 years [Lebedev and Nicolelis, 2006]. Using the activity of cortical neurons to control external devices as a possible method for restoring some motor function in paralyzed patients was proposed in 1980 [Schmidt, 1980], based on earlier experiments that showed the feasibility of learning to adjust the activity of individual neurons in monkeys [Fetz, 1969]. Around the year 2000, the first systems to enable the brain of rodents [Chapin et al., 1999, Talwar et al., 2002], non-human [Wessberg and Nicolelis, 2004, Serruya et al., 2002, Taylor et al., 2002] and human [Birbaumer et al., 1999] primates to directly interact with a machine appeared [Nicolelis, 2003, Donoghue, 2002].

These brain-machine interfaces (BMI) principally aim to develop a viable substitute for patients with impaired sensory-motor functionality. More recently, significant progress towards this aim was made as control of prostheses by human patients with cortical recording implants was demonstrated [Hochberg et al., 2006, 2012]. A relatively recent line of research has also advanced the sensory counterpart of BMIs towards providing the brain with sensory information via direct cortical stimulation [Bach-y Rita and W. Kercel, 2003, O'Doherty et al., 2011a, Tabot et al., 2013, Bensmaia and Miller, 2014].

BMIs are *de facto* modular as a result of the integration of an artificial component with a biological one. Their artificial part may be hard-wired to function in a predetermined way, but may also be equipped with cognitive functionality such as learning to recognize patterns of brain activity to interpret them as movements. In its interactions with the interface, the brain also maintains both its automatic and its cognitive functions. So, the development of BMIs is largely dependent on the understanding and the design of links of either direction between the cognitive and automatic, biological and artificial counterparts of the hybrid set-up.

1.6 Structure of the dissertation

This dissertation is concerned with theorizing about, experimentally testing, and implementing certain interactions between automatic and cognitive components of biological, artificial, and hybrid sensory-motor systems.

Specifically, this introduction is followed by chapter 2, where we propose a mechanism through which developmentally early spontaneous and reflexive automatic movements generated by the spinal cord may influence motor control and learning by the cerebral cortex. We demonstrate that a simulated artificial sensory-motor system modeled to capture aspects of the spinal cord, the cortex, and the body can benefit from and be strongly influenced by a mechanism which emerges from the system's and its components' properties, suggesting that biology may be taking advantage of such a mechanism, and that biologically-inspired robotic systems alike could benefit from making use of it.

In chapter 3 we describe an experiment designed to uncover how voluntary inhibition acts on spontaneous eye-blinks. The experiment involved recording neuromuscular activity around the eyes of human subjects who were occasionally instructed to stop blinking and subsequently to relax. The timing of blinks after periods of voluntary inhibition revealed mainly that the voluntary inhibition and its release stop and reset the automatic blink controller, as opposed to alternative hypotheses of volition (a) acting peripherally through opposite contractions of the eye muscles, or (b) negating the output of the blink generator while the generator itself continues outputting motor commands, or (c) pausing the blink controller in its pre-inhibition state.

In chapter 4 we experimentally investigate whether a voluntary reaction task such as clicking a computer mouse in response to mechanical stimulation of the fingertip can influence whether and when an automatic movement such as an eye blink is generated. The distributions of stimulus, mouse press and release, and eye blink timings reveal that the voluntary reaction introduces a trigger to an eye blink, and that eye blinks are likely triggered separately and not as a part of a single plan to

"click and blink".

In chapter 5 we describe how we configured a spiking neural network on a neuromorphic mixed digital-analog very-large-scale-integration electronic chip to learn to decode the intracortical activity of a rat's motor cortex into forces acting on an external object. The object's position was encoded through electrical microstimulation patterns into the rat's somatosensory cortex, thus forming a closed-loop bidirectional brain-machine interface (BMI). The rat in this implementation was anaesthetized, so cortical recordings represented largely automatic responses to stimulation, in contrast to the chip which was equipped with the cognitive function of learning. The network on the chip made use of the variability among silicon neurons and among silicon synapses, as well as of the chip's configurable features such as "stop learning". After training, the chip enabled the bidirectional set-up to function as a dynamical system approximating a force field. The BMI successfully guided the controlled object to a pre-defined target in every experimental session.

Finally, chapter 6 summarizes and discusses the dissertation's conclusions.

Chapter 2

The developmental role of reflexes as a tutor for cortical motor control

Disclaimer

The model was designed with Arko Ghosh and Matthew Cook, who also both guided the writing of the chapter.

2.1 Introduction

2.1.1 Sources of motor output in the nervous system

Different sources of motor commands in the mammalian central nervous system mature at different developmental timescales. The human spinal cord reaches its movement-initiating maturity very early. At birth it is able to produce a plethora of predefined reflexes while even prenatally it frequently generates largely stereotypical spontaneous movements [Robinson et al., 2000]. On the other hand, the generation of learned, planned, intentional movements by the cerebral cortex takes much longer to mature. For instance, human infants first learn to reach with their arms at four months after birth [Thelen et al., 1996], in contrast to movements of the arm produced by the spinal cord which occur even prenatally [Kurjak et al., 2002, McCartney and Hepper, 1999]. While intention has been attributed to movements occurring as early as 22 gestation weeks [Zoia et al., 2007], the corticospinal system, which transmits motor commands from the cortex, is the last of the motor systems to develop and takes years to fully mature [Martin, 2005], rendering the spinal cord the dominant source of early movement.

2.1.2 Conjectures of preparatory role of early movements

These developmentally early movements have been long regarded as preparatory for mature motor control. As soon as 1952, Piaget pointed out that early, stereotypical movements such as spontaneous movements and reflexes constitute a hereditary carrier of information about the body and its environment [Piaget and Cook, 1952]. A large recent body of literature on developmentally early movements, in particular twitches of sleeping rat pups, has provided convincing evidence that these movements play a significant role in the developing sensory-motor system (see [Blumberg, 2015] for a review). Specifically, these movements promote self-organization within the sensory-motor circuits that generate them, by associating motor output with sensory input [Blumberg et al., 2013]. For example, sensory feedback from spontaneous twitches is implicated in the wiring of spinal reflexes as has been demonstrated in artificial bimomimetic systems through computer simulations [Petersson et al., 2003, Marques et al., 2013]. Embedding these ideas in artificial sensory-motor systems not only promotes our understanding of biological development, but may also contribute to building better robots [Blumberg et al., 2013]. These synergistic advances in the developmental branches of biology and robotics, demonstrate the role of early spinal motor output in sensory-motor development, and specifically in the intra-spinal self-organization that gives rise to reflexes. Similar associative sensory-motor learning may occur in the supra-spinal circuits as a result of supra-spinally initiated movements. Nevertheless, whether and how the sensory-motor information contained in the circuits of the spinal cord can propagate and influence the motor development of the higher levels of the neuraxis such as the cortex remains unclear in the absence of cortical access to the spinal cord, such as during early development (Figure 2.1 A).

Similarities between early spinal and mature high-level movements in humans have led to the early movements being thought of as preparatory for mature, high-level motor control [Thelen et al., 1987, Thelen, 1985]. For instance, kicking movements in early infancy show similar spatiotemporal patterns with mature locomotive movements [Thelen et al., 1981]. Kinematic similarities also exist, in that both early spinal and mature high-level movements show a linear relationship between their peak velocity and their amplitude [Thelen et al., 1987]. The similarities can be attributed to the fact that mature, learned motor commands recruit the same low-level motor circuits that implement the early, stereotypical motor commands, possibly as a result of Hebbian strengthening of the descending connections with specific parts of the low-level circuitry. This picture still cannot account for a possible role of the early movements generated by the spinal cord in the absence of a causal link with cortical output.

Furthermore, despite the formation of motor skills in maturity through learning, performance level and learning rate in learned tasks have been documented to be

highly hereditary, according to studies comparing monozygotic to dizygotic twins [Williams and Gross, 1980, Bouchard and Malina, 1983, Fox et al., 1996, Missitzi et al., 2004, 2013]. There is a relative absurdity in this concept of heritable learned motor skills, that has not been sufficiently explained. This chapter is concerned with the possibility that there is a developmental influence of early genetically-defined spinal movements on the cortical circuits that learn, decide, plan, compute, and generate the mature motor commands. Such an influence could be a plausible explanation both for the transfer of genetically defined spinal movement characteristics to learned cortical movements, and for the hereditary component in learning and performance of acquired motor skills.

2.1.3 Activations of the cortex by early proprioception

A characteristic of early spinal movements that potentially establishes an influential link with the development of cortical motor computation is their resulting sensory information. In adults, the production of sensory information that reaches the cortex and results in the sense of proprioception is a fundamental common characteristic of all types of movement. Afferents from muscle spindles, Golgi tendon organs, joint mechanoreceptors, and skin stretch receptors supply a barrage of sensory inputs to the central nervous system [Prochazka, 2010], eventually processed by the cortex [Prud'homme et al., 1994]. Interestingly, even before the maturation of the cortical motor system, the cortex of neonatal rats becomes activated as a consequence of spinally-produced movements [Khazipov and Luhmann, 2006, McVea et al., 2012, Khazipov et al., 2004] which correspond to human fetal movements [Clancy et al., 2001]. These inputs, which arrive at this very plastic stage of development, are believed to have essential influences on the cortical wiring [Khazipov and Luhmann, 2006]. The reflection of these influences on the computations performed later by the cortex when it starts controlling the body movements, and ultimately on the movements themselves, has not previously been addressed systematically.

2.1.4 Spinal movements generate inputs to inverse internal models

Movement generation by the brain involves inverse internal models, which associate motor commands with internal representations of intended movements [Wolpert and Ghahramani, 2000, Oztop et al., 2013]. Essentially, when a representation of a movement is selected as a goal, inverse models are employed to compute the motor outputs that can achieve the goal. These premotor representations of conceivable movements are learned from observational experience, and among the earliest of experienced movements are those produced by the spinal motor generation circuits. The imprints of these sensory experiences on the developing cortex may be used later as

premotor sensory representations, i.e. sensory goals for cortical inverse-modelled motor control (Figure 2.1 B).

2.1.5 Our approach

In order to assess the influence of a developmentally early source of stereotypical motor commands on a later, plastic one, through a mechanism of sensory learning of movement representations, we performed simulations using a computational model of a joint with rich proprioceptive feedback. Our model intends to abstract those features of the biological motor system which are relevant to our enquiry, rather than simulate its components in detail. In our simulations we find that the sensory-motor system is well-positioned to employ a spino-cortical sensory tutoring mechanism that improves motor learning, and that such a mechanism can explain similarities between early spinal and mature cortical movements, and the heritability in learned motor skill performance and learning speed.

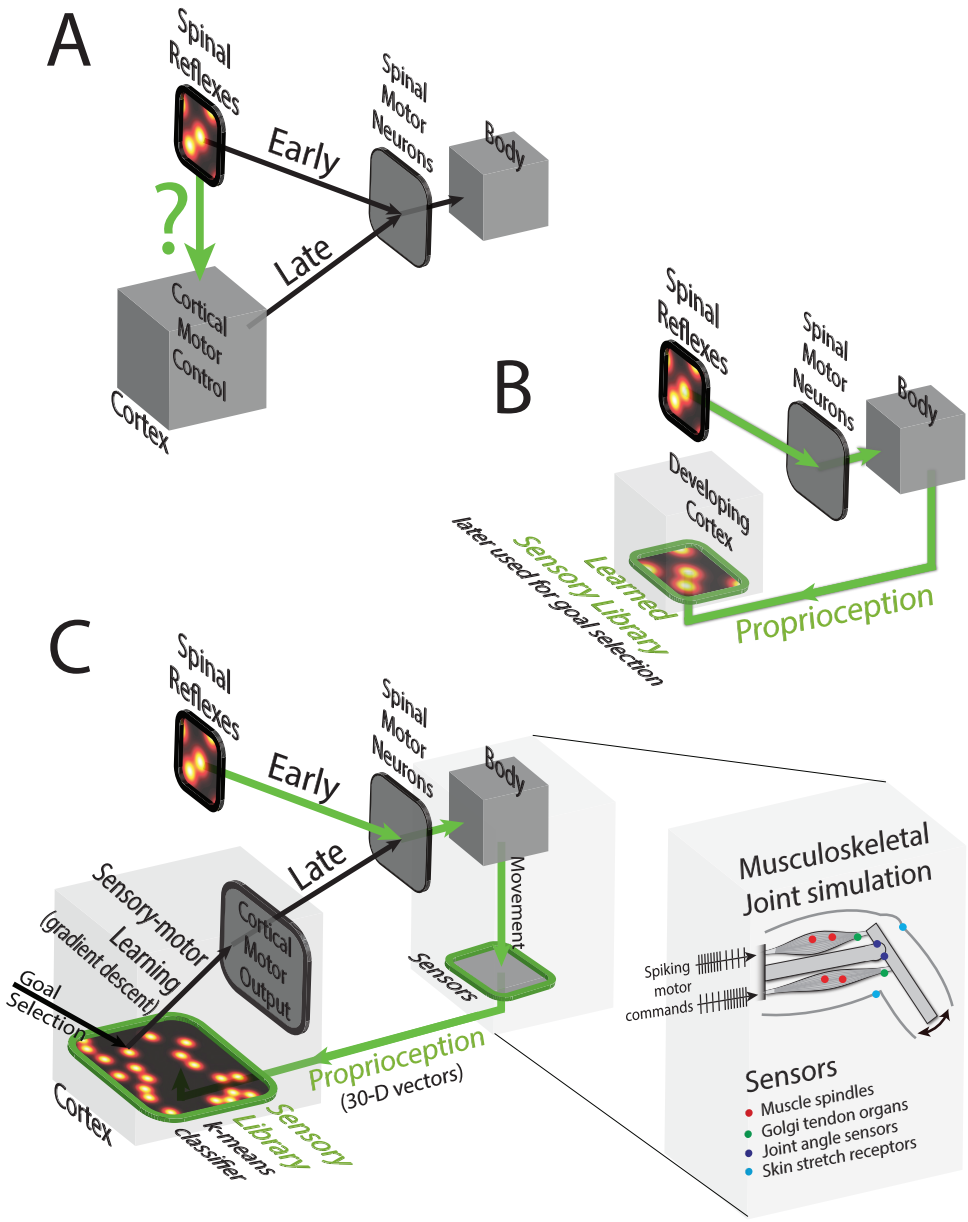

Fig. 2.1: ***The model.***

Fig. 2.1: ***The model.*** *(continued) (A) Motor commands originating in the spinal cord (Spinal Reflexes) activate Spinal Motor Neurons and move the Body early in development. Only certain parts of the space of possible motor outputs from the spinal cord are accessed by Spinal Reflexes (heat map schematic). Later in development, the Body is addressed via the Spinal Motor Neurons by commands originating from the Cortex. A potential influence of early spinal motor output on Cortical Motor Control has been hypothesized (green arrow) but how this may occur has not been addressed systematically (green question mark). (B) We propose that early spinal movements can influence later cortical motor control through their proprioceptive sensory consequences that enable the Cortex to learn sensory representations of movements from experience (Sensory Library). These sensory representations can later be used as goals for goal-driven cortical motor control. We call this mechanism "Reflex-tutoring". (C) In our model, the Cortex is capable of sensory learning (Sensory Library) which is implemented as a sequential k-means classification, which starts occurring when Spinal Reflexes are the only source of motor outputs addressing the body. Later, Cortical Motor Outputs take over control of the body. These outputs are goal-driven, with goals selected from the Sensory Library, according to a probability distribution (heat map schematic) defined by the Sensory Library's class centres. The mapping between the sensory space of the Sensory Library and the Cortical Motor Outputs is learned (Sensory-motor Learning) through gradient descent based on the errors between the goals and the resulting sensory feedback. The Body is simulated as a joint comprising two bones and two antagonistic muscles. Muscles are emulated based on Hill's model which comprises an active contractile element and a set of springs and dampers. Muscles receive input in the form of sequences of spikes. Motor commands from the Spinal Reflexes and the Cortex are encoded as pairs of firing rates addressing the muscles, for a variable duration. Cortical commands are filtered by Spinal Motor Neurons. The Body's kinematic and dynamic state is continuously monitored by pairs of five types of proprioceptors (Sensors), namely muscle spindles that monitor the muscles' length, Golgi tendon organs that monitor the force exercised by the muscles, joint receptors and skin stretch receptors that respond to changes in the angle of the joint. These receptors are simulated realistically based on data and models from the physiological literature. The output of these Sensors (Proprioception) is the input that the Sensory Library receives both before and after Cortical Motor Output takes over control of the joint's movements.*

2.2 Model

2.2.1 Model Overview

We modelled the motor system as comprising two independent sources of motor commands driving a musculoskeletal joint's movements (Figure 2.1 C). One source, Spinal Reflexes (SR), is the first to be active and produces tightly constrained motor commands addressing the joint's muscles, resulting in stereotypical movements. At a later time, a distinct, learning-capable source of goal-directed motor commands, the Cortex (Cx) takes over the control of the joint's muscles by replacing SR. Both the SR and the Cx address the joint's muscles via spinal motor neurons. The joint and its movements are monitored by sensors (proprioceptors). Proprioceptive information is forwarded to the Cx. The Cx includes a Sensory Library (SL), i.e. a space of sensory (kinaesthetic) representations of movements continuously shaped by a k-means classifier of kinaesthetic inputs. The Cx selects goals for its motor commands from a probability distribution defined by the SL. Each motor command is computed from its goal according to a sensory-motor mapping learned by a second learning mechanism employed by the Cx. This sensory-motor learning is implemented as a gradient descent that minimizes prediction errors, i.e. discrepancies between goals and actually fed-back sensory inputs. The model is programmed and simulated in MATLAB and Simulink.

The biomechanical model that we designed and used to simulate movements and their sensory consequences emulates a virtual single-joint limb, which receives spiking input commands from SR and Cx, through the spinal motor neurons. It consists of a proximal bone fixed at a horizontal position, articulated at a simple hinge joint with a distal bone, which is free to rotate about the joint, on the vertical plane. A pair of muscles – a flexor and an extensor – is attached to the distal bone and capable of actively moving it, by responding to received motor commands (Figure 2.1 C, inset).

Our model required that the joint's sensory-motor interface can accommodate the whole space of mechanically possible movements, as opposed to being optimized for one type such as rhythmic gait patterns. The functional independence of the two controllers in the model (SR and Cx) required a modular design. This design also allows easier extension and evolution of the model and its modules in future versions, which could add for instance a rhythmic pattern generator to the model's spinal motor neurons, or the ability for more complex motor plans to Cx. Furthermore, the SL was the key link between the SR and the Cx, so the rich sensory feedback from the joint's movements into the SL was essential and was reflected in the choice of a large array of proprioceptors. Finally, to increase the biological realism of the model, the sensors were modeled in agreement with physiological data. Some of these requirements are covered by previously described neuromuscular models in the

literature (e.g. [Wadden and Ekeberg, 1998, Taga, 1995, Dzeladini et al., 2014]), but our custom simulation meets their combination.

2.2.2 The joint

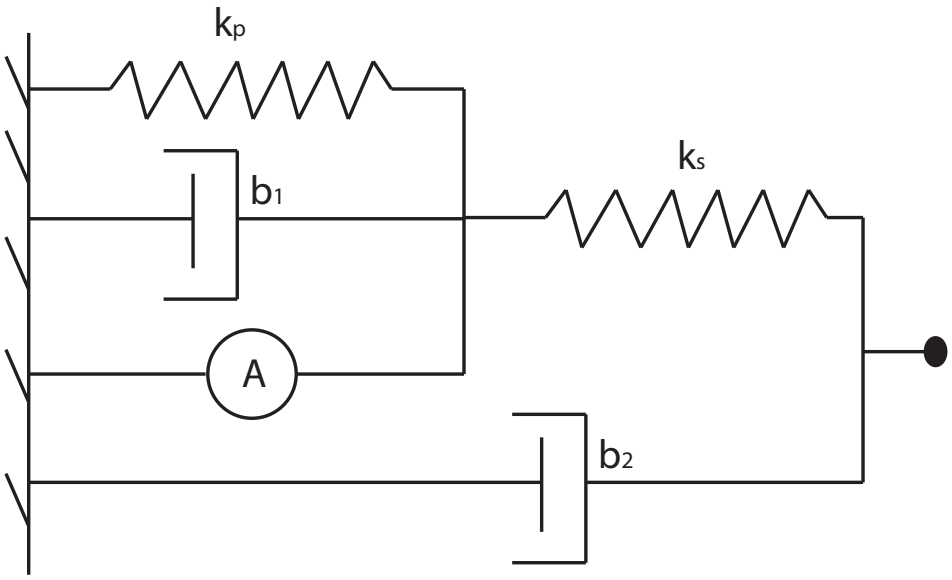

Fig. 2.2: ***The muscle model.*** *It comprises an active contractile element (A), two springs (k_s and k_p) and two dampers (b_1 and b_2).*

We used a Hill-type model [Zajac, 1989] to simulate the activity and the dynamics of the muscles of the musculoskeletal model. Our muscle model is a modification of the one described in [Shadmehr and Wise, 2005]. Each of the muscles comprises an active contractile element, connected in parallel with an elastic element (spring of constant k_p) and a viscous element (dashpot damper of constant viscosity b_1). A second elastic element (spring of constant k_s) is connected in series to the three aforementioned components. The muscle model is completed with a second viscous element (viscosity constant b_2) parallelly connected with the rest of the system (Figure 2.2).

Each muscle is actuated by motor commands in the form of spike trains that address the muscle's active contractile element, and is modelled as comprising one single motor unit. The force produced by the active contractile elements in response to the received spike trains was modelled as in [Shadmehr and Wise, 2005], i.e. it is dependent on the distribution of inter-spike intervals of the recent input, and principally on the rate of received spikes.

The force produced by the muscles' contractile elements is transferred through the passive elastic and viscous elements, exerting torque about the joint, rotating

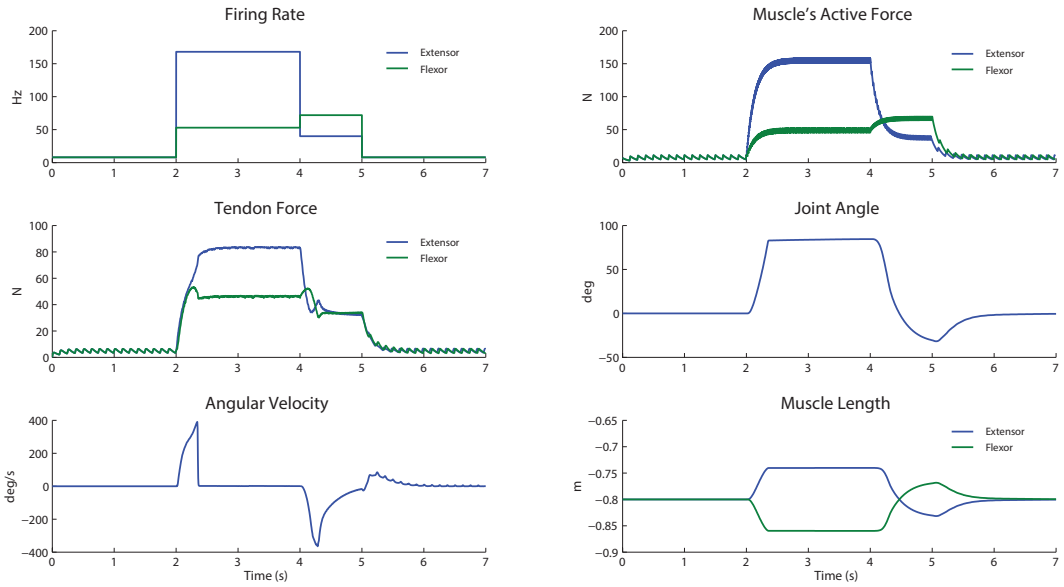

Fig. 2.3: ***Biomechanical joint kinematics and dynamics.*** *The firing rate of the input spike train to the two muscles is shown in the top left panel. The rest of the panels depict the resulting kinematics and dynamics.*

the movable distal bone. Kinematics and dynamics of an example of the joint's movement are shown in Figure 2.3.

2.2.3 Proprioceptors

The joint's movements are monitored by proprioceptors whose firing rates respond to the dynamics and kinematics of the joint (Figure 2.1 C, inset). Specifically, muscle spindles, Golgi tendon organs, skin stretch receptors and joint receptors are included. Each muscle's kinematics are monitored by a muscle spindle with a primary and a secondary afferent, discharging according to [Chen and Poppele, 1978] and [Prochazka, 2010]. One Golgi tendon organ responds to each muscle's force exerted on the bone as in [Houk and Simon, 1967]. One cutaneous receptor monitors each of the two directions of "skin stretch", with a discharge rate equal to the weighted sum of the joint angle and the angular velocity [Edin, 2001]. Two joint receptors respond to extreme angular displacements according to a fit to data from [Burgess and Clark, 1969]. Gaussian noise added to the firing rate of these 10 proprioceptive afferents shapes the final proprioceptive response. An example of the output of the sensors during movement is shown in Figure 2.4.

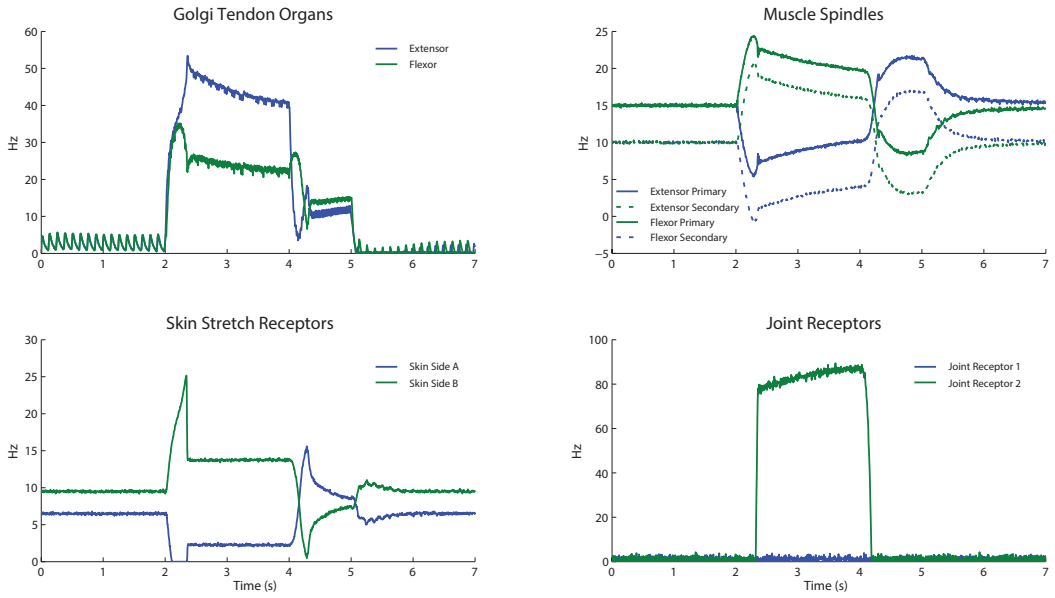

Fig. 2.4: ***Proprioceptor output.*** *The firing rate of the proprioceptors that monitor the joint, during the same time period as in Figure 2.3.*

2.2.4 The spinal motor neurons

Kinematic and dynamic changes of the joint, are produced by changes in the pair of forces exercised by the two muscles. As these forces are directly dependent on the firing rates (FR) actuating the two muscles, in a biological system functioning under these assumptions, a source of motor commands is ultimately a source of change of the spinal motor neuron's firing (Figure 2.1, Spinal Motor Neurons). In our model, each muscle is activated by one spinal motor neuron, comprising one motor unit. Motor commands at the level of the two motor units are modelled as a pair of firing rates ${}_{muscle}FR_1^{flex}, {}_{muscle}FR_1^{ext}$ activating the flexor and extensor muscles of the joint for a duration t, and ending as a subsequent pair of firing rates ${}_{muscle}FR_2^{flex}, {}_{muscle}FR_2^{ext}$. So, each motor command at spinal motor neuron level that directly activates the muscle is a 5-dimensional vector ${}_{muscle}\mathbf{MC} = \left({}_{muscle}FR_1^{flex}, {}_{muscle}FR_1^{ext}, t, {}_{muscle}FR_2^{flex}, {}_{muscle}FR_2^{ext}\right)$. In reality, single motor units demonstrate firing rates of up to a few tens of Hz [Borg et al., 1979, Fuglevand et al., 1993]. However, our muscle model does not include recruitment of multiple motor units. Instead, each muscle is modelled as a single motor unit, so we set the maximal FR at $200\,Hz$. When all commands are over, a FR of 8 Hz activates the muscles, accounting for the maintenance of muscle tone. The duration of commands ranges from 0.01 to 3 seconds. Commands arriving from the SR are directly translated to spinal motor neuron commands, unchanged, as they model commands

generated within the spinal cord. On the other hand, commands from the Cx are filtered to.

2.2.5 Spinal Reflexes (SR)

The SR is the early source of motor commands which drives the first, stereotypical movements of the joint, thus modelling the spinal cord's early reflexes and spontaneous movements (Figure 2.1, Spinal Reflexes). During normal functioning of the model, which we call the "reflex-tutored" condition of function, the movements that the SR produces provide the first sensory inputs to the SL. The SR's motor commands are transferred directly and unchanged through the motor neurons to the muscles, so that ${}_{muscle}MC = {}_{SR}MC$. The SR commands are tightly constrained. We chose to model the constraints on the SR by allowing commands to be of one of two types of muscle coordination patterns: (a) no co-contractions, or (b) high co-contraction level. In commands of type (a), each pair of FRs from the SR activates only one of the two muscles and deactivates the antagonistic one, similarly to the stretch reflex, so that the FR corresponding to the antagonist muscle is zero and the agonist's FR is randomly selected from a uniform distribution between 8 and $200\,Hz$. In condition (b), the agonist's FR is again selected from the same range, but the antagonistic muscle is always simultaneously activated as well, with a firing rate at 90% of the agonist's. The duration of the commands is randomly selected from a uniform distribution ranging from 0.01 to 3 s. The SR produces 10000 commands of both types (a) and (b) before the Cx takes over control of the joint. In two additional variants of the "reflex-tutored" condition designed to assess the effect of the type of spinally-generated movements on the Cx, the SR produced movements of either only type (a) or only type (b).

2.2.6 The Cortex (Cx)

Sensory Library

Sensory responses from the proprioceptors are forwarded to the Cx, and in particular to the model's key component, i.e. the Sensory Library (SL), where a description of the sensory space is produced through classifying kinaesthetic descriptions of movement (Figure 2.1 B, Sensory Library). The first inputs are provided by the SR's movements (Figure 2.1, arrow labelled "Early"), but SL classes continue being shaped by the Cx's sensory consequences (Figure 2.1, arrow labelled "Late"). Goals directing Cx motor commands are selected from the SL.

Sensory representations of movements

Each movement is described by the joint's state at the beginning of the movement, the joint's final state, and its trajectory and dynamics between these two states. Thus, each movement is represented in sensory coordinates by a 30-dimensional vector which includes the firing rates of the 10 proprioceptive afferents at the beginning and at the end of each movement, as well as their integrals over that interval.

Movement recognition

The beginning and the end of a movement are recognized by detecting kinematic and dynamic changes, through analysing the low-pass-filtered first three derivatives of the proprioceptors' discharge, for the detection of extrema. While, for a single movement, peaks in the firing rates of different receptors do not necessarily coincide due to different adequate stimulus for each of them, different sensitivity, and noise, the algorithm relates non-coinciding peaks of different receptors, by combining peak timing with a differential calculus approach, considering monotonicity and concavity of the first two derivatives.

Sensory learning (classification)

Assuming that the motor system has to represent the continuous sensory space of infinite movement possibilities in a finite set of district storage units, we model this representation as a classification of sensory descriptions of movements, i.e. the SL. In our model, the SL initially learns from sensory consequences of SR, but continues being updated by Cx movements thereafter.

Every 30-dimensional sensory vector $\mathbf{X} = (X_1,X_2,\ldots,X_{30})$ that describes a detected movement is fed as input to a sequential k-means classification algorithm, which forms the SL. The sequential k-means is implemented as follows. Each of the first k input vectors is used as the initial position of one of the k class centroids, and a counter for each of the classes is set equal to one, for $i = 1,2,\ldots,k$. For each new input vector $\mathbf{X}$, the closest sensory class centre $\mathbf{S_j}$ is found, so that $\|\mathbf{X} - \mathbf{S_j}\| \leq \|\mathbf{X} - \mathbf{S_i}\|$, for $i = 1,2,\ldots,k$, where $\|\cdot\|$ denotes the Euclidean norm. Counter n_j is increased by one for each new input belonging to class j and the centre of the class is moved to $\mathbf{S'_j} = \mathbf{S_j} + \dfrac{\|\mathbf{X} - \mathbf{S_j}\|}{n_j}$. To avoid domination of the distance metric by the largest dimensions, each dimension of the vectors is standardized by its variance before forwarding the vectors to the SL.

Each class centre in the SL represents in the sensory space a class of previously occurred movements. The choice of the precise number k of classes used for the k-means would be critical if the algorithm's purpose were data mining and qualitative understanding of the dataset. In our case, the purpose of k-means is rather to

segment the continuous space of sensory representations of possible movements to a finite number of classes that are used as the basis for movement selection and sensory-motor learning. We chose a number providing high segmentation of the sensory space within the range of computational resource limitations, and we thus set $k = 200$.

Cx motor output

The Cx is the later, learning-capable source of commands. The movements it produces are attempts to result in target sensory feedback selected from the SL. Each of the Cx's commands is also a 5-dimensional vector, with two dimensions corresponding to the activation FR of the two muscles, one duration dimension and two dimensions defining the muscles' activations after the end of this duration. Unlike the SR's commands which are directly sent to the muscles unchanged, the Cx's commands are transferred through the motor neurons to the muscles according to a filter function. Based on the fact that cortical neurons show inter-spike intervals of at least $2\,ms$ [Softky and Koch, 1993], we set the Cx's maximal FR, $\max({}_{Cx}FR) = 500\,Hz$. Transcranial magnetic stimulation (TMS) studies have shown thresholds for evoked motor potentials at levels of 30% to 60% of maximal stimulation intensity [Awiszus, 2003, Vucic and Kiernan, 2006, Caramia et al., 1991]. Although maximal cortical activity is likely to be evoked at a level different from maximal TMS intensity, we used TMS thresholds as a guide and chose 40% of maximal the Cx FR ($40\% \cdot 500\,Hz = 200\,Hz$) as the threshold for evoking a response at the lower motor neuron's level. Above threshold, we assumed a linear dependence:

$$ {}_{muscle}FR_i^j = \begin{cases} 8\,Hz & \text{if } {}_{Cx}FR_i^j \leq 200\,Hz \\ \left(\frac{200-8}{500-200} \cdot \left({}_{Cx}FR_i^j - 200 \right) + 8 \right) Hz & \text{if } {}_{Cx}FR_i^j > 200\,Hz \end{cases} $$

$$ i = 1{,}2; j = flex{,}ext $$

Goal selection

Motor decisions are the subject of a vivid theoretical field within motor control theory, principally including theories such as optimal control, Bayesian decision theory, and related frameworks [Friston, 2011, Shadmehr et al., 2010, Schaal et al., 2007, Körding and Wolpert, 2006, Liu and Todorov, 2007]. While these theories aim to describe the process of choosing the desired movement, we aim to explain the origin of the available choices. Namely, we argue that they are learned from previous sensory experiences, and are represented in a Sensory Library (SL). The purpose of our model and simulations is to demonstrate the influence of these sensory representations of

attemptable movements on the resulting movements. Our intention is not to model the decision process *per se*. Therefore, we reduced the decision process to random selection (Figure 2.1 C, bottom left, "Goal Selection"). Each movement's sensory goal is randomly chosen from the SL. The probability of selection of each point $\mathbf{S_0^*}$ in the 30-dimensional sensory space is given by the sum of Gaussian distributions, each centred at the centre of each class in the k-means SL.

Command computation

Around class centres $\mathbf{S_l}$, we assumed local linearity between sensory representations of movements $\mathbf{S_l^*}$ and the associated 5-dimensional motor commands from the Cx ($_{Cx}\mathbf{MC_l^*}$), so that for each class there exists a 5-by-30 weight matrix $\mathbf{W_l}$, for l = 1,2,...,k, such that $_{Cx}\mathbf{MC_l^*} = \mathbf{W_l} \cdot \left(\mathbf{S_l^{*T}} + 1\right)$, where l is a 30-by-1 vector of ones. For each selected sensory goal, the motor command is computed according to this relationship, by using a $\mathbf{W_l}$ stored with each class.

Sensory-motor learning (gradient descent)

Initially, the Cx produces random motor commands, as the initially stored weight matrices $\mathbf{W_l}$ are random. It learns to produce the correct motor commands for each desired movement, through error-based learning [Wolpert et al., 2011] by optimizing the weight matrices $\mathbf{W_l}$ through gradient descent (Figure 2.1 C, "Sensory-motor Learning") on the prediction errors E [Ajemian et al., 2010], defined as the Euclidean distance between resulting ($\mathbf{X}$) and desired ($\mathbf{S_l^*}$) sensory input $E = \|\mathbf{X} - \mathbf{S_l^*}\|$. After iteration p, the element of $\mathbf{W_l}$ at row i and column j becomes $W_{lij}^{p+1} = W_{lij}^{p} - \eta \cdot \frac{E^p - E^{p-1}}{W_{lij}^p - W_{lij}^{p-1}}$, l = 1,2,...,k; i = 1,2,...,5; j = 1,2,...,30; k = 200.

2.2.7 Experimental conditions for model assessment

To assess the influence of low-level inputs to higher movements, we compared three conditions (Figure 2.5 A). (a) In the normal condition ("reflex-tutored" condition), before the Cx takes over control of the joint, the SL is initialized with sensory consequences of the SR movements (Figure 2.5 A, "Reflex-tutored"). In the other two conditions, the SR's sensory consequences are ignored. In that case, the SL needs to be initialized in some other manner before the Cx can begin selecting desired movements, i.e. the initial classes in the SL need to be positioned. This was implemented in two ways. In condition (b), random motor commands from the Cx itself produce a few ($N = k = 200$) kinaesthetic inputs, assigning an initial position to each of the class centres. We call this the "self-tutored" condition of function (Figure 2.5 A, "Self-tutored"). In condition (c), the classes are initially positioned on random coor-

dinates. We call this way of initializing the SL the "untutored" condition (Figure 2.5 A, "Untutored").

2.3 Results

In order to assess the influence of early, low-level kinaesthetic inputs to the SL on the SR's function, we compared the model's performance for different conditions of function, by evaluating movement representation quality, determining accuracy of resulting movements relative to desired ones, measuring sensory-motor learning speed, and analysing movement characteristics such as muscular contraction patterns and movement kinematics.

2.3.1 Movement representation quality is reduced in the absence of reflex tutoring

Firstly, we considered the SL in the reflex-tutored condition immediately before the Cx starts producing commands, i.e. after 10000 SR commands, and compared it with the self-tutored condition, after 10000 random the Cx commands. We measured the average Euclidean distance of the centre of each class from the sensory inputs that produced it. This measure indicates the dispersion of the inputs that form a class. Due to the fact that the relationship between sensory representations of movements and motor commands is not constant throughout the sensory-motor space, the less dispersed the inputs per class, the better the representation quality of the class produced after the classification's averaging process. Commands of the SR are more tightly constrained compared to the self-tutoring random commands of the Cx. The SR's consequent sensory inputs to the SL are hence expected to be more concentrated, i.e. to yield classes of higher representation quality, compared to the self-tutored case. Our results show that, indeed, for all classes in the SL, the average dispersion of inputs to SL classes is larger for reflex-tutored SL classes than for SL classes in the self-tutored condition (Figure 2.5 B).

2.3.2 Description

2.3.3 Movement prediction errors increase in the absence of reflex tutoring and further increase in the absence of all sensory tutoring

Next, we evaluated the performance of the model under different conditions of function, in terms of prediction errors, i.e. the Euclidean distance between desired and actual movement, represented in the sensory space. Based on our result from the comparison of the quality of movement representations between the reflex-tutored

and the self-tutored SL, we predict that errors in the Cx's movements are on average larger for the self-tutored model, compared to the reflex-tutored one. The untutored model is expected to produce even larger errors, because attempts to result in kinaesthetic feedback similar to randomly positioned, non-kinaesthetically-created initial SL classes cannot be successful. To validate these predictions, we simulated 52000 Cx movement attempts, after each type of SL initialization. We calculated the average prediction errors over a moving window of 2000 attempts. We repeated the simulations of 52000 movements per SL initialization type four times, and averaged the four moving averages for each of the three conditions of model function to obtain the mean (Figure 2.5 C).

We first measured the prediction error in the first goal-directed movements attempted by the Cx, in the beginning of the sensory-motor learning process. The first point of the moving average of the prediction error, representing the first 2000 simulated movements, is for the self-tutored condition $14\% \pm 3\%$ (mean $\pm$ st. dev.) larger than the reflex-tutored one ($p = 10^{-3}$, two-tailed t-test). The same measure for the untutored condition is $31\% \pm 3\%$ larger than the reflex-tutored condition ($p = 2 \cdot 10^{-4}$, two-tailed t-test) (Figure 2.5 C).

We then compared the error at convergence level. Convergence level was defined as the average error of the last 10000 points of the moving average for each of the three conditions. In the self-tutored condition, movement errors converge to a level that is $41\% \pm 5\%$ (mean $\pm$ st. dev.) larger than in the reflex-tutored condition ($p = 5 \cdot 10^{-5}$, two-tailed t-test). In the untutored condition, errors at convergence are $54\% \pm 3\%$ larger than in the reflex-tutored condition ($p = 2 \cdot 10^{-4}$, two-tailed t-test) (Figure 2.5 C).

2.3.4 Sensory-motor learning speed is decreased in the absence of spinal tutoring

We defined learning speed as the rate of reduction of the average prediction errors. We calculated this speed as the ratio of the decrease in prediction errors from the beginning to the time of convergence, over the number of movement attempts it takes to first reach the convergence level. The learning speed for the self-tutored condition is $76\% \pm 7\%$ (mean $\pm$ st. dev.) lower than for the reflex-tutored condition ($p = 7 \cdot 10^{-4}$, two-tailed t-test). The untutored condition converges $45\% \pm 5\%$ slower than the reflex-tutored one ($p = 1.4 \cdot 10^{-2}$, two-tailed t-test) (Figure 2.5 D).

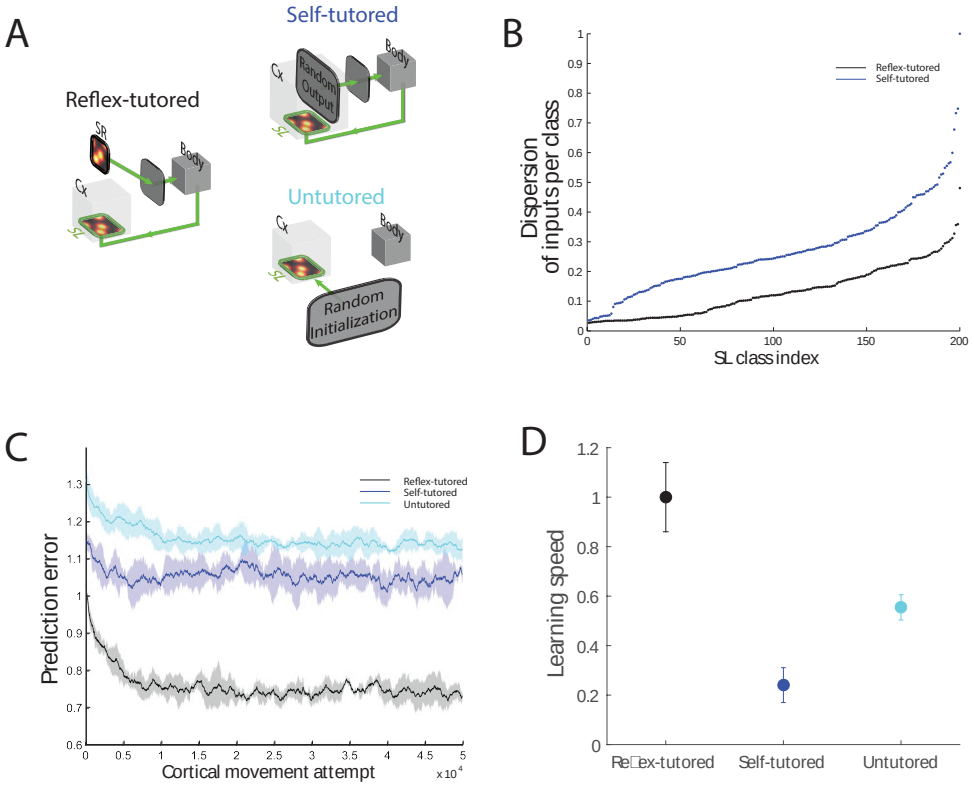

Fig. 2.5: ***(A) Experimental conditions.*** *To assess the SR's influence on the Cx, apart from the normal, "reflex-tutored" condition of function, we simulated two other conditions, in which the Cx ignores sensory consequences from the SR. In the "self-tutored" condition the SL is initialized by using sensory consequences of the Cx's own random commands, before goal-directed Cortical Motor Outputs begin to occur. In the "untutored" condition the SL's classes are positioned randomly in the sensory space.* ***(B) Reflex-tutoring improves movement representations in the Sensory Library.*** *Normalized average dispersion of kinaesthetic inputs per SL class, as a measure of movement representation quality. We define dispersion of a class as the average Euclidean distance between the class's centre and the inputs that created it. The scatter plot shows normalized dispersion values for all classes of the two conditions where tutoring takes place (the reflex-tutored and self-tutored conditions; black and blue points respectively), after 10000 tutoring movements. All self-tutored classes show wider dispersion than reflex-tutored ones, indicating better representation quality for the reflex-tutored classes.*

Fig. 2.5: *(continued)* ***(C) Reflex-tutoring decreases errors in motor control.*** *Normalized average prediction errors over a moving window of 2000 movements, for 52000 cortical movements, averaged over 4 repetitions of the simulation, for each condition. Black shows results for the reflex-tutored condition, blue for self-tutored, cyan for untutored. Shaded areas show standard deviation for the 4 simulations. During learning prediction error, i.e. the distance between cortical goals and actual sensory feedback, decreases, and converges to levels that are significantly lower for the reflex-tutored condition compared to the other two conditions. The self-tutored condition converges to lower prediction errors compared to the untutored condition. Average errors do not converge to zero because the ideal sensory-motor relationship is continuous, but is approximated by the finite capacity of the SL.* ***(D) Reflex-tutoring accelerates cortical sensory-motor learning.*** *Sensory-motor learning speed was measured as the ratio of the decrease in prediction errors by the time of convergence, over the number of movement attempts it took to reach convergence. Convergence level was defined as the average of the error in the last 10000 simulated cortical movement attempts. The graph shows the average and standard deviation over the 4 simulations for each condition. Learning speed is significantly higher for the reflex-tutored condition compared to the self-tutored or the untutored condition.*

2.3.5 Cx learned movement features are steered by the SR

We examined whether particular features in the SR's movements may be inherited by the Cx's learned movements. Strength of co-contraction of antagonistic muscles of learned Cx movements is partially inherited from SR movements We first measured the strength of co-contraction of antagonistic muscles in the Cx's movements. We defined co-contraction strength for each movement as , where are the firing rates activating the flexor and the extensor muscle respectively, during the movement. We measured co-contraction strength for each Cx-generated movement in two variants of the reflex-tutored condition (Figure 2.6 A): in variant (a) SR movements were characterized by no co-contractions (CS=0), while in variant (b) SR movements were characterized by strong co-contractions (CS=0.9). In each condition, after reflex-tutoring, we calculated the average co-contraction strength over a moving window of 2000 movements produced by the Cx. The results shown in Figure 2.6 B demonstrate the convergence of muscle co-contraction to strengths directly related to co-contraction strength in the SR movements that the Cx has been tutored by. Strong co-contractions in SR movements during reflex-tutoring ultimately lead to strong co-contractions in the Cx's learned movements (Figure 2.5 A, black line) and, conversely, no co-contractions in SR movements result in weak co-contractions in the movements learned by the Cx. The average co-contraction strength of the last 2000 simulated movements is significantly different between the two conditions ($p < 10^{-3}$, two-tailed t-test).

2.3.6 Peak velocity of learned Cx movements depends on SR

In addition, we assessed the influence of reflex-tutoring on the kinematics of the resulting learned movements. We measured the peak velocity of movements of the joint generated by the Cx, after learning has converged. When SR movements that provide the reflex-tutoring to the Cx are characterized by strong co-contractions, the average peak velocity of the movements caused by the Cx is significantly higher compared to the peak velocity of movements learned from the Cx after reflex-tutoring with no co-contractions ($p < 10^{-3}$, two-tailed Wilcoxon rank-sum test) (Figure 2.6 C).

2.4 Discussion

Through computer simulations, we showed that the sensory-motor development of the cortex is boosted in learning speed and learned accuracy if the learning of possible movement goals begins early in development by classifying sensory experiences from spinally-generated movements, a mechanism which we name "reflex-tutoring".

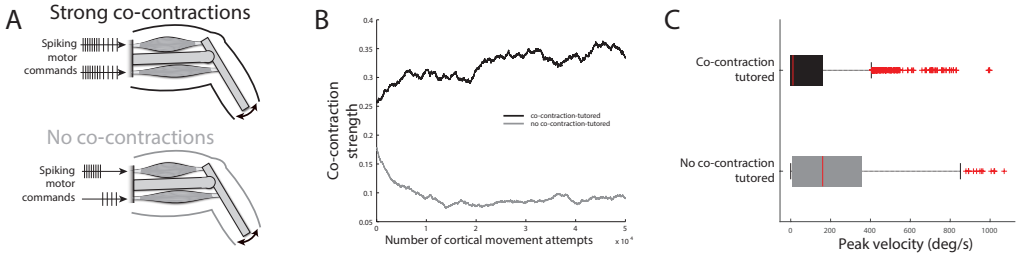

Fig. 2.6: ***Inheritance of features by the Cortex from Spinal Reflexes.*** *(A) Two variants of the reflex-tutored in which commands from the SR were constrained to cause different muscle coordination patterns. In the one variant, SR commands activated both muscles with similar firing rates so that they contracted concurrently (strong co-contractions). In the second variant, each SR motor command activated only one of the two muscles (no co-contractions). (B) Moving average (moving window of 2000 movements) of strength of co-contraction of antagonistic muscles for the reflex-tutored learned cortical movements, for tutoring with strong-co-contraction (black) and no-co-contraction (grey) SR movements. Sensory-motor learning after tutoring with strong-co-contractions from the SR yields strong co-contractions in learned Cx movements and vice versa. (C) Box plot of peak velocity of the last 1000 simulated reflex-tutored learned cortical movements for the two variants of reflex-tutoring, i.e. tutoring through strong co-contractions of antagonistic muscles, and tutoring with no co-contractions (black and grey respectively).*

Furthermore, cortical motor control partially inherits features of these early movements. Finally, eliminating reflex-tutoring of the cortex, and instead preceding cortical sensory-motor learning with a self-tutoring phase through random cortical motor outputs diminishes learned movement accuracy, but improves it compared to a complete absence of a sensory learning phase. Our results provide a plausible explanation to biologically observed hereditary effects on learned skills.

2.4.1 Model assumptions

These results emerge from the combination of seven properties of the mammalian sensory-motor system that we assumed in the model. First, it is assumed that both the spinal cord and the cortex can independently generate motor commands. Second, that the cortical and spinal motor output become effective in different developmental landmarks. Third, that spinally-initiated motor output is constrained compared to cortical possibilities. Fourth, that the cortex is capable of unsupervised classification of sensory inputs. Fifth, that the cortex produces goal-directed motor behaviour. Sixth, that the space of possible goals is learned from sensory experience. Finally, seventh, that the cortex learns the inverse model underlying goal-directed behaviour by use of errors in the movements it produces.

2.4.2 Dependency of results on chosen methods

According to our simulations, a source of initial sensory inputs is a necessity for accurate learning of movements, as reflected in the comparison between randomly- and kinaesthetically-initialized SL ("untutored" and "self-tutored" conditions of function respectively; Figure 2.5 C, cyan and blue lines). This is a result of movement-irrelevant SL classes produced by the randomly-initialized condition. Specifically, as the k-means algorithm only updates the class which is closest to the input, many of the random classes remain non-representative of movement, and therefore the error in the motor learning attempts remains large. A clustering algorithm which updates all of the classes simultaneously with each input, e.g. fuzzy k-means [Burrough et al., 2000], could eventually overcome this issue, but would cost more in terms of number of iterations, keeping sensory initialization superior to the random one.

We implemented the sensory-motor learning as an optimization of a linear sensory-motor function for each SL class, through gradient descent minimization of prediction-feedback errors. Gradient descent is a standard algorithm for error-based learning [Wolpert et al., 2011]. Our results show that sensory-motor learning is faster and converges to more accurate movements when the initial sensory learning phase is provided by the stereotypical movements of an early, pre-developed controller (reflex-tutored condition), compared to the self-tutored condition, where initial sensory inputs to the SL are provided by random movements from the the Cx controller before learning (Figure 2.5 B and C; black and blue lines). The reason for this superiority of reflex-tutoring lies in the fact that, due to tight constraints in the pre-developed motor output of the SR, the subsequent inputs create more concentrated classes, i.e., each class is dedicated to a smaller region of the sensory space (Figure 2.5 B). As the sensory-motor relationship varies along the sensory space, while a classification algorithm must group multiple inputs into a single class, the quality of movement representation by a class is inversely related to the spread of inputs producing the class. Therefore, in the case where sensory tutoring to the the Cx is provided by the SR, each of the classes is more concentrated, leading to better learning of the approximated linear sensory-motor relationship for each class, while the same range of the sensory space can be covered by the SL as a whole. Notably, although we assumed linearity for simplicity, other assumptions for the type of relationship would still produce better learning results for the more concentrated classes of the inter-level tutoring case, for the same reason.

Movement selection from the SL in our model is random and does not incorporate any decision process. Theories of motor control such as optimal control or Bayesian decision theory have addressed how the nervous system selects the movement that it will attempt [Friston, 2011, Shadmehr et al., 2010, Schaal et al., 2007, Körding and Wolpert, 2006, Liu and Todorov, 2007]. This decision process implies

selection of a representation of a desired movement from among all the available options of attemptable movements, which must also be internally represented. While the selection process has indeed been previously addressed, the origin of the internal representation of the attemptable movements remains theoretically unexplored. For instance, optimal control describes the selection of a desired movement through minimizing a cost function $u(x)$ over all possible movements x:

$$\hat{x} = \arg\min_{x} u(x)$$

However, the domain of definition of $u(x)$ is left undefined, or assumed to be the set of every possible movement allowed by the body's mechanical properties. Here we argued that, as the representation of this domain needs also be learned, past movement experiences form it, and the earliest ones, i.e. those provided by the independent early motor source, have a strong influence on this formation. While a complete detailed model would incorporate measures of cost and usefulness in the selection of desired movements, we chose to model the selection of a desired movement as being dependent solely on past experience, to isolate the influence of the process of sensory learning by the pre-programed movements on higher motor control. Additionally, our choice is consistent with experimental observations of muscle activation patterns that were previously habitually employed even if they contradict the predictions of optimal control [de Rugy et al., 2012], suggesting that muscle activation patterns are decided based on past experience.

2.4.3 Related theories

Our results are compatible with theories in the field of motor learning and beyond. For example, the development of the visual system is dependent on spontaneous coordinated rhythmic retinal activity which appears even before vision occurs [Penn et al., 1998, Stellwagen and Shatz, 2002, McLaughlin et al., 2003, Chandrasekaran et al., 2005, Huberman et al., 2006]. While the similarity to our concept of sensory tutoring from early spinal movements is clear, the so-called retinal waves have been associated with the development of a purely sensory system.

In sensory-motor systems, it has previously been proposed that sensory activity in the cerebral [Khazipov et al., 2004, Khazipov and Luhmann, 2006] and the cerebellar [Sokoloff et al., 2015] cortices caused after movement may be contributing to motor development, however, through which mechanism this may happen and what its possible effects are had not been previously addressed.

The importance of sensory feedback has also been noted in artificial models of central pattern generators, where it has been proposed as a means of entraining the passive biomechanics with the active oscillators [Lewis et al., 2003].

Our model has similarities to learning by imitating external tutors, which is a common strategy followed by humans and other primates attempting to acquire a new motor skill [Romanes and Darwin, 1884, Piaget, 1952, Meltzoff and Moore, 1983, Tomasello et al., 1993]. This process is believed to involve the mirror neuron system, and is commonly modelled using frameworks of reinforcement learning [Arbib, 2011, Rizzolatti and Craighero, 2004, Schaal, 1999, Schaal et al., 2003]. However, it is distinct from this article's scope, in that it necessitates translation of the visual description of the external tutor's movements into the student's own body's proprioceptive coordinates, in contrast to reflex-tutoring which is provided directly by the body's own movements.

An analogous mechanism exists in songbirds. Songbirds undergo a period of sensory learning during which they memorize the song of a tutor that they subsequently learn to reproduce [Brainard and Doupe, 2002, Hahnloser and Kotowicz, 2010, London and Clayton, 2008, Mooney, 2009]. While also in this case the tutor is external, there is conceptual agreement with our model in that the sensory representations do not require a translation between sensory domains. In addition, our result that shows transfer of features from early spinal movements to the learned cortical ones is consistent with the similarity between the tutor's and the student's birdsong. Besides, the learned birdsong shows reduced structure for untutored animals [Brainard and Doupe, 2002, Williams et al., 1993], drawing parallels with our results of reduced accuracy and learning speed for the untutored and self-tutored conditions.

2.4.4 Implications of results and conclusions

Our findings of impaired motor learning and performance for hypothetical conditions which do not make use of the sensory inputs from the spinally-generated movements speak for a developmental advantage offered to vertebrates by movements such as reflexes, distinct from these movements' direct protective and behavioural roles. Specifically, these movements might provide crucial information for sensory-motor development to an animal which is blind or otherwise isolated from external tutors, increasing the likelihood of survival.

We also demonstrated a transfer of features from the pre-developed to the later learned movements, by using the strength of co-contractions of antagonistic muscles, and the peak velocity of movements as examples of transferrable features. The long, ongoing debate of nature versus nurture currently follows a compromising line of reasoning which integrates the fields of evolutionary psychology and developmental systems theory [Goldhaber, 2012]. Our results suggest that even if high-level sensory-motor circuits such as the cortex begin as a *tabula rasa* [Kalisman et al., 2005], i.e. completely unshaped and entirely susceptible to nurture, this susceptibility might in fact expressly allow them to be tutored by largely genetically-defined,

independently-functioning low-level circuits such as those that control spinal reflexes and spontaneous movements. Notably, the results match biological observations of consistent kinematics and dynamics across developmentally early and mature human movements [Thelen et al., 1981, 1987, Thelen, 1985], and thus suggest that reflex-based sensory tutoring of mature motor control may underly the long hypothesized preparation of the motor system by early movements.

Additionally, taken together the results on motor performance judged by movement accuracy, on motor learning judged by learning rate, and on the inheritance of movement features are remarkably similar to the strong hereditability of these same measures in humans acquiring new skills [Williams and Gross, 1980, Bouchard and Malina, 1983, Fox et al., 1996, Missitzi et al., 2004, 2013]. Based on this, our model of reflex-tutoring provides a simple plausible mechanism for passing genetic seeds to largely nurtured motor skills, which may explain the previously unclear mechanism of hereditary learned motor performance.

There is further significance in the steering of the learning-capable circuits towards particular types of movement. The mature, learnt movements generated by high-level sources such as the cortex are implemented by recruiting spinal circuits. Therefore, the guidance of the high-level movements towards movements similar to the early ones might signify a routing of the high-level commands through the same spinal circuits which are established *a priori* by the early sources of motor output. This routing could act synergistically with proposed Hebbian strengthening of descending connections to the low-level spinal circuits [Martin, 2005, Meng and Martin, 2003, Eyre et al., 2001]. Therefore, the sensory link between the differentially developing sources of motor output bears implications for the nervous system's economy, as it assists in preventing the *de novo* development of low-level circuitry for the implementation of high-level commands.

Moreover, the comparison between the untutored and the self-tutored cortex in our model revealed a decline in the efficacy of motor learning when sensory-motor learning is not preceded by a phase of sensory exposure. This result suggests that sensory-motor associative processes might rely on efference-independent mechanisms of sensory learning, to an extent worthy of further exploration both theoretically and experimentally.

2.4.5 Biological relevance

The components used in our model do not replicate the biological ones precisely. Nevertheless, the assumptions on which the model is based are abstractions of known biological mechanisms (see subsection 2.4.1 and subsection 2.4.2). The biological relevance of the model is further corroborated by the variety of well-established analogous biological models that operate on similar principles (see subsection 2.4.3).

Importantly, the results of our simulations closely match qualitative biological observations that were not adequately explained previously (see subsection 2.4.4, lending the model further biological credibility and relevance.

To summarize, our simulated model demonstrates that mammalian motor control may be steered by and benefit from sensory inputs from movements, particularly early-developed ones, and proposes a plausible mechanism for this. Our results suggest that the spinal cord is well-positioned to guide higher-level, plastic controllers like the cortex towards fast and accurate learning of movements and steer them to recruit the pre-established spinal circuits. We propose that sensory consequences of movement are an influential channel that enables sensory-motor information to propagate from developed low levels of the neuraxis to still-developing higher ones, thus promoting bottom-up inter-level self-organization of the sensory-motor system. Further work in the rapidly advancing field of sensory-motor development and its intersection with developmental robotics could reveal to what extent and with what added sophistication mammals do and robots should exploit the underpinning of this mechanism.

Chapter 3

Voluntary inhibition of spontaneous eye-blinks

Disclaimer

The experimental paradigm was largely designed with Arko Ghosh. The experiments were performed with help from Gina Paolini. The chapter's text was written with Arko Ghosh. A partial version of the text is published in [Moraitis and Ghosh, 2014].

3.1 Introduction

In chapter 2 we explored how the development and the mature behaviour of a cognitive controller like the cortex is influenced by an automatic one such as the spinal cord. While we explored the influence of the automatic controller on the cognitive one, the cognitive part in that system, when developed, is the one that exerts control over the automatic one as cortical motor outputs recruit spinal circuits. How this latter type of hierarchical relationship is implemented was not in the scope of the previous chapter and was not addressed. In the present chapter we do explore a hierarchical interaction of this type, i.e. of an automatic component controlled by a cognitive one. Eye blinks offer a convenient paradigm of automatic movements due to their frequency, spontaneity, and relative simplicity, and here we analyze through both theory and experiment how volition exerts control over automatic blinks when blinks are voluntarily inhibited.

In 2012, Fergal "Eyesore" Fleming won a staring contest by willfully inhibiting spontaneous eye blinks for 40 min and 59 s. There is little data on the inhibition of spontaneous blinks that would allow us to compare Fergal's celebrated record with the rest of the population. Research has traditionally focused on the mechanisms

for the generation of spontaneous blinks and the variations of the blinking behavior in health and diseases [Hall, 1945, Karson, 1983, Ponder and Kennedy, 1927]. Interestingly, the blinking behavior, in particular the blink rate may contribute to the diagnosis of psychiatric illness such as depression and schizophrenia [Mackintosh et al., 1983]. Still, few neuroscientific studies have focused on the aspects of the blinking behavior that make the voluntary inhibition of spontaneous blinking possible. Our anecdotal experiences suggest that we can successfully inhibit spontaneous blinking albeit for a limited period.

The established function of spontaneous blinking is to lubricate the eye [Doane, 1980]. Blinks also "milk" the meibomian gland to increase lipid secretions and help form a stable tear film [Korb et al., 1994]. However, only a small fraction of the spontaneous blink rate is sufficient to keep the eye lubricated [Doane, 1980, Karson, 1983]. In addition to their protective role, blinks may influence higher brain functions such as by modulating the neuronal circuits involved in attention and introspection [Nakano et al., 2013]. Blinks may also serve a role in nonverbal communication. EEG measurements suggest that viewing another person blink results in significant neuronal activations [Nakano et al., 2013].

Spontaneous blinks occur without apparent sensory inputs and are very likely driven by an endogenous blink generator in the brain [Doughty, 2001, Kaminer et al., 2011]. There are two main lines of evidence for a central generator. First, the blink rate is strongly associated with central dopamine activity. For instance, the administration of dopamine agonists in non-human primates increases the spontaneous blink rate [Karson, 1983]. Further, the depletion of dopamine such as in Parkinson's disease decreases the blink rate and treatments that elevate dopamine increase the blink rate [Biousse et al., 2004, Karson, 1983]. Consistent with all this, the higher than normal blink rate in schizophrenic patients is reduced by neuroleptic medications [Mackert et al., 1990]. Second, the blink rate is closely related to cognitive processing. For instance, in visuo-motor tasks the blink rate decreases with task difficulty [Drew, 1951]. The rate is also modulated while reading texts, listening to sounds and watching movies, and entrained by rhythmic movements such as finger tapping [Cong et al., 2010, Doughty, 2001, Fukuda, 1994, Nakano et al., 2013, 2009]. Nevertheless, sensory inputs from the eye also modulate the blink rate. Anaesthesia of the cornea reduces the blink rate but it does not abolish blinking, whereas dry eyes or damage to the ocular surface increase the blink rate [Nakamori et al., 1997]. Therefore the pace of the hypothetical central blink generator is determined by both intrinsic and peripheral factors.

The blink rate may be dramatically altered at will and brain imaging studies reveal a surprising number of cortical areas associated with this ability [Chung et al., 2006, Yoon et al., 2005]. In a PET study, the inhibition was associated with the

insular cortex, primary and supplementary motor cortices [Lerner et al., 2009]. The same areas were unveiled by using fMRI and a more detailed examination of the insular cortex suggested that this area is involved in encoding urge – which presumably builds up during the period of inhibition [Berman et al., 2012]. The pre-frontal cortex is also associated with blink inhibition [Berman et al., 2012]. Surprisingly, the primary visual cortex is also activated (in the dark) and this is not resolved using corneal anaesthesia [Tsubota et al., 1999]. In sum, the variety of brain structures associated with blink inhibition not only reflects the complexity of voluntary control of spontaneous blinking but also underlines that movement inhibition may trigger a range of cortical consequences beyond motor inhibition such as the rise in the sense of urge. However, these findings provide little insight into how exactly the cortical motor outputs countermand the spontaneous blinks.

The empirical focus on spontaneous blinking and its voluntary inhibition has not been matched by theoretical efforts to address this involuntary-voluntary interaction. Based on the rhythmic nature of spontaneous blinks it is safe to assume that the blink generator can be depicted as an oscillator. Perhaps due to the complex mix of factors that can influence this oscillator the outputs are not entirely regular. Most published inter-blink interval (IBI) distributions are positively skewed, or "j-shaped" [Cruz et al., 2011, Naase et al., 2005, Ponder and Kennedy, 1927]. The "j-shaped" irregularity of the generator's outputs could be described by a log-normal curve [Cruz et al., 2011] or using a stochastic statistical Ornstein-Uhlenbeck model [Hoshino, 1996]. A separate study theoretically explored the inhibition of blinks by assuming a linear buildup of urge, but this linear model primarily aimed towards the analysis of fMRI data [Berman et al., 2012]. The aim of our study is to address the neuronal mechanisms involved in the voluntary control of spontaneous blinking by exploiting behavioral measurements from the period post-inhibition.

Hypothetically, the voluntary inhibition of spontaneous blinks may be implemented by any one of four distinct strategies and reflect on the first spontaneous blink post inhibition ("after-blink") (Figure 3.1).

First, voluntary inhibition may involve a positive motor command to antagonize the (eyelid-closing) orbicularis oculi muscle. This mechanism is rather unlikely, as previous recordings from the inhibition period did not detect any blink-like activity in the orbicularis oculi muscle (our measurements from the inhibition period also confirm this) [Chung et al., 2006]. Still, if such a mechanism were to operate then it would leave the generator in an on state such that it continues to generate excitatory outputs during the inhibition period. Essentially, the withdrawal would have no systematic influence on the timing of the after-blink.

Second, voluntary inhibition may involve a negative motor command to intersect and null the outputs after the generator emits them. Similarly to the first strategy,

here too the blink generator would be left in an on state and the withdrawal would have no influence on the after-blink. But efferent signals from the blink generator could inform the rest of the nervous system about the timing of the next blink and then the system could respond by directly influencing the blink generator without needing the intersection. Notably, efferent signaling may explain visual suppression even before the eyelids cover the pupil in reflexive blinking [Manning et al., 1983].

Third, voluntary inhibition may withhold the generator's outputs so as to achieve a pause state. Such a pause could be achieved for instance if the inhibitory command acted on the oscillating drive of the blink generator by stabilizing it at its pre-inhibition phase. The stabilization effect might be enabled by a feedback control loop between the generator's potential and the inhibition. As in the previous two scenarios, the after-blink in this case would not be dictated by the inhibition offset and would be determined by the pre-inhibition phase of the oscillation.

Finally, voluntary inhibition may involve negative motor commands that target and stop the blink generator entirely, and thus require the generator to reboot upon the withdrawal of inhibition. In this case and in contrast to the previous three, the after-blink would be time-locked to the offset of the inhibition and dictated only by the time taken by the generator to restart.

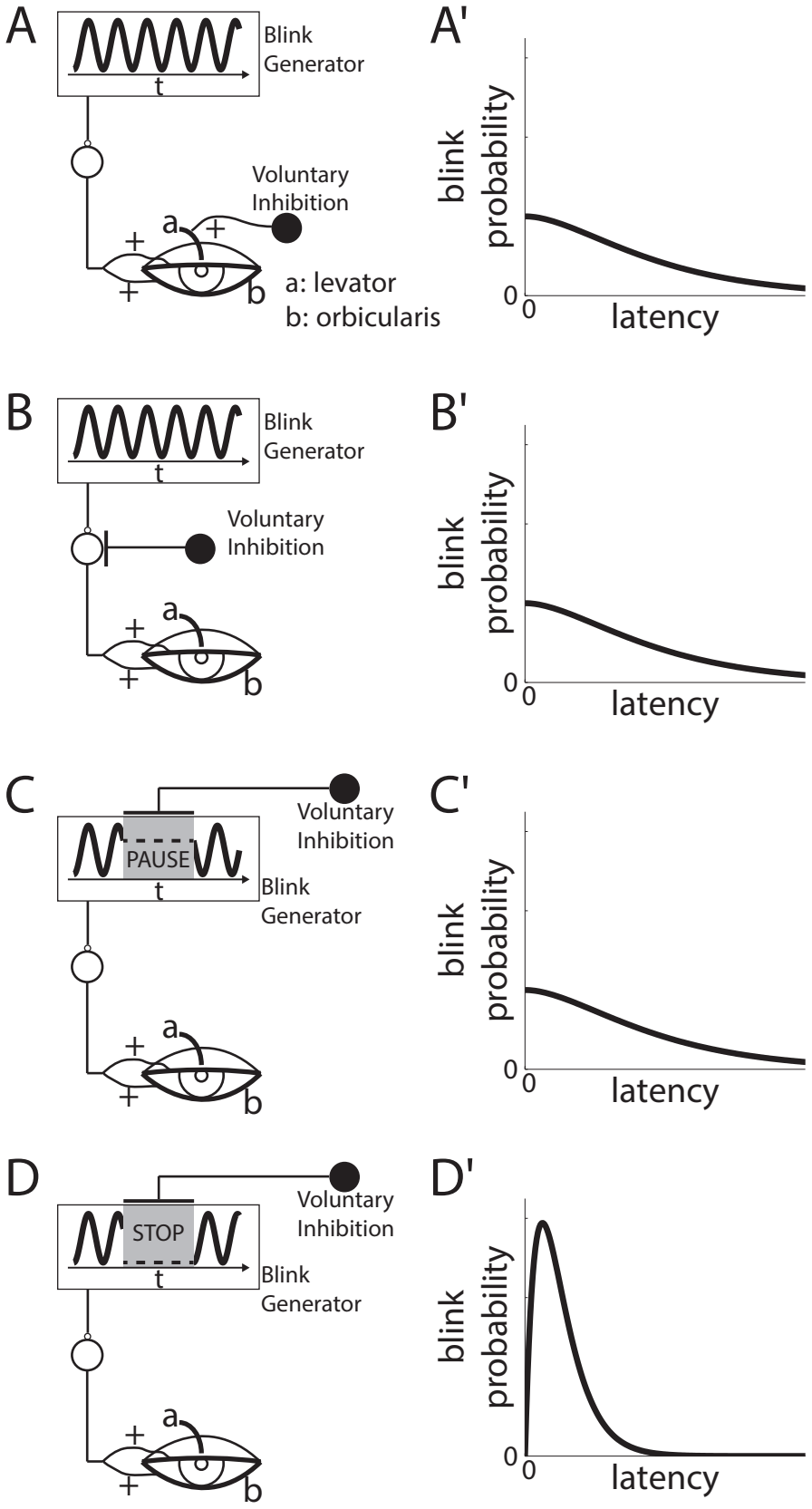

Fig. 3.1: ***Hypothetical strategies of voluntary inhibition of spontaneous blinks and associated predictions.***

Fig. 3.1: *(continued) (A) Peripheral inhibition, through strong excitation of the levator palpebrae superioris muscle antagonizing the closing of the eye by the orbicularis oculi, while the blink generator is kept in an on state, still emitting outputs. (A') Upon the withdrawal of inhibition the outputs would continue to flow as during inhibition. Therefore, the withdrawal would have no systematic influence on the timing of the after-blink. Instead, the distribution of the after-blinks would be uniform within a range of one inter blink interval. (B) Action of voluntary inhibition via intersecting commands which null the generator's outputs after they are emitted. (B') Similarly, the generator would be left in an on state, and the withdrawal of inhibition would have no effect on the after-blink. (C) Action of voluntary inhibition through a motor command which counter-balances the generator so as to achieve a pause state. (C') Here the after-blink would be dictated by the random timing of the pre-inhibition blink relative to the onset of the pause state. (D) Voluntary inhibition targets and stops the blink generator, setting it to an off state. (D') In this case only, the after-blink would be time-locked on the offset of inhibition and dictated only by the time taken by the generator to restart.*

In this study we focused on the relationship between voluntary inhibition offset and the after-blinks. We instructed volunteers to inhibit blinks in response to a sound tone and found that the after-blinks were consistently time-locked to the offset of the tone. In addition, we were able to opportunistically address the influence of voluntary excitation on spontaneous blinking, by asking the subjects to voluntarily blink at the offset of the sound tone, and found that the first spontaneous blink was delayed by the presence of the voluntary blink.

In the theoretical part of the study we constructed a neuronal network that reproduced the pattern of our results by using a voluntary-involuntary interaction architecture that allowed the voluntary commands to nudge the blink generator into an off state.

3.2 Methods

3.2.1 Volunteers

For the main experiments on blink suppression we recruited 15 volunteers (7 males) between the ages of 20 and 28. A separate group of 6 volunteers (3 males) in the same age range were used for related control experiments but these did not involve blink suppression. All the volunteers gave informed consent for the experiments and the local ethical committee approved the experimental procedures.

3.2.2 Experimental paradigm

Volunteers were randomly presented with two distinct sound tones that lasted for 12 different equally spaced durations from half of the mean inter-blink interval (IBI) measured at rest to 7 x mean IBI. The stimuli were presented in four blocks of 24 intermixed trials. A separate block acclimatized the volunteers to the experimental set-up. A gap of a random time sample between 3 x mean IBI and 4 x mean IBI was used to separate the trials. For one of the two sound tones they were instructed to "inhibit spontaneous blinking for the entire duration of the tone"; for the other tone they were instructed to "inhibit spontaneous blinking and generate one blink at the end of the tone". For the latter instruction, volunteers were briefly trained not to squeeze their eyes but instead to voluntarily blink as rapidly as spontaneous blinks. The tones were allotted randomly to each volunteer. The sound tones were delivered using a MATLAB script. The subjects watched a silent nature documentary through the experiment and this, based on our pilots, prevented them from falling asleep in the hour-long experimental session involving a rather simple task.

A separate control group of subjects (n = 6) were exposed to sound tones of the two distinct frequencies and were instructed to report the tone type by using a track pad.

3.2.3 Recording blinks

Blinks were recorded by using a pair of ocular EMG surface electrodes placed around the eyes to target the orbicularis muscle. The signals were grounded by using a salt band placed around the neck. The raw signals from the surface were amplified with a gain of x1000 and digitized at 2500 Hz using a data acquisition board (USB-6008, National Instruments). The sound tones were digitized on the same board.

3.2.4 Automatic detection of blinks

The recorded EMG data were filtered offline with two different settings offline. The data was low-pass-filtered (20 Hz) to get confirmation of the blink movements by exploiting the movement artifacts and in parallel the data was band-pass-filtered (70 Hz – 200 Hz) to detect the neuromuscular activations. We further processed each of the two filtered signals by subtracting the mean and converting to absolute values.

We detected peaks crossing a threshold set to one standard deviation of the signal for the low-pass-filtered data and to 3 times the standard deviation for the band-pass-filtered data. A peak detected in the band-pass-filtered signal was assumed to be associated with a blink when it coincided with a peak in the low-pass-filtered signal. Peaks spaced closer in time than 50 ms were assumed to belong to the same

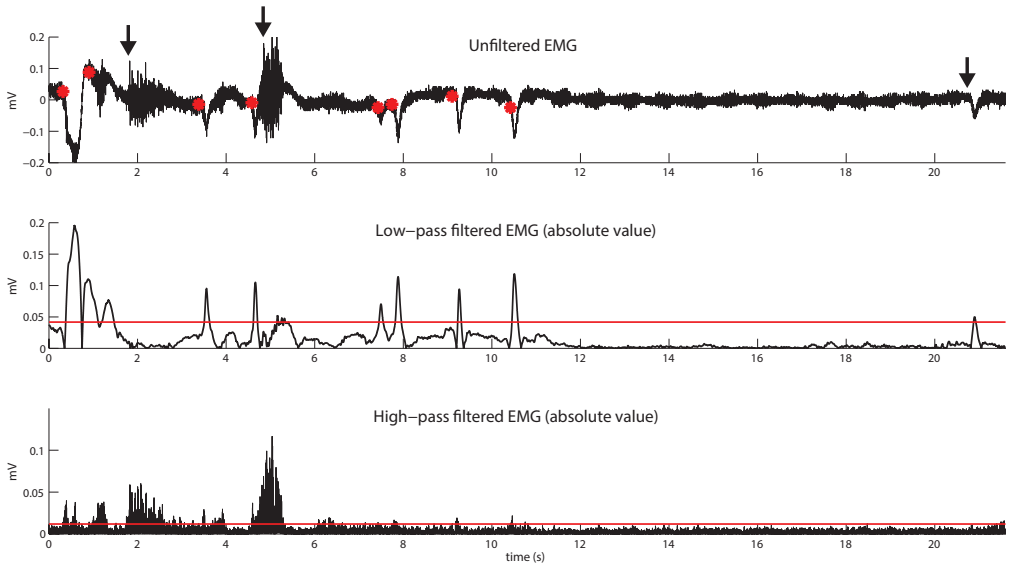

Fig. 3.2: ***Automatic detection of blinks.*** *A sample of about 20 s of recorded EMG activity (top). Combinations of peaks detected in a high-pass- (bottom) and a low-pass-filtered (middle) EMG signal were used to detect blinks robustly (red points, top), while excluding false positives that any of the signals alone could have yielded (arrow locations, top).*

blink. The first of such a block of peaks was taken as the onset of a blink's EMG activity (Figure 3.2).

3.2.5 Derivation of distribution of blinks in general, and of post-inhibition after-blinks

Distribution of blinks in general during the experiment

- ***General IBI distribution during the experiment***

  Having detected N_{blinks} blinks at time points t_i, $i = 1,2,\ldots,N_{blinks}$, we obtained the general distribution of IBIs for each subject during the experiment by subtracting the time stamps of consecutive blinks, after excluding the periods of inhibition, and uninhibited periods between an instruction to voluntarily blink and the next inhibition:

$$\left\{{}^{N_{blink}-1}_{i=1} IBI_i\right\} = \left\{{}^{N_{blink}-1}_{i=1}(t_{i+1} - t_i)\right\} \tag{3.1}$$

  .

  As expected, we found IBIs to follow a positively skewed "j-shaped" distribution.

- ***Blink distribution after a random time point***

  From the distribution of IBIs, we derived the probability distribution of blinking at time $t = t0 + \Delta t$ for the first time after any random time point t0 during the experiment, as follows:

  Blink's $i+1$ latency from each of the time points t_0 in between t_i and t_{i+1}, is $\Delta t = t_{i+1} - t_0$. But t_0 are uniformly distributed, such that $t_0 \sim U(t_i,t_{i+1})$.

  Therefore the latency of blink $i+1$ from a random point t_0 after blink i is uniformly distributed between 0 and IBI_i:

$$\Delta t \sim t_{i+1} - U(t_i,t_{i+1}) = U(0,IBI_i)\,. \tag{3.2}$$

  Thus, the latencies of all blinks from all random points during the experiment for each subject – after normalization to obtain probability – are distributed as

$$P_{random}(\Delta t) = \frac{\sum_{i=1}^{N_{blinks}-1} U(0,IBI_i)}{\int_{\Delta t=0}^{\infty} \sum_{i=1}^{N_{blinks}-1} U(0,IBI_i)}. \tag{3.3}$$

Distribution of after-blinks

We measured the latency of the after-blink from the offset of inhibition, i.e. of the sound tone. Subsequently, linear regressions were used to examine the relationship between inhibition length and latency.

For each subject we measured the number of after-blinks that occurred per bin of $125\,ms$ and divided with the total number of trials, to obtain a binned distribution of relative frequencies of the latencies of after-blinks:

$$n_{real}^{bin} = \frac{N_{blinks}^{bin}}{N_{trials}}. \tag{3.4}$$

3.2.6 Comparison of after-blink timing with unperturbed expectations

Comparison of after-blinks with random blinks

For the sake of comparison with the probability density $P_{random}(\Delta t)$ we transformed the real relative frequencies of after-blinks into relative frequency densities by dividing by the bin time-length:

$$P_{real}^{bin} = \frac{n_{real}^{bin}}{0.125\,s}. \tag{3.5}$$

We found the bin with the maximum relative frequency $n_{real}^{peak\,bin} = \max\left(n_{real}^{bin}\right)$ and compared this relative frequency with the predicted probability of blinking within this bin ${}_{random}n_{pred}^{peak\,bin}$ according to the $P_{random}\left(\Delta t\right)$ distribution.

Comparison of after-blinks with blink timing expected from last blink

A different form of analysis was used on a subset of inhibition trials, which were only a fraction of the mean IBI. We predicted the expected latency of the after-blink from the offset of inhibition with a second method based on the timing of the last blink pre inhibition, t_{last} and the probabilistically expected value of IBI computed as the mean of the "j-shaped" IBI distribution (see subsection 3.2.5 *General IBI distribution during the experiment*). The expected timing was $E\left[t_{blink}\right] = t_{last} + E\left[IBI\right]$, thus the expected latency from the offset of inhibition was $E\left[\Delta t_{blink\,inh}\right] = E\left[t_{blink} - t_{inh}\right] = E\left[t_{blink}\right] - t_{inh} = t_{last} + E\left[IBI\right] - t_{inh}$. We compared this with the actual latency of the after-blink, t_{real} . To avoid inhibition periods far from a (pre-inhibition) blink we considered only those trials where the last blink (pre-inhibition) occurred such that the expected after-blink latency, ${}_{single\,trial}^{min\,inh\,dur}E\left[\Delta t_{sp_1\,inh}\right]$, was longer than the mean inhibition-locked blink latency as per our result for all inhibition durations, $mean\left({}_{single\,trial}^{all\,inh\,dur}\Delta t_{sp_1\,inh}\right)$.

3.2.7 Model of Voluntary Inhibition – Spontaneous Blink interaction

We constructed a neuronal model of a spontaneous blink generator that could be inhibited using motor commands akin to the voluntary outputs. The architecture of our model and its resulting behavior were directed towards reproducing key features of our empirical observations. A component of the model was an oscillator composed of a pair of an excitatory (G) and inhibitory neuron (C), connected to an integrator (S) of spontaneous and voluntary drive that provided continuous flow of inputs to the pair. The firing rate of each of the neurons in the oscillator (G, C, and S depicted with an i below) was modeled as a sigmoid function of the neuron's membrane potential.

$$F_i = \frac{c_i}{1 + \exp\left(-g_i \cdot U_i - \theta_i\right)} \tag{3.6}$$

c_i is a scaling constant, g_i is the gain of the sigmoid function, θ_i is the neuron's firing threshold, and U_i is the membrane potential of the neuron.

U_G changed linearly with respect to the firing of the pre-synaptic neurons S, C, and I. The neuron I inhibited G. The membrane potential of G was returned to rest by using a term of decay.

$$\frac{dU_G}{dt} = w_{SG}F_S - h_{CG}F_C - h_{IG}F_I - \alpha_G \cdot \left(U_G - U_G^0\right) + j_G \cdot F_G \tag{3.7}$$

w_{SG}, h_{CG}, and h_{IG} are the weights of connections from S, C, and I respectively, α_G is the constant of decay, U_G^0 is the resting potential, and j_G is the weight of self-excitation. The membrane potential of neuron S, i.e. U_S was changed similarly with time, while it received inputs from neurons D and V, and self-excitatory feedback.

$$\frac{dU_S}{dt} = w_{DS}F_D + w_{VS}F_V - \alpha_S \cdot \left(U_S - U_S^0\right) + J_S\left(U_S, \frac{dU_S}{dt}\right) \tag{3.8}$$

w_{DS}, and wVS are the weights of connections from D and V respectively, α_S is the constant of decay, U_S^0 is the resting potential. The self-excitatory feedback was a function of C_I's membrane potential, such that it resisted to decreases in the membrane potential:

$$J_S\left(U_S, \frac{dU_S}{dt}\right) = \begin{cases} -j_S \cdot U_S + \frac{dU_S}{dt} & \text{when } \frac{dU_S}{dt} < 0 \\ 0 & \text{otherwise.} \end{cases} \tag{3.9}$$

Its firing rate F_S was given similarly to neurons G, C, and S by Equation 3.6 The membrane potential of neuron C, i.e. U_C was changed with time, by receiving weighted inputs from S, G, and from an additional inhibitory interneuron C_I, and by a term of decay to the resting potential, but with no self-excitation involved.

$$\frac{dU_C}{dt} = w_{SC}F_S + w_{GC}F_G - h_{C_IC}F_{C_I} - \alpha \cdot \left(U_C - U_C^0\right) \tag{3.10}$$

The neuron C_I was used as an oscillation modulator and received inputs from S. Its membrane potential changed linearly with respect to the firing of the pre-synaptic neuron S, and was allotted a term of decay.

$$\frac{dU_{C_I}}{dt} = w_{SC_I}F_S - \alpha_{C_I} \cdot \left(U_{C_I} - U_{C_I}^0\right) \tag{3.11}$$

w_{SC_I} is the weight of the connection from neuron S, α_{C_I} is the constant of decay, and $U_{C_I}^0$ is the resting potential.

Its firing rate was given by a non-linear relationship with the membrane potential.

$$F_{C_I} = \frac{C_{C_I}}{1 + \exp\left(-g_{C_I} \cdot V_{C_I} - \theta_{C_I}\right)^2} \tag{3.12}$$

An important neuron in the network was neuron V which was responsible for nudging the oscillator into its off state via neurons I and S when V's firing rate was set to 1. It was set to 0 otherwise. Finally, D was responsible for sustaining the oscillation

through its constant and continuous firing rate that was set to 1.

3.3 Results

3.3.1 The after blink is time-locked to the inhibition offset

Volunteers were instructed to inhibit spontaneous blinks throughout the duration of two types of sound tones. At the offset of one tone type volunteers were instructed to relax and at the offset of the other type they were instructed to voluntarily blink. All the volunteers were able to successfully inhibit their blinks through the duration of the sound tones. We reasoned that the blink that spontaneously occurred right after the offset of inhibition would inform us on the strategy used by the brain to implement voluntary inhibition (in the inhibition followed by the "relax" instruction). To briefly re-iterate, if voluntary inhibition were to nudge the blink generator into an off state then the spontaneous after-blink would be time-locked to the withdrawal of inhibition, i.e. when the sound turned off. The voluntary condition allowed us to compare spontaneous after-blink with voluntary blink and these comparisons shall be stated in the following section.

Across all the subjects the spontaneous after-blinks were consistently time-locked to the withdrawal of inhibition (Figure 3.3 A). To quantify this, we relied upon the distribution of the blink latency (from the sound offset) obtained from each subject by using an arbitrary bin size of $125\,ms$ (Figure 3.3 B). The peak of this distribution (${}_{random}n_{real}^{peak\,bin}$) was in all subjects considerably higher than the prediction (${}_{random}n_{pred}^{peak\,bin}$) for the same bin based on the general blink probability distribution $P_{random}(\Delta t)$ (see subsection 3.2.5 *General IBI distribution during the experiment*, Figure 3.3 C and D; $mean\left({}_{random}n_{real}^{peak\,bin}\right) = 0.18s^{-1}$, $mean\left({}_{random}n_{pred}^{peak\,bin}\right) = 0.06s^{-1}$, $p = 9.38 \cdot 10^{-5} < 0.05$, two-tailed paired-sample t-test, t = 5.40, n = 15).

We assumed that periods of inhibition that lasted only for a fraction of the mean IBI would not be associated with significant changes of the tear film and alter sensory drive from the cornea. And a broken tear film could not be entirely ruled out where the inhibition periods were a couple of folds longer than the mean IBI. To quantify the impact of short periods of inhibition (subset of all inhibition periods) we first predicted the expected latency of after-blink from inhibition withdrawal ${}_{single\,trial}^{min\,inh}E\left[\Delta t_{sp_1\,inh}\right]$, based on the last pre-inhibition blink and the expected IBI (see section 3.2.6), and then compared it with the real blink latency ${}_{single\,trial}^{min\,inh}\Delta t_{sp_1\,inh}$ (Figure 3.3 E). We found the expected latencies (${}_{single\,trial}^{min\,inh}E\left[\Delta t_{sp_1\,inh}\right]$) across this subset of inhibition trials to be significantly larger than the real ones (${}_{single\,trial}^{min\,inh\,dur}E\left[\Delta t_{sp_1\,inh}\right]$) (Figure 3.3 F; ${}_{single\,trial}^{min\,inh\,dur}E\left[\Delta t_{sp_1\,inh}\right] = 2403\,ms$, ${}_{single\,trial}^{min\,inh\,dur}\left[\Delta t_{sp_1\,inh}\right] = 698\,ms$, $p = 2 \cdot 10^{-7} < 0.05$, two-tailed paired-sample t-test, t = -6.83, n = 29). Essentially, even for inhibition periods that lasted only for a fraction of the mean IBI the spon-

taneous after-blinks were time-locked on the inhibition withdrawal and not on the last blink before inhibition.

Listening to the sounds alone and discriminating between the two clearly distinct tones (250/,Hz vs 400/,Hz) had no impact on the blinking behavior measured here (mean blink latency from 250 Hz tone: 5. 38 s, mean blink latency from 400 Hz tone: 5. 98 s, p = 0.36, two-tailed paired-sample t-test, t = -1.01, n = 6).

In sum, the withdrawal of inhibition triggered after-blinks that were time-locked close to the inhibition offset.

3.3.2 Comparison of the after blink with voluntary blinks

We addressed whether the time taken for an after-blink reflected a dead time in the system induced by the inhibition or whether system is in fact capable of producing an endogenous blink even faster than the after-blink. To address this we instructed volunteers to produce a blink in response to the offset of the sound. The mean of means of spontaneous after-blink latencies was 2420 ms, significantly longer than the mean voluntary blink median latency, 1628 ms (p = 0.0092 $<$ 0.05, two-tailed paired-sample t-test, t = 3.05, n = 15). Therefore, the period from the withdrawal of voluntary inhibition to the after-blink does not reflect a general dead time in the system and specifically represents the time taken to restart the spontaneous blink generator.

3.3.3 Relationship between inhibition duration and the after blink

Spontaneous blinking inhibition is expected to build up neuronal activity that may contribute to sensations such as urge and we addressed whether such inhibition-duration dependent processes also influences the speed of the after-blink production [Berman et al., 2012]. Does inhibiting for longer periods result in a shorter after-blink latency from the inhibition offset? We used linear regressions to relate the duration of inhibition and the timing of the after-blink. We found the mean slope of this relationship to be -0.0820 (for inhibition durations and blink timings measured in seconds), but not significantly different from 0 (p = 0.337 $>$ 0.05, two-tailed one-sample t-test, t = -0.994, n=15).

3.3.4 The impact of the inhibition beyond the after blink

To address whether the impact of inhibition spilled beyond the after blink we quantified the inter-blink interval (IBI) before inhibition and compared it to the interval after inhibition. The former was estimated by using the total number of blinks in the two seconds prior to the inhibition periods. The latter was estimated by the latency

of the second blink post-inhibition from the first one. The mean of median differences between these parameters (pre IBI – post IBI) was significantly above zero (1415 ms, $p<0.05$, one-sample t-test, $n=15$). Simply put, a period inhibition not only generated an after blink but also subsequently introduced a different blinking behavior.

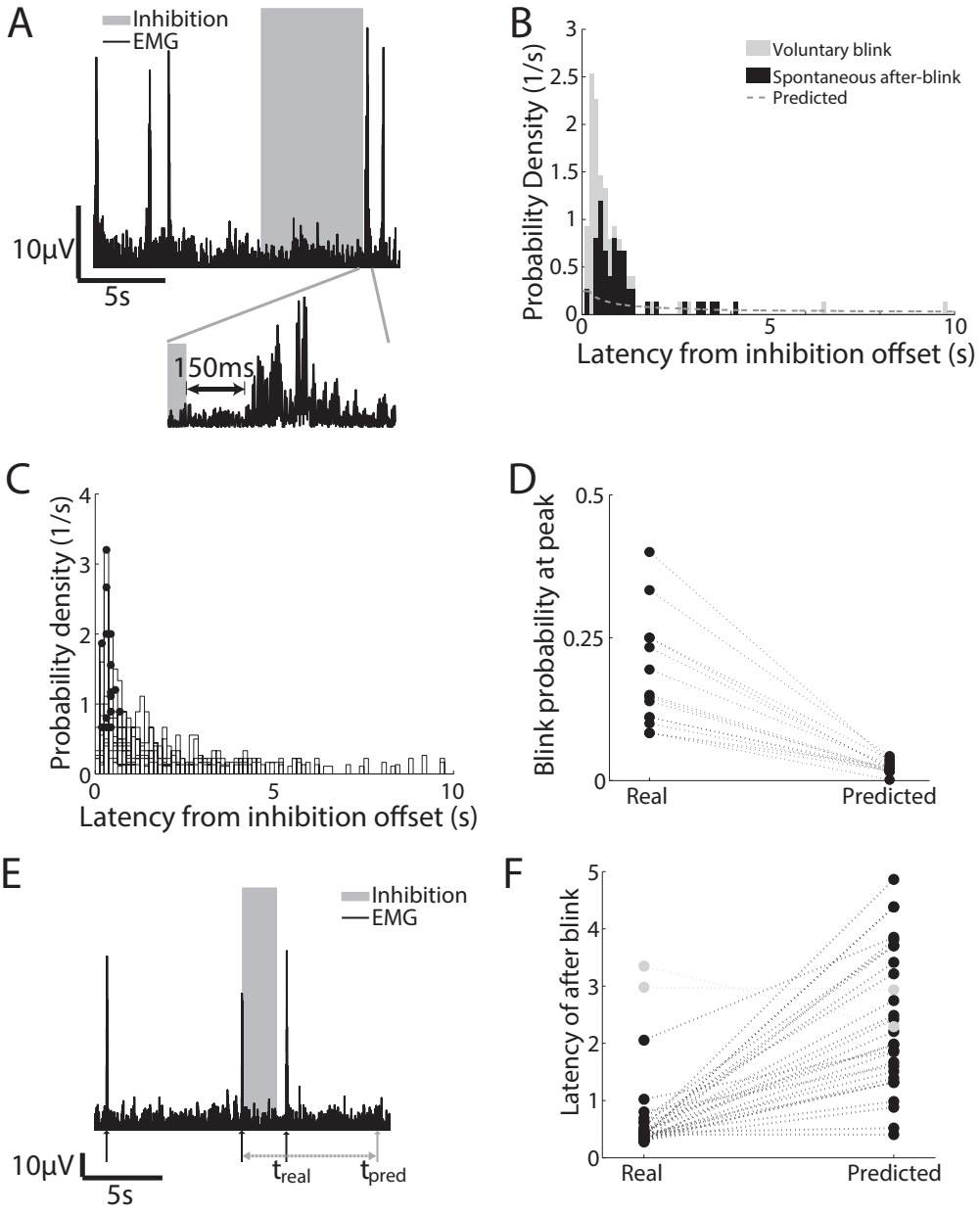

Fig. 3.3: ***Empirical investigation of the period post inhibition.*** *(A) An example of the EMG data, showing three blinks followed by a period of voluntary inhibition and then followed by two blinks. The insert shows the after-blink's EMG signal in detail and illustrates its latency from the offset of inhibition. (B) Histograms depicting the relative frequency of after-blink events across different latencies in a representative subject. Grey bars are for the voluntary blinks elicited post inhibition offset. Black bars are for the after-blinks elicited post inhibition offset. Bins are 125 ms wide. The dashed line depicts the probability distribution of after-blinks, based on the distribution of IBIs measured during the experiment.*

Fig. 3.3: *(continued)(C) Histograms of probability densities derived from relative frequencies of after-blink events across different latencies for each subject. The black dots depict the peak relative frequency of each subject. (D) Comparison of real probability of after-blink at peak time bin, versus probability of blinking in this same bin as predicted by IBI. (E) Example of a trial of minimum inhibition duration. Here, the timing of the after-blink is predicted based on the expected IBI and the timing of the last pre-inhibition blink. (F) Real latencies of after-blinks versus predicted ones for minimum inhibition periods, for all relevant trials. Predictions were based on expected value of IBI and last blink pre inhibition. Grey are the trials where the predicted latency was shorter than the real one. This result suggests that the blink generator is nudged into an off state also by very short periods of inhibition, and then it restarts upon withdrawal of inhibition.*

3.3.5 Architecture and behavior of the neuronal model

A neuronal architecture consisting of seven firing-rate-based neurons were used to model the key features of the inhibition of spontaneous blinking. A key component of the model was the oscillator that produced excitatory motor outputs for blinks (Figure 3.4 A). This was achieved by coupling an excitatory neuron (G) with an inhibitory neuron (C). The oscillator was sustained by a constant source of excitation (S). Therefore, C, G and S, all operated to produce oscillations in G's membrane potential and generated rhythmic outputs from G. An additional connection between S and C was mediated via an inhibitory interneuron (CI), and this allowed the same oscillator to produce different frequencies in response to changes in S.

The source of excitation (S) was sensitive to a range of factors including the voluntary commands responsible for blink inhibition (V). But, in the default state the spontaneous oscillation was sustained by constant current input to S by excitatory drive from a neuron (D). For inhibition, the voluntary commands reached the oscillator's excitatory neuron via an inhibitor neuron (I). Due to simultaneous impact of V on S and G (via I), the oscillator achieved a step-like behavior in response to the inputs from V, and when V ceased, G was equipped to rebound.

When simulated, this network reproduced several of our experimental observations. First, the network spontaneously produced rhythmic outputs with a constant frequency. Second and importantly, activation of neuron V, akin to voluntary commands, nudged the oscillator to an off state. And the withdrawal of inhibition resulted in a new sequence of blinks, with a time-locked after blink. Third, the latency of the after blink was independent from the duration of inhibition (Figure 3.4 C). Finally, the blink rate after withdrawal also increased by a constant value in comparison to the pre-inhibition levels only to transiently return pre-inhibition values (Figure 3.4 D). Notably, the transient relaxation was due to the damping effect introduced by the self-excitation term of the driving integrator S.

In sum, we used a neuronal architecture that allowed neuronal outputs akin to voluntary commands to directly drive the inhibitory neuron associated with the oscillator and in parallel excited an integrator also wired to the oscillator. This architecture allowed the voluntary outputs for inhibition to nudge of the network in to an off state.

3.3.6 The impact of a voluntary blink on the timing of the spontaneous after-blink

The "must" condition was originally designed to test the ability to voluntarily blink in the time between inhibition and the after-blink (see subsection 3.3.2). Nevertheless, we could additionally use it to address the impact of the voluntary blink

on spontaneous blink generation by measuring the timing of the first spontaneous after-blink in the "must" and "relax" conditions. One possibility was that the first spontaneous blink would remain uninfluenced by the presence of a voluntary blink. I.e., in the "must" condition, the latency of the first spontaneous blink from inhibition offset, $\Delta t^{must}_{sp_1 inh}$, would be the same as in the "relax" condition, $\Delta t^{relax}_{sp_1 inh}$. Instead, we found that the first spontaneous blink in the "must" condition occurred later than in the "relax" condition ($mean\left(mean\left(\Delta t^{must}_{sp_1 inh}\right)\right) = 4713\,ms$, $mean\left(mean\left(\Delta t^{relax}_{sp_1 inh}\right)\right) = 3317\,ms$, $p = 4.5 \cdot 10^{-4} < 0.05$, two-tailed paired-sample t-test, t = -4.55, n=15) (Figure 3.5 C and E).

To explain this difference between "must" and "relax" conditions in the distributions of first spontaneous blinks we formulated two testable ad-hoc explanations: (a) the voluntary excitation in the "must" condition merely added to the voluntary control processes used to inhibit blinks. If that were the case, the difference in the latency of the first spontaneous blink relative to the offset of inhibition between the two conditions would be due to the delay in restarting the spontaneous blinking sequence introduced by the extension of volition. That is, the latency of the after-blink from the inhibition offset in the "relax" condition would be analogous to the latency of the first spontaneous blink from the voluntary blink in the "must" condition. Alternatively, (b) the voluntary blink in the "must" condition was the initiator of the blinking sequence, similarly to the spontaneous after-blink in the "relax" condition. In this case, the latency of the second blink from the first blink – voluntary or otherwise – would be the same between the two conditions.

To test explanation "a", we compared the latencies of the first spontaneous from the voluntary blinks in the "must" condition, $\Delta t^{must}_{sp_1\, vol}$, with the latencies of the after-blinks from the inhibition offsets in the "relax" condition, $\Delta t^{relax}_{sp_1\, vol}$. We found their means to be significantly different ($mean\left(mean\left(\Delta t^{relax}_{sp_1 inh}\right)\right) = 3182\,ms$, $mean\left(mean\left(\Delta t^{must}_{sp_1 vol}\right)\right) = 2481\,ms$, p = 0.0255 < 0.05, two-tailed paired-sample t test, t = -2.500, n=15). We suggest that spontaneous after-blink latencies from the preceding voluntary processes in the two conditions were not the same; in turn suggesting that the voluntary excitation was not a mere extension of the proceeding voluntary process. As the measures of the offset of inhibition (tone offset vs voluntary blink) as well as the sign of the last part of the voluntary process were different between the two conditions (inhibition vs excitation), we make this suggestion cautiously. To test the alternative explanation (b) we compared the latency of the first spontaneous from the voluntary blinks in the "must" condition, $\Delta t^{must}_{sp_1\, vol}$, with the latencies of the second blinks from the after-blinks in the "relax" condition, $\Delta t^{must}_{sp_2\, sp_1}$. We did not find their means to be significantly different ($mean\left(mean\left(\Delta t^{must}_{sp_1 vol}\right)\right) = 2481\,ms$, $mean\left(mean\left(\Delta t^{relax}_{sp_2 sp_1}\right)\right) = 2750\,ms$

p=0.3033>0.05, two-tailed two-sample t test, t=-1.0717, n=15) (Figure 3.5 D and F).

Although our data did not allow us to confidently favour one explanation over another, the lack of difference in the post-inhibition inter-blink temporal relation (tested for explanation (b)) suggested that the voluntary blink post-inhibition (in the "must" condition) initiated spontaneous blinking just as the first spontaneous after-blink did (in the "relax" condition).

In summary, our data strongly suggested that voluntary inhibition of spontaneous blinking involves switching the central blink generator off and we did see signs of the generator being influenced by voluntary excitatory commands as well.

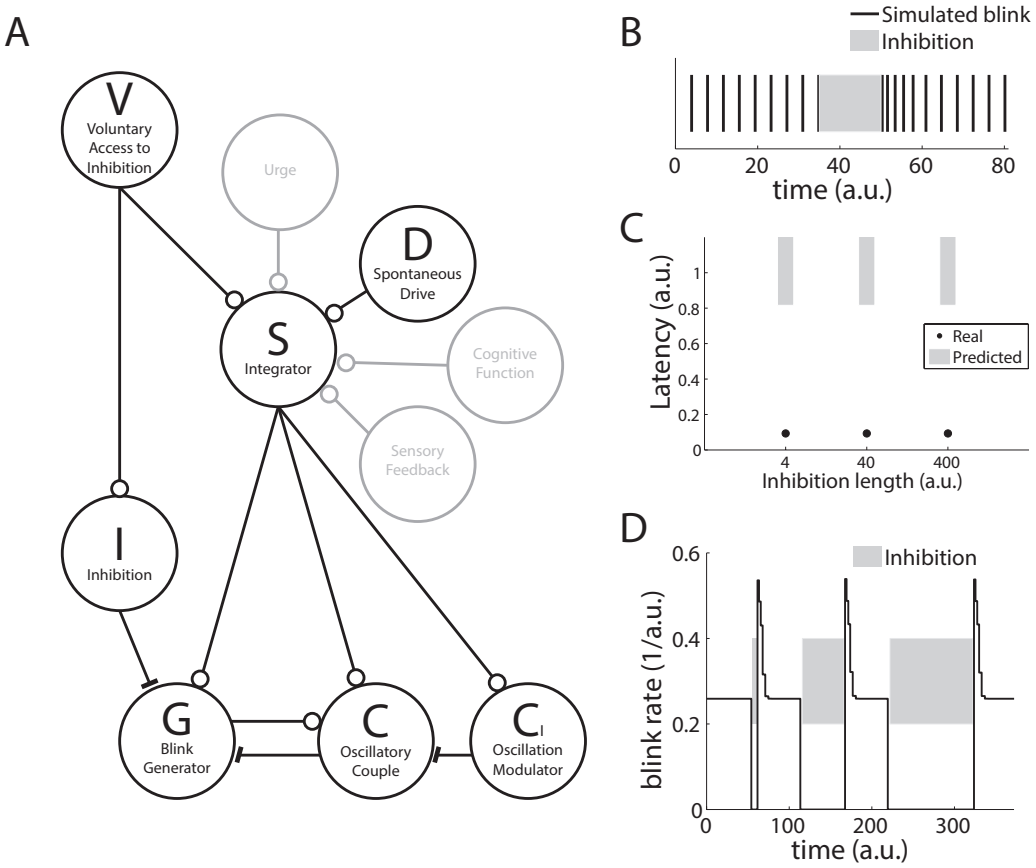

Fig. 3.4: ***Neural network simulation addressing the voluntary inhibition of spontaneous blinks.*** *(A) A neuronal model of a spontaneous blink generator that can be inhibited using motor commands akin to the voluntary outputs. It consists of seven firing-rate-based neurons. The network's output unit is an excitatory neuron (G). G is driven by the continuous input from another excitatory neuron (S) and by the inhibitory feedback from a coupled inhibitory neuron (C). This system produces oscillations in G's membrane potential and therefore in the network's output firing rate. The oscillation is sustained by driving input, which is provided by S. Oscillation frequency depends on S's input current to the oscillator's components G and C. An additional connection between S and C is mediated via an inhibitory interneuron CI to modulate this current. Spontaneous oscillation is sustained by constant current input to S by excitatory drive from neuron D. G receives a connection from inhibitory neuron I. When I is active, excitatory inputs to G are balanced by I's inhibition, and G's output is prevented. I is accessed and activated by an excitatory neuron (V). V also provides input to S, so the activation of I's inhibition on G is coupled with an influence on the oscillator's frequency. S receives self-excitatory feedback J, which delays its relaxation after withdrawal of inhibition. (B) A sequence of blinks interrupted by inhibition, and rebounded, as produced by a simulation of our model. Time is given in arbitrary units. (C) Latency of after blinkafter-blink from offset of inhibition for various inhibition lengths. In grey is shown the lower part of the range of latencies within two standard deviations, predicted by the IBI. In black is shown the actual latency as produced by our simulations, which is time-locked on the offset of inhibition. Time is in arbitrary units. (D) The rate of simulated blinks which are interrupted by three inhibition periods of different durations. Each inhibition period is followed by a blink rate increased by a constant that is independent from the duration of inhibition. Blink rate transiently relaxes to pre-inhibition levels.*

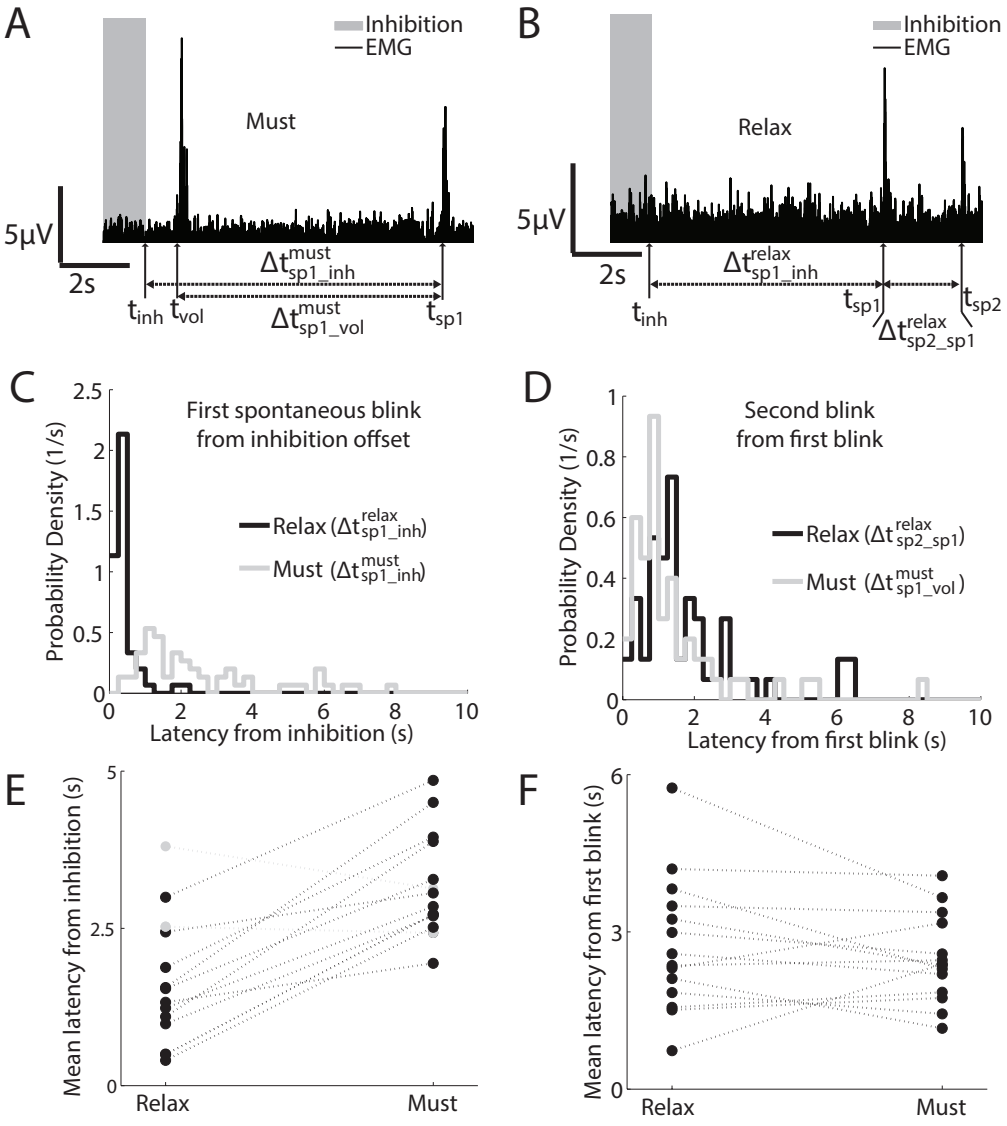

Fig. 3.5: ***Impact of voluntary blinks on the spontaneous after-blinks.*** *(A) EMG recording from a post-inhibition period in the "must" condition. Inhibition ended at time t_{inh}. The voluntary blink occurred at time t_{vol}. The first spontaneous blink occurred at time $t_{sp_1} = t_{inh} + \Delta t^{must}_{sp_1\,inh} = t_{vol} + \Delta t^{must}_{sp_1}$. (B) EMG recording from a post-inhibition period in the "relax" condition. Inhibition ended at time t_{inh}. The after-blink (first spontaneous blink) occurred at time t_{sp_1}. The second spontaneous blink occurred at time $t_{sp_2} = t_{inh} + \Delta t^{relax}_{sp_2\,inh} = t_{sp_1} + \Delta t^{relax}_{sp_2\,sp_1}$. (C) Probability density distribution of the latency of the first spontaneous blink from the offset of inhibition in the "must" condition ($\Delta t^{must}_{sp_1\,inh}$; grey) and in the "relax" condition ($\Delta t^{relax}_{sp_1\,inh}$; black) in a representative subject. The delayed occurrence of the first blink in the must condition with respect to the offset of inhibition is apparent, as well as the qualitative difference between the two distributions. (D) Probability density distributions of the interval between the two first blinks post inhibition in a representative subject. Grey: between first spontaneous blink and voluntary blink in the "must" condition ($\Delta t^{must}_{sp_1\,vol}$). Black: between second spontaneous blink and first spontaneous blink in the "relax" condition ($\Delta t^{relax}_{sp_2\,sp_1}$). The similarity between the two distributions is evident. (E) Visualization of the means of the two probability distributions depicted in C, for all subjects. The delay in the "must" condition is consistent across most subjects (grey are the inconsistent with the trend subjects). (F) Visualization of the means of the two probability distributions depicted in D, for all subjects. The lack of consistent difference is obvious.*

3.4 Discussion

Previous measurements on voluntary (externally-triggered) inhibition mainly focused on the preparation and execution stages of the movement (for review see: [Filevich et al., 2012b]). In this study we focused on the interval after the voluntary inhibition of spontaneous blinking. Volunteers withdrew voluntary inhibition at the offset of a sound tone that was played for an unpredictable duration. While they were able to successfully inhibit their blinks, the offset of the inhibition was accompanied by an after-blink. The after-blink was time-locked to the inhibition offset. This suggests that voluntary commands countermanded spontaneous blinks by turning off the central generator and the generator rebooted upon the withdrawal of voluntary inhibition.

It must be noted here that our usage of the term voluntary is perhaps more in line with the motor control framework – i.e. a cortical control mechanism distinct from reflexive or spontaneous (pattern generator like) controller – than the idea of intentional action control set forth in cognitive neuroscience. Simply put, the inhibitory motor commands would have been more endogenous if the volunteers inhibited spontaneous blinks by choice rather than in response to an external trigger as in this study. However, given the considerable overlap between the mechanisms for external-trigger-induced inhibition and intentional inhibition it is likely that the mechanism implied here is shared by both forms of inhibition [Filevich et al., 2012a, Swick et al., 2011].

A core assumption in this study was that an endogenous blink generator exists. While this is widely considered to be the case, the location and neuronal description of this generator remains elusive [Doughty, 2001, Karson, 1983, Mackintosh et al., 1983]. Alternatively, spontaneous blinks may reflect the corneal inputs that report on the tear film. In this case, there may be an entirely different account for the after-blinks. In face of such hypothetical sensory dominance, successful inhibition reflected the voluntary suppression of the peripheral inputs. Essentially, when inhibition was withdrawn the circuit regained its responsiveness to the corneal changes. However, we do not believe this to be the case as after-blinks occurred even for short periods of inhibition that would not alter the corneal sensory inputs. Our findings are compatible with the idea that spontaneous blinks are centrally generated under the influence of several factors including peripheral inputs and volition.

Our data on the after-blink post-inhibition of spontaneous blinking suggest that the blink generator rebounded after a period of inhibition. The idea of such post-inhibition rebound is not new for neuronal systems. For instance, the neurons responsible for saccadic eye movements burst at high rates when released from inhibition [?]. Our results suggest that post-inhibition rebound also applies for voluntary inhibition

at least when an endogenous pattern generator is involved.

Previous experiments suggested that there is a build-up of urge when inhibiting spontaneous blinks [Berman et al., 2012]. These results indicated a form of neuronal activity that is proportional to the duration of inhibition. Intuitively, the longer the inhibition lasts the more the urge increases. We hypothesized that the outputs of the blink generator post-inhibition were also responsive to inhibition duration. However, this was not found. Taken together with the previous report on urge build-up the blink generator is not responsive to the extent of the neuronal activity built up during inhibition.

We constructed a model of the voluntary-involuntary interactions by using a small number of neurons. The formulation of these neurons was biologically inspired. For instance, at the core of the model was an oscillator that essentially consisted of an excitatory-inhibitory couple. Such excitatory-inhibitory interactions are frequently observed in the brain [Donner and Siegel, 2011, Wilson and Cowan, 1972]. It must be noted here that inhibitory neurons alone may result in network oscillations. Notably, the excitatory neuron in our model enabled the network to discharge motor outputs. Here the key enabler of inhibition was an excitatory voluntary motor command. While part of this excitation was wired to an inhibitory inter-neuron of the oscillator, the rest excited a separate neuron that excited the oscillator. Our empirical results on the after blinks post voluntary inhibition could be reproduced by allowing the two voluntary influences to operate at different time constants. Obviously, a much larger number of neurons may be involved in the voluntary-involuntary interaction in reality. However, our simulations demonstrate that such interactions may be possible via strategic connectivity that allows voluntary commands to act both on the inhibitory interneuron wired to the blink generator and on the factors that provide the generator with excitation.

Interestingly, the spontaneous after-blinks were slower than the voluntary blinks generated upon the withdrawal of inhibition. We believe that the latency of the spontaneous after-blink reflected the time taken for blink generator to reboot post inhibition. There are two distinct lines of untested explanations as to why the voluntary blinks were faster. First, the voluntary excitatory commands may have employed the spontaneous blink circuit to produce a blink and the commands may have hastened the generator's reboot time. Second, the voluntary blinks may bypass the spontaneous blink generator to produce the movement and the latency reflected the reaction time of that pathway. The latter implies that the voluntary and spontaneous blink pathways are largely distinct. This may indeed be the case as voluntary and spontaneous blinks are associated with distinct neuronal signatures, EMG, and kinematic patterns [Bodis-Wollner et al., 1999, Evinger et al., 1991]. Furthermore, patients with Parkinson's disease show rather distinct influences on voluntary vs.

spontaneous blinks [Agostino et al., 2008].

We also addressed a complex form of voluntary inhibition – excitation – spontaneous blink interaction, by observing the consequences of inserting a voluntary blink post-inhibition. The main result was that the first spontaneous blink post inhibition occurred at a longer latency from inhibition with the voluntary insertion than without. Although this reflects on a form of voluntary-spontaneous movement interaction, it was unclear as to why this delay occurred. A more in-depth analysis revealed that the time elapsed between the voluntary blink and the subsequent spontaneous blink was indistinguishable from the inter-blink period between the first two spontaneous blinks in the relaxed condition. It is tempting to suggest that post inhibition and after the first blink, the blink generator timed its outputs according to the most recent blink – irrespective of the exact nature of the blink (spontaneous vs. voluntary).

The mechanisms for the voluntary suppression of inhibitory blinks implied here may also apply to other forms of blink suppression. It is well known that the rate of spontaneous blinking is reduced by various factors including the load of cognitive processing. The offset of such inhibition has been previously associated with an increase in the blink rate [Fukuda, 1994]. Such behavior suggests that the cognitive processing directly perturbs the blink generator akin to the action of voluntary commands.

A major challenge to the study of voluntary inhibition is the absence of a read-out to confirm the implementation of inhibition. The voluntary inhibition of spontaneous blinking was empirically verifiable and by focusing on the period post-inhibition we were able to draw important mechanistic insights for inhibitory motor control. Our experiments suggest that voluntary inhibition is implemented by perturbing the source of involuntary movements i.e., the spontaneous blink generator. The direct access of volition to the blink generator may provide the higher areas with an effective instrument to take control of the involuntary movement.

An interesting line of thought is triggered by the questions why and how the motor system chooses or is led to the specific implementation of voluntary inhibition on automatic movements such as eye blinks, among the alternatives. The choice may be made based on how effectively the possible mechanisms can enforce the inhibitory control, and how economical they are in terms of energy consumption. The hypothesis supported by our results is both an effective and an economical choice. The action of voluntary inhibition directly on the source of blinks, i.e. their generator, prevents the motor system from generating any motor outputs at all. This may be more effective than attempting to negate motor outputs that have already been generated. Furthermore, the direct prevention of any energy-consuming motor outputs from the generator is a more economical strategy than an *a posteriori*

negation of the blink motor outputs. The specific strategy of stopping and resetting the blink generator further contributes to the economy of the system as it does not require keeping a working copy of the state of the generator in memory, as opposed to a hypothetical alternative strategy through pausing the generator.

The "stop and reset" strategy of voluntary inhibition may be the result of evolutionary processes. Alternatively, or additionally, the sensory-motor system may achieve this effective and economical strategy through learning during development, within the "reflex-tutored" framework that was presented in chapter 2. Automatic generation of blinks presumably precedes its inhibition in developmental terms. In addition, sensory inputs from automatic blinks, including not only proprioception from the eyelids but also visual changes, may be available to the cognitive areas of the brain. As shown in chapter 2, these two ingredients, namely the developmental precedence of automatic movements and the sensory link, can enable the cognitive controller to learn more effectively to control the body. Therefore, the experimental results reported in the present chapter may as well be an outcome of a reflex-tutored voluntary inhibition of eye blinks.

In fact, such a learning and developmental process in the controller of voluntary inhibition may be assisted by the automatic movements. In chapter 2 we demonstrated that automatic movements may provide tutoring to a cognitive controller for more effective learning and control, as long as sensory consequences of the automatic movements reach the cognitive controller. Sensory inputs from automatic blinks, include not only proprioceptive information from the eyelids, but also visual changes which could further enhance the sensory representation of the movement that voluntary inhibition learns to control.

Chapter 4

Voluntary-involuntary movement cascade: eye-blinks resulting from voluntary finger reactions

Disclaimer

The experiment was designed by Arko Ghosh. Experimentation and data acquisition were performed with Myriam Balerna and Magali Chytiris.

4.1 Introduction

Behaviour of moving organisms is composed by combinations and sequences of motor outputs of multiple motor controllers. Shared resources between the controllers allow in many cases one controller to influence when a second controller triggers a movement. To explore the extent and generality of this type of link in the sensory-motor system, in this chapter we test a pair of controllers that are largely unrelated to each other, not least because the one is involuntary whereas the second involuntary.

The known reasons why a controller may affect the trigger of an other one have not been previously categorized, but there are essentially three known types of such links. Firstly, a motor controller can be triggered by another when it acts as the target or intermediary of the latter controller's motor commands. This is the expression of various types of functional hierarchy between components of the motor system, and between tasks and subtasks that they control [Adams et al., 2013, Uithol et al., 2012]. Interestingly, not only targeted excitation, but also the withdrawal of inhibition in such a hierarchically related pair of controllers may result in triggering the hierarchically lower counterpart of the pair [Moraitis and Ghosh, 2014] (see chapter 3). Secondly, a motor controller can be triggered indirectly by a change in

its environmental or sensory context caused by a different controller. This could be a planned sequence, such as grasping a key and then unlocking a door, or unplanned, such as mis-typing a letter and then deleting it. Thirdly, the motor system enables certain motor controllers to determine the timing of the outputs of others that operate concurrently. Specifically, between-task interference with effects on the time at which motor outputs are produced has been evidenced as a delay in the reaction to a stimulus when a subject focuses on a primary task to react on a different stimulus. This delay has been dubbed the "psychological refractory period" (PRP) [Pashler, 1994]. Currently, there are two candidate theoretical models that suggest a cause for PRP effects [Pashler, 1994, Fischer and Plessow, 2015, Marti et al., 2015]. The serial processing model suggests that access to computational resources is performed serially, due to a central bottleneck that processes only one task at a time [Pashler and Johnston, 1989, Sigman and Dehaene, 2005]. The resource sharing model suggests that the processing mechanism can handle multiple tasks simultaneously, but the shared computational resources are limited [Kahneman, 1973, Tombu and Jolicœur, 2003]. Both models therefore attribute this corollary effect to competition between the controllers.

PRP effects are very widespread [Marti et al., 2015] in pairs of reaction tasks. It has been reported that some pairs of tasks may not interfere with each other under certain conditions [Greenwald and Shulman, 1973, Hazeltine et al., 2002, Schumacher et al., 2001, Yamaguchi et al., 2012]. However, many of these negative results have been contradicted or unsuccessfully replicated [Levy and Pashler, 2001, Lien and Proctor, 2002, Shin et al., 2007, Tombu and Jolicoeur, 2004]. The astounding ubiquity of between-controller trigger-influencing links presents the possibility that all concurrent controllers in the human sensory-motor system are inherently coupled in this respect. In attempting to falsify this hypothesis, pairs of controllers that are minimally related are good candidates for experimental paradigms. Involuntary controllers of reflexive and spontaneous movements have traditionally been studied separately from those of voluntary movements, even though potential interactions between the two classes of controllers could be revealing of general principles of interactions within the motor system. It is possible that the autonomous function of some involuntary controllers allows them to escape the interference with their trigger from concurrently operating voluntary motor controllers.

Endogenous, involuntary eye blinks offer a convenient model for the empirical study of interactions between voluntary and involuntary motor controllers, by virtue of their relative simplicity and their frequent spontaneous generation, including in concurrence with voluntary movements. Periodical blinks continue to occur in the absence of sensory input from the eye [Nakamori et al., 1997], suggesting that they are governed by an internal rhythm generator [Kaminer et al., 2011]. Blinks can be

triggered at will, and voluntary inhibition of spontaneous blinks triggers a blink after inhibition [Moraitis and Ghosh, 2014] (see chapter 3).

Whereas only few effects from voluntary motor control on the blink generator are known, blinking is subject to sensory and cognitive sources of influence. The rate of rhythmic blink generation is influenced by peripheral factors such as corneal anaesthesia, dry eyes, and damage to the ocular surface [Nakamori et al., 1997], as well as by intrinsic factors such as Parkinson's disease [Biousse et al., 2004], schizophrenia [Karson et al., 1990, Mackert et al., 1991] and related medications [Biousse et al., 2004, Karson, 1983, Mackert et al., 1990, 1991]. Cognitive tasks also influence the blink generator. The blink rate increases with increasing cognitive task difficulty [Drew, 1951], while individual blink timing has been found to coincide with salient events of cognitive tasks, such as punctuation points when reading text [Orchard and Stern, 1991], sounds in an auditory discrimination task [Goldstein et al., 1985], and scene breaks in movies [Nakano et al., 2009]. Finally, blinks can be generated reflexively in response to abrupt intense light or sound, and to somatosensory stimulation.

Despite the known array of influences on blink timing, it is still unclear whether the timing of individual blinks depends on concurrent unrelated actions. Here we measured the timing of eye blinks and of an action that was chosen to make the pair largely unrelated. Mouse-click reactions with the finger to mechanical stimulation of the fingertip were used. The lack of relation lies in the separation of voluntary vs involuntary control, finger vs eye sensory-motor control, and endogenous vs reactive movement.

4.2 Methods

4.2.1 Experimental setup

During the experiment, volunteers were seated on an armchair, looking at a screen placed high in the visual field in front of them showing a silent nature documentary. We amplified and recorded at a 2000 Hz sampling rate the electromyographical (EMG) activity of the orbicularis oculi, i.e. a key muscle participating in the control of the eyelid during blinking (Figure 4.1, top left). In addition we provided tactile stimulation to the fingertip of the subjects' right index. The stimuli were mechanical and were provided instantaneously (stim duration?) 400 times in random intervals of 1.5 to 2.5 seconds by a magnetic mechanical tapper on which the finger was resting (Figure 4.1, middle left). The stimulus was strong enough to be easily detectable by the subjects. Subjects wore earbuds playing white noise at a level that covered environmental sounds. The tapper was attached to the left button of a computer mouse, so that pressing the tapper with the finger and releasing it would result in a mouse click (Figure 4.1, bottom left). The mouse output was recorded as well. The

Fig. 4.1: ***The experiment.*** *We recorded the electromyographical (EMG) activity around the eye of volunteers (left, top). Subjects received a tactile stimulus to the fingertip in random intervals (left, middle). They were instructed to immediately react to stimuli by clicking a mouse button on which their finger was resting (left, bottom). From the EMG activity, eye blink timings were detected, and recorded along with stimulus, and button press and release timings (right).*

subjects' hands were resting with the computer mouse and the attached tapper on a light board on their lap. The experiment was performed in two different conditions for each subject. In the experimental ("task") condition, subjects were instructed to click as soon as possible each time a stimulus was provided to their fingertip. In the control condition ("rest"), subjects were instructed to relax.

4.2.2 Data analysis

By band-pass filtering and thresholding the EMG signal we detected blinks and registered their onset's timing. Mouse button presses and releases were also timed through the recorded mouse output. The timing of provided stimuli was recorded as well. (Figure 4.1, right). From 71 participants, data from 44 subjects were used for the analysis, after excluding noisy EMG recordings and rarely-blinking participants (average inter-blink interval at rest of more than 15 seconds).

For each blink that occurred first after a stimulus, its onset's latency from the last stimulus was computed. The distribution of stimulus-to-blink latencies was characterized and compared between the task and rest conditions.

Furthermore, each subject's distribution of inter-blink intervals and of inter-stimulus intervals were obtained from the timestamps of the events. Based on these two distributions, a prediction for the stimulus-to-blink latency distribution was produced. The predicted distribution was statistically compared to the actual one in

both the rest and the task condition, through the Kolmogorov-Smirnov test. Finally, the distribution of stimulus-to-blink latencies was compared with the distribution of click durations in terms of its skewness, measured through the Fisher-Pearson skewness coefficient, adjusted for sample size.

4.3 The reaction task influences blink timing.

To explore the effect of the mouse-click reaction task on the timing of blinks, we measured how soon after tactile stimuli blinks occurred in the task and the rest condition. The distribution of stimulus-to-blink latency visibly changes with the introduction of the reaction task (Figure 4.2 A vs B, grey histogram). In particular, in 40 of the 44 analysed subjects, we found the peak of the distribution to increase, indicating that blinks became more likely to consistently occur at a particular latency after the stimulus. As a consequence, at the group level, the average change of the maximum of the stimulus-to-blink latency distribution, after the introduction of the reaction task is positive and significant (t test, $p = 1.1 \cdot 10^{-5}$) (Figure 4.2 C). Therefore, the timing of the endogenous blink generator changes by the introduction of the voluntary mouse click reaction task. In addition, the probability of blinking immediately after the stimulus is very low, or zero in the condition where the reaction task is performed (Figure 4.2 B). This suggests that blinks may be inhibited prior to the execution of the reaction.

4.4 The effect is on individual blink timing.

The apparent consistency of the first post-stimulus blink's timing with respect to the stimulus in the task condition may be a consequence of a change in the distribution of inter-blink intervals, such as a change in the mean blink rate. In this case, the distribution of stimulus-to-blink intervals would be accounted for by the combined distributions of inter-blink and inter-stimulus intervals. Alternatively, it may be a direct influence on individual blink timing from the reaction task. In this case the inter-blink and inter-stimulus intervals will not suffice to explain the distribution of individually determined stimulus-to-blink intervals.

To explore whether the observed effect is on individual blink timings are or on their distribution, we computed the theoretical distribution of stimulus-to-blink latencies based on inter-blink and inter-stimulus interval distributions, assuming that individual blinks were randomly timed according to the inter-blink interval distribution (see Methods section). In the rest condition we found the theoretical prediction to fit very well the experimentally obtained distribution, being insignificantly different from the actual distribution in 42 of the 44 subjects (KS-test, $p>0.5$). In the

task condition the actual distribution was significantly different from the theoretically predicted in each of all 44 subjects (KS-test, $p<0.02$; in 41 subjects, $p<0.001$). The differences in the goodness of the theoretical distribution's fit as expressed by the Kolmogorov-Smirnov distance is visible in Figure 2D. This result indicates that the stimulus-to-blink interval distribution in the task condition cannot anymore be explained by random selection from an inter-blink interval distribution, but rather each stimulus-to-blink interval is individually determined by the execution of the stimulus-click reaction task.

The combined results that (a) the reaction task makes blink timings more consistent with respect to the stimulus, and that (b) each blink is timed individually suggest that the reaction task introduces a trigger of an individual blink.

4.5 What is the trigger of blinks?

The operation of the cognitive mouse-clicking task causes the automatic blink decisions to be triggered by evidence originating from the clicking reaction task. Specifically, the decision to blink might be triggered by evidence from either the sensory or the motor component of the clicking task, i.e. the tactile stimulus, or the action of clicking the mouse. Alternatively, it is also possible that neither the sensory nor the motor component is exclusively providing evidence for the blinking decision, but rather that the stimulus-reaction pair as a whole is.

4.5.1 Comparison of dispersion of latency distributions

We tested the hypothesis that blinks are triggered by one of the two landmarks of the stimulus-click reaction task. In particular, we reasoned that blinks are triggered by the stimulus if the timing of a blink is independent of the timing of the click before it, but dependent on the timing of the stimulus. Or, equivalently, if the stimulus-blink latency is less dispersed than the click-blink latency. We compared the standard deviations of the two latency distributions (stimulus-blink and click-blink) and we found that there is no significant pairwise difference (two-tailed t-test). Therefore, the hypothesis that the trigger for blinks is either the stimulus or the click action could not be confirmed by this comparison.

4.5.2 Blinks analyzed as reactions

We used a second method, based on principles prevalent in the decision-making literature to reveal which component of the stimulus-click reaction task is the evidence for the blink decision process.

Decision time

For most types of reactions, the time from the presentation of a stimulus until the reaction is far longer than what axonal conduction and synaptic delays would predict, suggesting that reaction time is significantly accounted for by the time taken to form the decision to respond to the sensory stimulus. Thus, reaction time offers valuable proxy access to decision time. In turn, a direct link between decision time and a process of evidence accumulation that leads to a decision has been proposed and this model has been remarkably successful in explaining a wide array of experimental observations concerning decision-making.

LATER model

In reaction tasks, reaction times are variable between repetitions of the same stimulus-action pair, even under controlled conditions. The distribution of reaction times is positively skewed, i.e. there is higher probability for short reaction times than long ones. However, the reciprocal of reaction time is normally distributed, suggesting that the variability in observed reaction times is a consequence of a reaction rate that governs the underlying decision process and varies from trial to trial in a way randomly sampled from a normal distribution. This model is called the Linear Approach to Threshold with Ergodic Rate (LATER) model [Noorani and Carpenter, 2016] and has emerged from the study of saccadic eye movements [Carpenter, 1981, Gold and Shadlen, 2007].

If a LATER decision model underlies the trigger-blink latency distribution, it is meaningful to compare the dispersion of the *reciprocal* stimulus-blink and click-blink latencies. So, we first looked for evidence that blink decisions are taken by a LATER decision-maker. We found that distributions of blink latencies (either with respect to the stimulus or with respect to the click), are positively skewed. Secondly, we found latency reciprocals in each subject to be sampled from quasi-normal distributions. Based on this, it is plausible that the variability in blink latencies is an expression of the variability in the rates of two processes of linear approach to threshold, and hence it is sensible to compare the reciprocal stimulus-blink and click-blink latencies.

Comparison of dispersion of reciprocal latency distributions

The fact that stimulus-blink latencies are longer than click-blink latencies applies a downward pressure on the reciprocal of stimulus-blink latencies and hence on its dispersion, relative to click-blink latencies. We reason that if despite this the reciprocal click-blink latency is less dispersed than the reciprocal stimulus-blink latency, then blinks are triggered by evidence originating from the clicks rather than the stimuli.

Through pairwise comparison of the standard deviations of reciprocal stimulus-blink and click-blink latencies we find standard deviations of reciprocal click-blink latencies to not be smaller than reciprocal stimulus-blink latencies. In fact, they were found to be significantly larger (t-test, p=0.008). Therefore, the hypothesis that blinks are triggered by clicks could not be confirmed.

Note that this result does not confirm the hypothesis that blinks are triggered by clicks, but it does not reject it either. The reason why the standard deviation of the reciprocal of stimulus-blink latency is smaller than the standard deviation of reciprocal click-blink latency is possibly that stimulus-blink latency is longer than click-blink latency, and latency is inversely related to the standard deviation of its reciprocal.

4.5.3 Comparison of measured to predicted dispersion of latency distribution

We ultimately used a third method to approach our aim to reveal which component of the stimulus-reaction task provides the relevant evidence to the blink decision-making process. We estimated what the dispersion of the stimulus-blink latency distribution would be (a) if blinks were triggered based exclusively on evidence from the mouse click, and (b) if blinks were triggered exclusively by evidence from the stimulus. The estimates were calculated based on the dispersion of the measured stimulus-click and click-blink latencies. We then compared the estimates to the dispersion of the measured blink latency.

If blinks triggered after a stimulus-click reaction were decided based on evidence from the mouse click and not from the stimulus, then the variance in the stimulus-blink latency would be due to the variances in both two constituent time intervals, i.e. stimulus-to-click and click-to-blink. We estimated how the standard deviations of stimulus-to-click and of click-to-blink latencies would propagate to the standard deviation of stimulus-to-blink latency if blink timings were produced by a click-triggered process. For this, the standard formula for propagation of uncertainty from the summands to the sum was used, assuming uncorrelated summands:

$$\delta SB^2_{click} = \delta SC^2_{measured} + \delta CB^2_{measured}, \tag{4.1}$$

where δ denotes the standard deviation.

On the other hand, if blinks were decided based on evidence from the stimulus, the variance of the stimulus-to-blink latency would be independent from the variance in click timing, and thus smaller than an estimate for the click-triggered case. We can predict exactly how much smaller the stimulus-blink latency variance would be in the stimulus-triggered blink scenario than in the blink-triggered scenario, as follows.

In the stimulus-triggered scenario, the variance in the click-blink latency would be due to the variances in both stimulus-click and click-blink latencies. In particular, because click-blink latency is the difference of stimulus-click from stimulus-blink latency, again based on propagation of uncertainty, we have:

$$\delta SC^2_{measured} = \delta SB^2_{stim} + \delta CB^2_{measured}, \tag{4.2}$$

or, equivalently,

$$\delta SB^2_{stim} = \delta CB^2_{measured} - \delta SC^2_{measured}. \tag{4.3}$$

We found the mean of the difference between the measured and the estimated value of the square of the standard deviation not to differ significantly from zero. So, the hypothesis that blinks decisions are click-based could not be rejected.

If blink decisions were click-based, then the standard deviation of the square of the measured stimulus-blink latency should be equal to the estimate from equation 4.1. Therefore,

$$\begin{aligned} \delta SB^2_{measured} = \delta SB^2_{click} &= \delta SC^2_{measured} + \delta CB^2_{measured} \\ &= \delta CB^2_{measured} - \delta SC^2_{measured} + 2 \cdot \delta SC^2_{measured}. \end{aligned} \tag{4.4}$$

So, using equation 4.3,

$$\delta SB^2_{measured} = \delta SB^2_{stim} + 2 \cdot \delta SC^2_{measured}. \tag{4.5}$$

Therefore, the difference between the two estimates of the squared standard deviation of stimulus-blink latency is

$$\delta SB^2_{click} - \delta SB^2_{stim} = 2 \cdot \delta SC^2_{measured} \tag{4.6}$$

.

We calculated the mean of the difference of the square of the standard deviation of the measured stimulus-click latency δSB^2 from each of its two estimates δSB^2_{click} and δSB^2_{stim} for all subjects and we found it not significantly different from zero. Therefore, neither the hypothesis that a blink decision is taken based on evidence accumulated from the mouse click, nor that it is based on evidence accumulated from the stimulus could be rejected.

Nevertheless, the difference between the two estimates $2 \cdot \delta SC^2_{measured}$ (from equation 4.6) is significantly different from zero, as expected from a square. This is significantly different from zero, therefore if the stimulus-triggered blink hypothesis is true, the squared standard deviation of the measured stimulus-blink latency must be significantly different from the estimate corresponding to the click-triggered

blink hypothesis, and vice versa. We compared the standard deviation of our measurements of stimulus-blink latency to both estimates and we didn't find it to be significantly different from either of them, rejecting both hypotheses.

We conclude that blinks are not triggered by evidence from either the sensory stimulus or the motor reaction exclusively.

4.6 Blinks are likely planned separately from clicks.

It is possible that the triggered blink in the "task" condition is part of a single motor plan that the brain initiates as a reaction to the stimulus, and that includes the mouse button press and release, and the blink in a single sequence. For this to be the case, a single sequencing process (Figure 4.3 A, process $P(\mu)$) must be triggered that determines the time intervals between mouse button press, mouse button release, and blink onset. In this case, and assuming that the mouse button press and release do belong to a single planned sequence, the distribution of the mouse button press-to-release intervals, i.e. the distribution of click durations (Figure 4.3, t_{12}), would be expected to be qualitatively similar to the distribution of mouse-button-press-to-blink intervals (Figure 4.3, t_{13}) as both distributions are determined by the same underlying process (Figure 4.3 A, green arrow). If the two distributions are qualitatively dissimilar, this would suggest that blink timings are determined by a separate process (Figure 4.3 A, $Q(\mu)$, red arrow).

By measuring the skewness coefficients we find that mouse duration distributions (Figure 4.3 B) are visibly qualitatively different from mouse-press-to-blink interval distributions (Figure 4.3 C). In particular, we find click-to-blink interval distributions to be positively skewed, significantly more than click duration distributions (t test, p=0.003, t=-3.1945) (Figure 4.3 D). So, assuming that the two movements pertaining to the mouse click, i.e. button press and release, do belong to a single planned sequence, this result suggests that blinks belong to a separate plan, planned and timed by a separate sequencing process.

4.7 Discussion

By measuring the timing of eye blinks of participants that reacted by clicking a mouse in response to fingertip stimulation, we found that the reaction task introduces a trigger of an individual blink, which is likely planned separately from the click.

Our results suggest that the blink is not part of a single unified click-and-blink reaction to the stimulus, but rather that the blink is triggered as a separate direct or indirect consequence of the stimulus-click reaction task. The triggered blink may be a consequence of the operation of cognitive processes engaged by the motor task, such

as detecting or attending to the stimulus, similar to how an auditory discrimination task increases the blinking probability after the task's execution [Goldstein et al., 1985]. Alternatively, the blink could be a consequence of the completion of the motor readiness to react to the stimulus. Our data is consistent with a period of inhibition of blinks before the triggered blink (Figure 4.2). It was recently reported that the motor system is inhibited in a broad manner during response preparation [Greenhouse et al., 2015], while in chapter 3 we found that inhibition of blinks causes an excitatory after-effect [Moraitis and Ghosh, 2014]. We propose that inhibition of eye blinks, introduced by the cognitive and motor processes that prepare the finger's reaction, is a plausible cause of the triggered after-blink.

The mechanism that leads to the triggered blink may alternatively be related to the specific type of reaction task employed in the experiment. Firstly, mouse clicks are most commonly produced in response to a visual stimulus provided by a computer screen. Therefore a learned association between the clicking movement and a blink that follows the computer-provided visual stimulus is possible, even though blinking during computer is very sparse [Blehm et al., 2005]. Secondly, the fact that in the experiment the motor reaction addresses the body part that also receives the stimulus, might lead to an amplification of the somatosensory blink reflex (SBR). Top-down amplification of the SBR has been previously described in the case of wrist nerve stimulation within the face's peripersonal space [Sambo et al., 2012].

Implications of the "triggerable blinks" finding

Our first result, i.e. that eye blinks are time-locked to the stimulus-click reaction task, indicates that even though the decision to blink in our experimental paradigm is endogenous to the nervous system, it is not spontaneous but rather triggered as a reaction to an event that is extraneous to the spontaneous, rhythmic blink-generating signal. This is a result with two principal implications, one regarding endogenous blinks specifically, and two concerning decision processes in general.

- ***Involuntary endogenous blinks can be non-spontaneous*** Firstly, it reaffirms that endogenous blinks cannot be considered synonymous to spontaneous blinks. This is in agreement with a long line of evidence prior to this work, which has shown that endogenous eye blink generation is far from being an isolated, self-contained process. Endogenous influences on blinking have been previously shown to be possible, expressed both as a modulation of the rate of the spontaneous rhythmic process and through directly, voluntarily triggering blinks, or as an excitatory after-effect following voluntary blink inhibition. However, no previous study had demonstrated blinks or any other endogenous movement to be triggered as a consequence of an unrelated motor task. Our

experimental paradigm revealed that a blink can be endogenously induced by the operation of a separate motor task.

- ***Actions can determine the relevant context for other decisions*** Secondly, this first result demonstrates that a mouse click in response to a tactile stimulus shifts the orientation of the blink decision-making process from the spontaneous signal that normally governs it, to a different, non-spontaneous signal. This suggests that one motor controller can cause a different controller to re-evaluate the relevance of available sources of information to its own decisions.

- ***Endogenous decisions can be action-triggered*** Furthermore, these suggest that one sensory-motor task can itself become a relevant source of evidence for an endogenous decision. The relevance of each source of evidence to a motor controller is dependent on context shaped by task instructions internal to the sensory-motor system that orient the controller to environmental cues and endogenous signals. Our result shows that the context for a decision can also be provided by concurrently operating tasks, and in the absence of voluntary instructions regarding what information is behaviourally relevant to the decision. This might be the expression of a mechanism that allows an urgent action to directly influence and align other decision processes to its own goals, without the need to access and engage the higher, conscious levels for this purpose.

Sensory vs motor triggering of eye blinks by mouse click reactions

Our results are a consequence of the addition of a motor reaction task (mouse click reaction) to the automatic sensory detection (conscious salient tactile stimulation), demonstrating the potential impact of the motor component of a sensory-motor task on other decisions, possibly through the cognitive processes it invokes. Therefore, the result that blinks are time-locked to the stimulus-click reaction task demonstrates that the operation of a motor task can influence another motor controller's decisions. Furthermore, the motor task does so by re-orienting the second controller to be receptive to signals generated or engaged by the sensory-motor task. Our data shows that the blink decision-triggering evidence was likely not of pure sensory or pure motor nature, hence the sensory-motor task possibly contributes to the blink triggering decision through both its sensory and its motor components. Alternatively, the blink may be triggered by the operation of internal cognitive processes engaged by the reaction task.

4.7.1 The possibility of hierarchical, cognitive-to-automatic effects

Our empirical observations do demonstrate that influences on the decision-making of endogenous motor controllers from unrelated controllers are possible, but they might be limited to influences from a cognitive, voluntary motor task onto an automatic movement. Voluntary controllers are high in the functional hierarchy of the sensory-motor system, and top-down influences in this hierarchy are not surprising. Nevertheless, the interactions we observed are between utterly disparate tasks that are in no apparent *de facto* functional hierarchical interdependence. Hence, if the effects we observed are due to the different degrees of cognition between the interacting decisions, they suggest the presence of a *de jure* hierarchy that governs the relationship between cognitive and automatic components of the sensory-motor system regardless of their functional relationship.

Our results demonstrate that an endogenous involuntary motor controller can be highly susceptible to a concurrently-operating voluntary one, up to the extent of being compelled to produce a movement when it would otherwise be silent. This implies that there are unknown mechanisms through which a motor controller influences the function and decision-making of concurrently-operating controllers. Further experimentation could reveal the extent to which the candidate underlying mechanisms proposed here enable interactions between voluntary and involuntary, or other pairs of motor controllers.

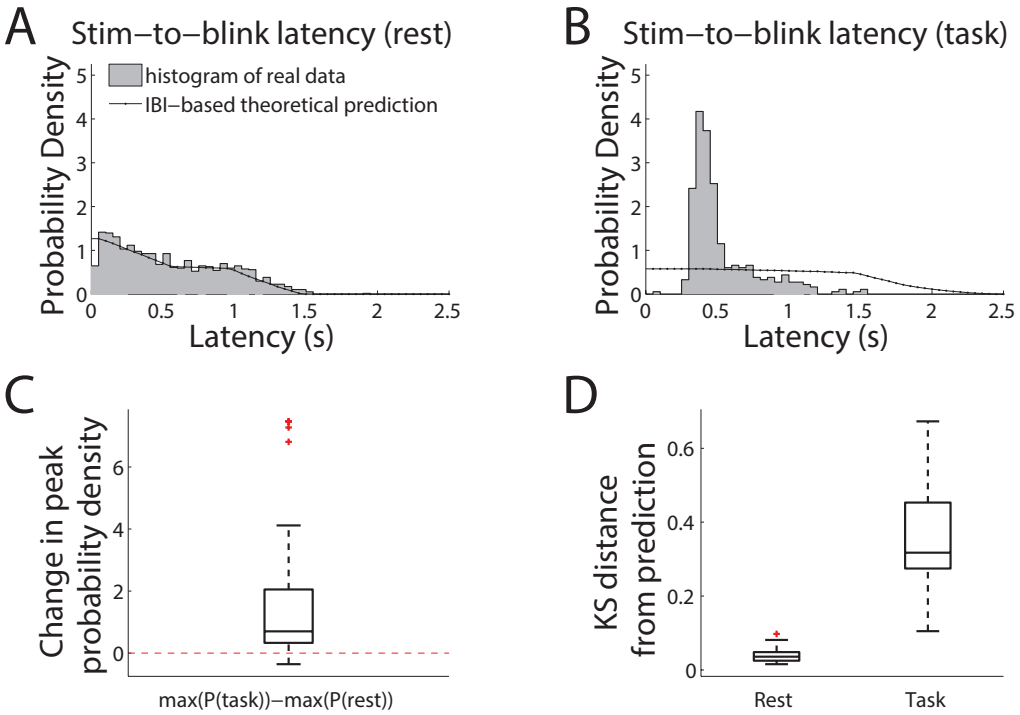

Fig. 4.2: ***Blink timing results.*** *(A) The gray area shows a histogram of probability densities of blink latencies from finger stimulations in the resting condition for one participant. The black line shows a theoretical prediction based on the distributions of inter-blink and inter-stimulus intervals. The prediction matches the real data histogram very closely. (B) Same as in previous panel, but for data recorded during the execution of the reaction task by the same subject. The histogram is visibly different from the resting condition in the previous panel. Additionally, the theoretical prediction is very different from the real data. (C) Box plot of the change in peak probability latency by the addition of the reaction task in all subjects. The significantly positive change shows that the addition of the task caused a specific time bin after the stimulus to be very probably containing a blink. (D) Kolmogorov-Smirnov distances between histogram of real stimulus-to-blink latencies and theoretical predictions during rest (left) and in the "task" condition for all subjects. The significantly large KS distance in the "task" condition shows that inter-blink and inter-stimulus interval distributions could not account for the stimulus-to-blink distribution, indicating that each blink's timing was decided individually.*

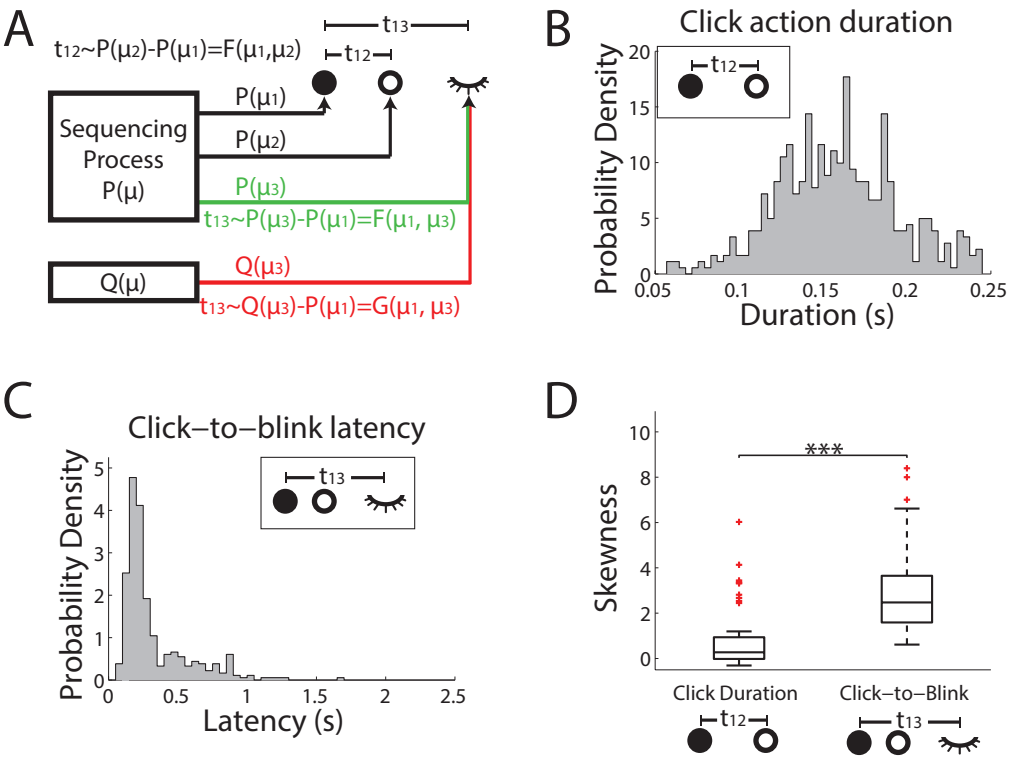

Fig. 4.3: ***Evaluation of the possibility of a click-and-blink motor reaction plan.*** *(A) The conceptual models of common vs separate plans for clicks and blinks and implications for timing. A sequencing process in the brain ($P(\mu)$, black arrows) determines the timing of mouse button presses ($P(\mu_1)$, filled black circle) and releases ($P(\mu_2)$, empty black circle), and thus the distribution of mouse click durations t_{12} is determined by a process $F(\mu_1,\mu_2)$ representing the difference of the two individual timings. Eye blinks may also be timed by the same process that sequences button presses and releases ($P(\mu_3)$, green arrow), so that the distribution of click-to blink intervals t_{13} is determined by a process $F(\mu_1,\mu_3)$ similar to $F(\mu_1,\mu_2)$. Alternatively, if t_{13} is distributed very differently from t_{12}, this would indicate that click-to-blink intervals are determined by a separate process $G(\mu_1,\mu_3)$, $G \neq F$, and thus that blinks are planned separately (process $Q(\mu)$, red arrow). (B) Distribution of click durations in a single subject. (C) Distribution of click-to-blink latencies in the same subject. (D) Comparison of the skewness of the two distributions in all subjects, as a quantitative measure of the strong qualitative difference visible in panels C and D.*

Chapter 5

Neuromorphic decoding of motocortical activity in a bidirectional brain-machine interface

Disclaimer

The spike-based learning and decoding algorithm was implemented with Giacomo Indiveri.

The following collaborators are affiliated with the Italian Institute of Technology. The physiological experiments were performed by Fabio Boi and Alessandro Vato. Fabio Boi, Vito De Feo, Francesco Diotalevi, and Chiara Bartolozzi designed, built, and debugged the hardware and software infrastructure for the BMI, except the neuromorphic part.

All the experiments were performed in accordance with DL116/92 of the Italian legal code and approved by the institutional review board of the University of Ferrara and by the Italian Ministry of Health (73/2008-B).

A part of the chapter is published in [Boi, F. and Moraitis, T. et al., 2016].

5.1 Introduction

5.1.1 Brain-machine interfaces

The possibility of controlling a prosthetic device through a direct interface with the central nervous system represents a promising solution for restoring sensory-motor functionalities in patients with limb amputations or peripheral and neurological deficits due to spinal cord injury, amyotrophic lateral sclerosis, or stroke. In the last two decades, a fast-growing field has made large progress towards the development of clinically applicable hybrid brain-machine or brain-computer interfaces

(respectively BMIs or BCIs) [Lebedev and Nicolelis, 2006].

The first documentation of monkey's ability to learn to control the activity of individual neurons [Fetz, 1969] led to proposals to use external devices controlled by the activity of cortical neurons to restore motor function in paralyzed patients [Schmidt, 1980]. By the turn of the century, technological advances enabled the first systems that allowed the brains of rodents and primates, including humans, to directly interact with machines [Chapin et al., 1999, Birbaumer et al., 1999, Talwar et al., 2002, Wessberg and Nicolelis, 2004, Serruya et al., 2002, Taylor et al., 2002]. Interfaces that allowed the use of the controlled machine to manipulate physical objects followed [Velliste et al., 2008], along with an increase in the understanding of the plastic changes that the brain undergoes to accommodate the interface with the machine [Jarosiewicz et al., 2008].

These seminal studies additionally showed the importance of coupling visual feedback with the control of the interfaced machine, as its presence increased the performance of the subjects in manipulating the machines. This reconfirmation of the importance of sensory feedback for motor control and suggested that lack of somatosensory feedback, i.e. sensory feedback directly from the controlled body to the central nervous system (CNS), could be partially responsible for the relatively poor performance of BMIs, implying that an ideal BMI would be bidirectional [Bensmaia and Miller, 2014]. The tools to provide artificial sensory stimulation to the brain had been developing independently. Already in the 1930s, electrical stimulation was shown to elicit somatosensory percepts [Penfield and Boldrey, 1937], and much later the possibility to modulate the evoked sensation by changing parameters of intracortical microstimuli was documented [Romo et al., 1998a, London et al., 2008, Fridman et al., 2010, Semprini et al., 2012, Zaaimi et al., 2013] including strategies attempting to mimic natural sensations and successfully conveying information about contact location, force and timing [Tabot et al., 2013]. The first bidirectional BMIs was described in 2009, when monkeys were instructed by intracortical microstimulation (ICMS) and moved a computer cursor according to the instruction with their motocortical activity [London et al., 2008, O'Doherty, 2009]. The sensory-motor loop in a bidirectional BMI was closed, when monkeys moved a cursor with their motocortical activity while they were informed about the cursor's movements through electrical stimulation of their somatosensory cortex [O'Doherty et al., 2011b].

A closely related group of studies developed prostheses artificially activating central-pattern-generator (CPG) networks in the cat's spinal cord to support walking [Saigal et al., 2004], and demonstrated the importance of closing the sensory-motor loop by modulating the artificial stimulation according to sensory feedback [Holinski et al., 2011, Mazurek et al., 2012]. The closed-loop control performed by the spinal cord in healthy subjects is not expressed only in the case of CPGs. The spinal cord

is also able to control limb movements by applying a force field mapped to different positions of the limb such that this mapping guides the limb to follow predetermined trajectories that can for instance stabilize the limb to a position that the force field converges to [Mussa-Ivaldi and Bizzi, 2000, Mussa-Ivaldi et al., 1994]. The state of the limb is fed back to the spinal cord by sensory input. This sensory input can cause corrective spinal motor outputs, similar to how CPG activity is modulated by sensory input. Descending efferents from the brain into the spinal cord can activate or modulate this spinal dynamical system, also similar to how CPGs are modulated by descending signals. The brain's outputs also depend on sensory inputs that may be consciously perceived, thus closing another, longer loop. Bidirectional BMIs address the long brain-centered loop, but the on-line closed sensory-motor loop that the spinal cord normally provides is not present, as the spinal cord is bypassed. While an analogous control loop in the hardware could perform this function, bringing both loops within the CNS reduces reliance on added artificial components that are hard to properly integrate. In cases where restoring this coordination between the brain and the spinal cord is infeasible, the brain itself may be able to accommodate both closed loops. The path towards this implementation has been followed in two recent variants [Vato et al., 2012, 2014] which implement the analogue of the short, spinal loop within the brain. These systems communicate the state of a device to a rat's sensory cortex with ICMS and interpret the immediate motocortical response to a mechanical force moving the device. This interpretation of the neural response as a force is configured such that the automatic closed sensory-motor loop that results corresponds to a pre-specified force field that acts on the device. The BMI presented in this chapter is of this type as well.

The main contribution of the chapter is the demonstration of a spiking neuromorphic chip configured to learn to interpret the motocortical activity to forces that act on the controlled device in a closed-loop bidirectional BMI. The hybrid sensory-motor interactions in this type of BMI may allow future clinically mature systems to benefit from biological interactions such as those presented in the previous chapters, and may as well provide a platform to test these mechanisms. Therefore this chapter's contribution to maturing this type of BMIs is bidirectionally linked with the work presented in the rest of the dissertation. The specific links are discussed in the subsection that follows.

5.1.2 BMIs and interactions of automatic and cognitive controllers

Successful integration of an artificial part into a coherent hybrid system requires that fundamental functional principles of biology are preserved in the interface. For instance, in healthy subjects motor processes are firmly conjoined with sensory feedback signals in a closed sensory-motor loop. Nevertheless, bidirectional BMIs that

both decode brain activity into motor commands and encode information descriptive of the state of the controlled device back into the brain have only recently been proposed [O'Doherty et al., 2011b, Vato et al., 2014]. What the optimal sensory encoding strategy is, what the sensory-motor interactions involved in the neural processing are, and how to integrate these interactions in the decoding algorithms to close the loop remain open questions.

In the previous chapters, biological and artificial systems were studied from the aspect of interactions between their cognitive and automatic components. BMIs are also *de facto* composite systems, and due to this, the framework that is used in the previous chapters of this thesis is particularly applicable to BMIs as well. The biological mechanisms studied in the other chapters can be used to preserve the biological principles in the hybrid interface. Furthermore, inter-controller interactions found to be beneficial to biological or artificial systems could be used to engineer better BMIs. In this chapter we present a BMI that preserves several biological principles, including those that evidence presented in the previous chapters suggests that they exist in a biological system.

One type of biological interaction that is studied in previous chapters is the hierarchy in the sensory-motor system combined with closed sensory-motor loops at its lower levels. The spinal cord is able to autonomously control the body through reflexive sensory-motor loops, but supraspinal structures can exert control over the spinal circuits. Similarly, eye blinks are produced by a generator that integrates sensory inputs from the eyes to its automatic function, but volition can overtake its control. Aspects of these systems were studied in chapter 2 and chapter 3. The present chapter is concerned with a BMI that preserves the principle of integrating sensory inputs in an automatic bidirectional closed loop which is intended to be voluntarily controlled by higher cognitive counterparts. It does so by informing the system with sensory feedback about the controlled body, and by integrating this feedback in reflexive motor responses. In the current implementation of the system which is described in this chapter the function of the automatic sensory-motor loop is demonstrated, but its integration with the higher, voluntary counterpart is not implemented yet.

In chapter 3 it was revealed that voluntary inhibitory control of the automatic part of eye-blink generation is applied directly on the automatic blink generator, rather than further down the path of motor output, suggesting a close integration of the cognitive with the automatic controller, and potential advantages from this approach were discussed. The BMI studied in this chapter reproduces such a close integration of voluntary with automatic control by closing the automatic sensory-motor loop within the brain as opposed to outsourcing it entirely to the artificial part of the BMI. This is achieved by providing the sensory feedback directly into the

brain which closes the loop with its automatic motor responses.

In chapter 2 it was demonstrated that a motor controller with some of the learning abilities of the cerebral cortex can benefit from receiving sensory inputs from movements of the body controlled by a second, automatic motor controller, such as those from reflexes produced by the spinal cord. This model has direct links with bidirectional BMIs that integrate the cortex. Firstly, the BMI itself can benefit from employing an implementation of reflex-tutoring, as the results in chapter 2 show that the cortex can benefit from a phase of learning from sensory inputs from automatic movements, improving the cortical learning and motor control. In the BMI, the reflex-tutoring of the cortex can be provided by movements controlled the automatic components of the system, or by cortical stimulation simulating the sensory consequences of movements. Conversely, the understanding of the purely biological system can benefit as well, as a bidirectional BMI provides a platform for testing the model of reflex-tutoring with the cortex itself, as opposed to our simulations in chapter 2. It offers the possibility to enable or disable reflex-tutoring provided to the cortex by the automatic components of the BMI. This would be equivalent to the less feasible option to disable reflexes in the purely biological system. This chapter contributes towards establishing a BMI that can test directly the possible benefits of BMIs or biological systems from reflex-tutoring, in a system that engages the cortex and the integrated artificial components in a manner very much analogous to the cortical and spinal functions, and their developmental and hierarchical sensory-motor links in the purely biological system.

5.1.3 Potential advantages from neuromorphic hardware in BMIs

In addition to the contributions of this chapter towards linking BMIs with biological interactions, this work's main contribution is in integrating spiking neuromorphic hardware in the system as an interpreter of cortical motor activity that learns to perform its task. The development of a BMI system aiming for large clinical application necessitates crucial improvements of the hardware and software components. The hardware components need to be (a) fully implantable for long term use and therefore miniaturizable; (b) able to reliably process neural signals with a limited power budget; (c) powerful enough to implement non-trivial computational tasks involved in a BMI system. Additionally, the decoding algorithms need to be (d) flexible enough to be implemented with different types of hardware components and (e) able to dynamically adapt to changes in the neural activity due to the interaction with the artificial device [Orsborn et al., 2014, Dangi et al., 2011].

To address the challenging hardware and software requirements to develop portable and implantable BMIs, we tested the applicability of neuromorphic hardware in a BMI system. Neuromorphic devices offer the perspective of compact, energy-efficient,

and adaptive operation that has been demonstrated to be best-suited for tasks that involve learning from real-world observations in an on-line fashion [Chicca et al., 2014]. They achieve this by employing silicon emulations of biological neurons and synapses that can be physically configured to implement algorithms inspired by the asynchronous massively parallel computations performed in biological neural networks. Additionally, input to and output from neuromorphic chips is provided with asynchronous digital pulses that encode information in their analog timing, similarly to action potentials of biological neurons. Because of these features, neuromorphic processing chips are very promising candidates for implementing reliable and energy-efficient decoding of neural activity, that could ultimately be evolved to be portable, implantable, and directly interfaced with neural tissue. [Chen et al., 2016] demonstrated the use of a neuromorphic chip for efficient decoding of cortical activity. However, integration of such a chip in a working BMI has not been described before the work presented here. As a fist step in this direction, we tested a neuromorphic chip as a learning decoding module for the motor activity acquired from rat's barrel cortex in a well-consolidated experiment [Vato et al., 2012].

5.2 Overview of the complete physical implementation

The BMI is based on the Dynamic Neural Interface described in [Vato et al., 2012]. Here, the neural activity recorded from the motor cortex of an anesthetized rat, and the state of an object which is fed back through stimulation of the animal's sensory cortex define a dynamical system and control its movements.

The neural signals collected from the motor cortex are transformed by a Decoder into a force vector to be applied to the controlled device that moves according to its dynamics. In this implementation the Encoder maps each position of the device to one of 4 different patterns of intracortical microstimulation (ICMS) delivered to the somatosensory cortex in order to produce artificial proprioceptive information about the state of the dynamical system. This mapping is obtained during a calibration of the Encoder that divides the workspace into 4 different contiguous sensory regions. Over several iterations of this recording-stimulation loop the BMI is capable of driving the controlled device from different starting positions to a predefined target region within the workspace. Importantly, the whole system is implemented in reality, with ICMS provided to the cortex and corresponding to the actual position of the controlled device, and with simultaneous recording from the motor cortex that is provided to the Decoder for learning and decoding. During the testing phase, the Decoder's output force is applied to the controlled device, moving it to a new position. The Decoder is implemented in the neuromorphic hardware, which is configured beforehand through a python programming interface. This results in a fully

working and physically implemented closed-loop system. The 4 stimulation patterns are delivered to S1 with a $1\,Hz$ frequency, and they differ from each other only in the combination of stimulating electrodes. The waveform remained constant (trains of biphasic pulses delivered at $100\,\mu A$, $333\,Hz$, $300\,ms$). After each stimulation, the Decoder considers the first $256\,ms$ of the evoked motor neural signal to produce the driving force for the dynamical system.

5.2.1 Simulated work

Some simulations were performed additionally. A simulation of the chip was programmed and used as an initial aid in getting accustomed with its neural and synaptic mechanisms. Furthermore, we also implemented an additional decoding scheme that involved partly the neuromorphic hardware and partly a software component that improved the purely-hardware-based learning and decoding and is described in section 5.5.

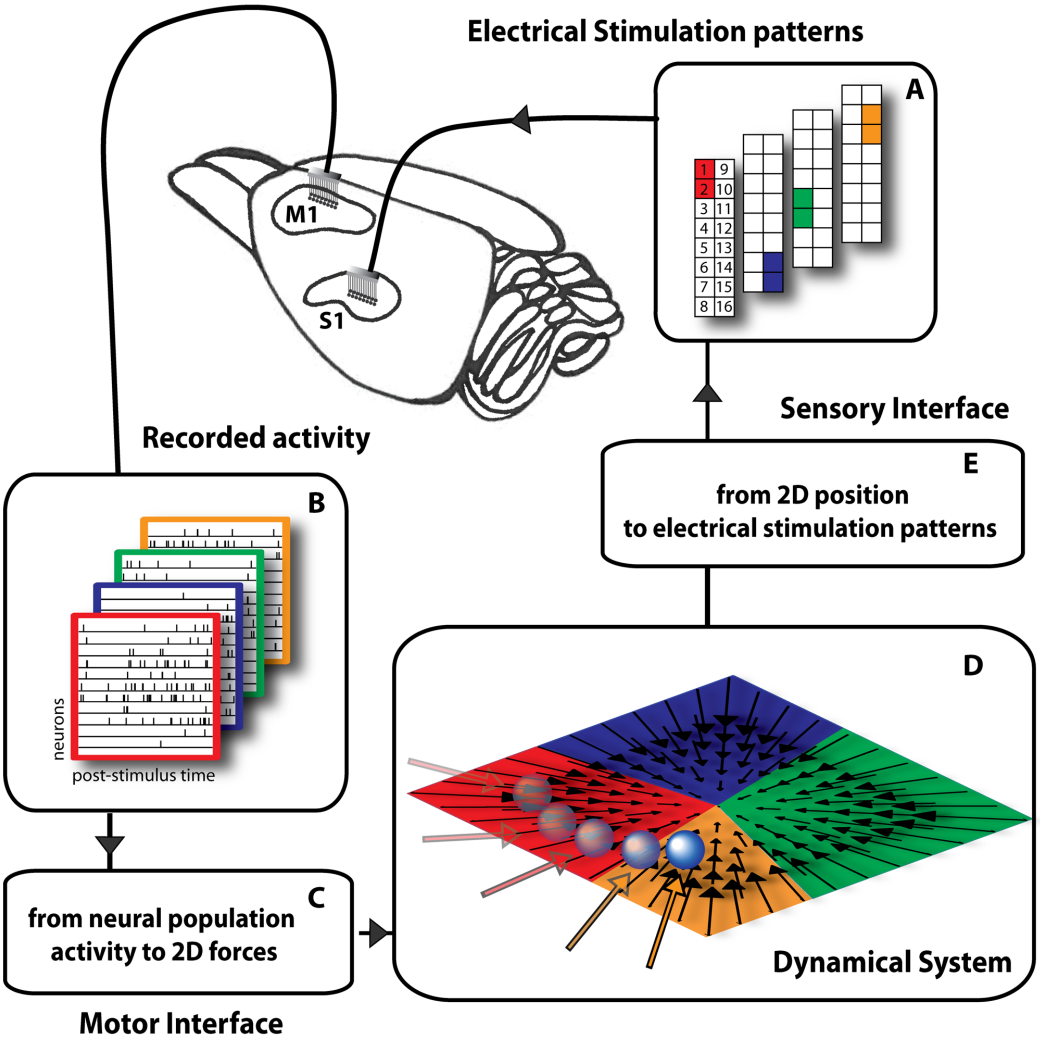

Fig. 5.1: ***The bidirectional BMI*** *(adapted from [Vato et al., 2012]). (A) One of four stimulation patterns is provided to the somatosensory cortex of a rat. (B) The activity in the rat's motor cortex is recorded after the stimulus. (C) The recorded activity is decoded into a force. Here, we performed the decoding on a chip equipped with electronic circuits emulating biological neurons with plastic synapses. (D) The decoded force moves an object in a viscous material. (D and E) Different positions of the object in space are associated with different stimulation patterns subsequently provided to the rat's brain, closing the loop. The closed loop system defines a dynamical system through approximating a force field that can cause the object to move in predictable trajectories, for instance converging to a target location. The figure is adapted from [Vato et al., 2012], a study which also used this set-up, but with the decoding performed on a conventional computer.*

5.3 The ROLLS neuromorphic processor

5.3.1 Description

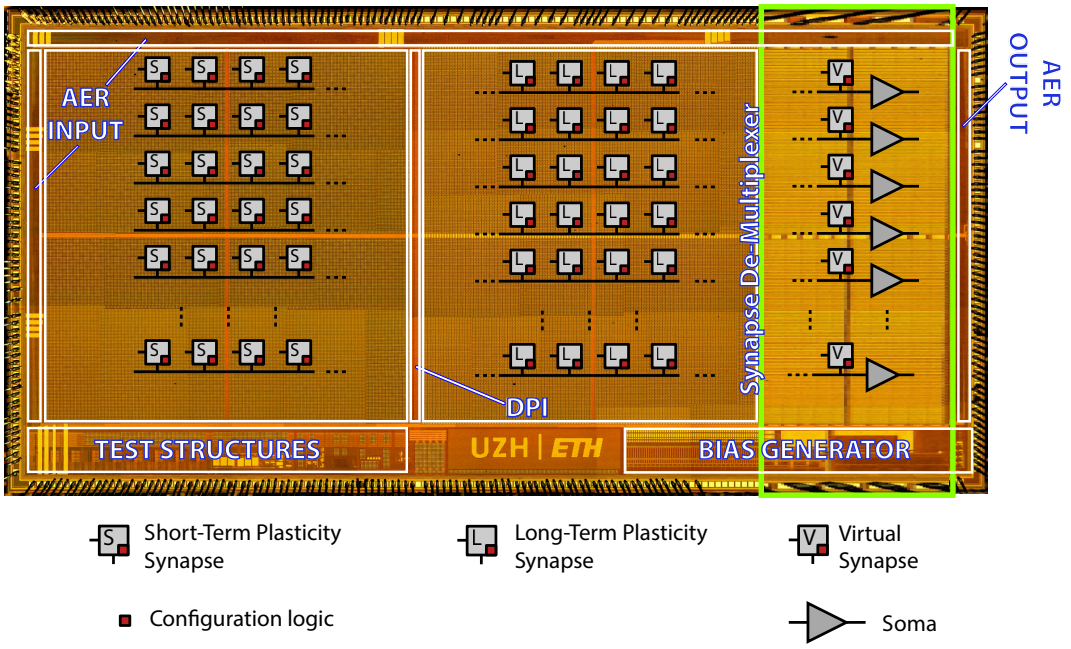

Fig. 5.2: ***ROLLS Neuromorphic Processor.*** *Micrograph of the neuromorphic processor chip that was used to learn to perform the decoding task in the BMI. It allocates most of its area to non-linear synapse circuits for memory storage and distributed massively parallel computing. The test structures in the lower left part of the chip contain low-power neural amplifier circuits and neural signal Analog-to-Digital conversion circuits.*

The Reconfigurable On-line Learning Spiking (ROLLS) Neuromorphic Processor is a general-purpose spiking neural network chip [Qiao et al., 2015]. Fig. 5.2 shows the chip micrograph. It was fabricated using a standard 6-metal $180\,nm$ CMOS process, occupies an area of $51.4\,mm^2$ and has approximately 12.2 million transistors. It comprises 256 adaptive exponential integrate-and-fire neurons implemented in a mixed signal analog/digital design. There are $128\,K$ synapses, of which $64\,K$ that can implement a Hebbian plasticity rule [Brader et al., 2007, Mitra et al., 2009] (Long-Term Plasticity (LTP) synapses), and $64\,K$ that can exhibit short term depression and short-term facilitation dynamics (Short-Term Plasticity (STP) synapses), and which have a resolution of two possible programmable weights, in addition to the possibility to configure them as either excitatory or inhibitory. These two synaptic matrices allow arbitrary on-chip connectivity thanks to a crossbar structure. In principle all-to-all connections are possible, through the programmable logic state of the synapses. The LTP synapses comprise pre-synaptic spike-based learning circuits with bi-stable synaptic weights [Mostafa et al., 2014]. Additional circuits are also

instantiated next to the neurons array, needed to implement the spike-based weight update algorithm [Brader et al., 2007], and they represent the calcium concentration at the post-synaptic side. The internal dynamics of the synapse are analog but its state is binary. This removes the need of storing analog variables on long-time scales and simplifies the circuit implementation. We refer the reader to [Qiao et al., 2015] for detailed circuits description. Both the neural network architecture and the parameters of the neuromorphic core are fully programmable via a high-level Python framework [Stefanini et al., 2014]. The combination of reconfigurable hardware with the Python-based configuration framework supports the exploration of a wide range of spiking neural network architectures, and their real-time emulation in closed-loop setups. This setup enabled us to configure a hardware implementation of a spiking neural network that learns on-line to decode patterns of recorded spike sequences.

5.3.2 The learning synapse

The synapses that were key to the chip's learning of its task were its learning (LTP) synapses. These synaptic circuits implement physically a plasticity rule described in [Brader et al., 2007] (Figure 5.3). These synapses are excitatory and their weights are bistable, spontaneously drifting linearly to either 0 or 1, depending on their value relative to a threshold. In addition, the weight may increase, i.e. potentiate, or decrease, i.e. depress, between 0 and 1 when a presynaptic spike arrives, depending on the value of two variables characterizing the postsynaptic neuron soma: the calcium variable, and the membrane potential of the neuron's soma. The calcium variable represents the concentration of calcium in the neuronal soma, it spikes with every postsynaptic action potential, and decays exponentially. Below one threshold Ca_{min} and over a threshold Ca_{pot} no potentiation or depression of the synaptic weight is allowed. Between Ca_{min} and a threshold Ca_{dep} depression is allowed. Between Ca_{min} and Ca_{pot} potentiation is allowed. For potentiation, or depression, these conditions need to be simultaneously satisfied with a condition related to the membrane potential. When the membrane potential is below a threshold V_th, only depression is allowed, and when it is above the threshold, only potentiation is allowed. The thresholds, the amplitudes of incremental increase and decrease of the weight, the weight drift rates, the calcium variable spike amplitude and calcium concentration decay time constant, as well as the dynamics of the neuronal membrane potential are all independently configurable through analog parameters.

The spike-based plasticity rule, translates to a rate-based rule, whereby a range of low postsynaptic firing rates permits synaptic depression, and a range of high postsynaptic rates permits potentiation (Figure 5.4).

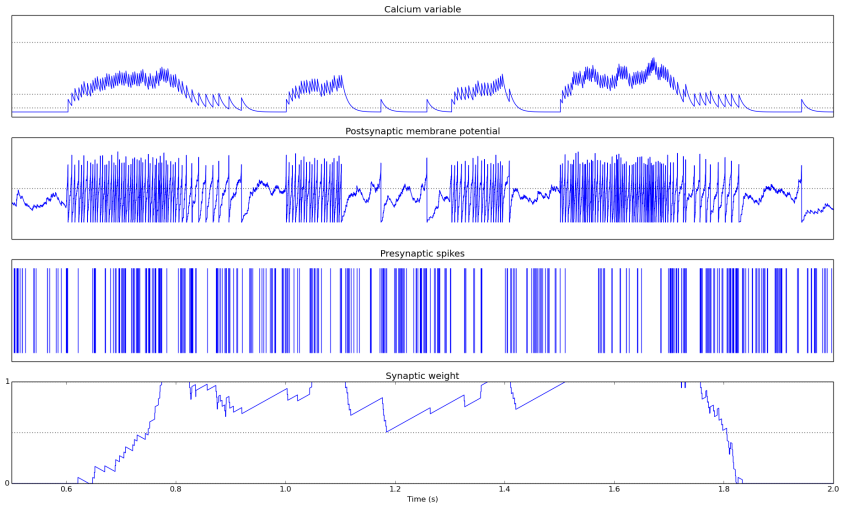

Fig. 5.3: ***The learning synapse in operation.*** *These data, taken from our simulations of the chip's neurons and synapses, demonstrate the operation of the chip's learning synapses in parallel with relevant somatic variables, as described in subsection 5.3.2. The calcium variable of the neuron and the thresholds determining the potentiation and the depression regime are in the top panel. The postsynaptic membrane potential with visible spiking activity is in the second panel. A threshold decides whether either potentiation or depression is possible. The third panel shows a set of presynaptic spikes to a synapse of the neuron. The last panel shows the evolution of this synapse's weight with time. The effect of each presynaptic spike according to the condition of the somatic variables is visible. In addition they bistability of the weight is shown by the drifting behaviour towards either zero or one. These data are the only ones in this section that are the result of simulation as opposed to real physiological or neuromorphic recordings.*

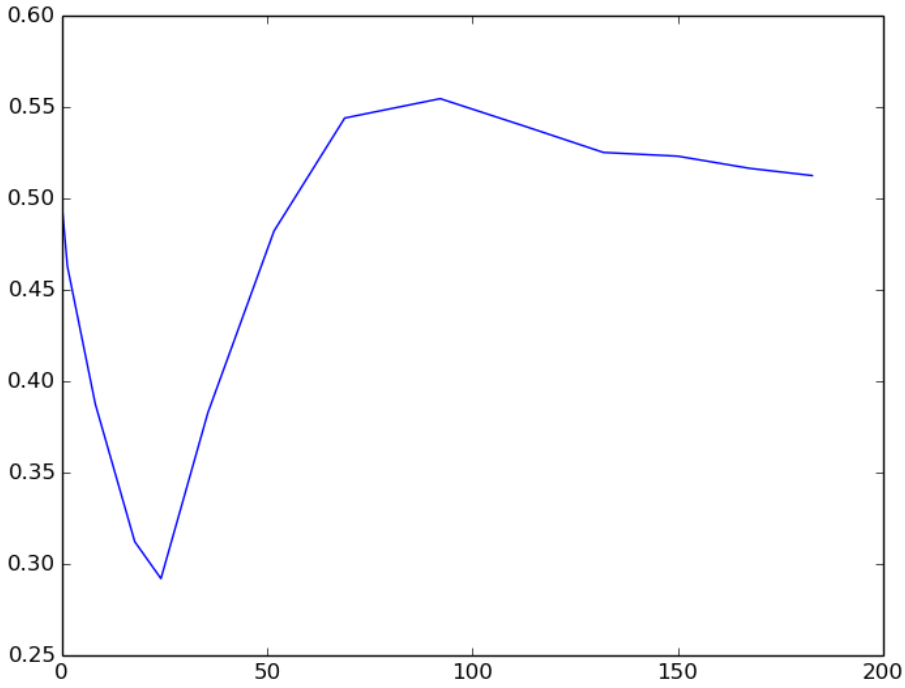

Fig. 5.4: ***Synaptic depression and potentiation probability as a function of postsynaptic firing rates.*** *Each point in this curve was obtained by first setting a half of all the learning synapses of the chip at their potentiated state. Subsequently, a Poisson spike train of a fixed mean rate (100 Hz) was provided for 100 ms to all learning synapses, simultaneously with an excitatory current provided to the post-synaptic neurons, which varies on the horizontal axis. The mean output rate of all the neurons at each datapoint, and the proportion of synapses that were in the potentiated state was measured and is shown. The ranges where depression or potentiation are likely are visible. Also, the "stop learning" feature for high output rates is shown at the decreasing right-hand part of the curve.*

5.4 Decoding on the ROLLS

5.4.1 Choosing the decoding algorithm

The BMI's intended effect on the controlled device was the approximation of a force field that converges to a target in the center of the working plane. Specifically, in the implementation reported here, the working plane was divided into four equal regions, and the desired field at any point of each region was defined by a force vector parallel to the vector pointing from the region's center to the target. The Decoder's task included decoding each motocortical response to stimulation into a resulting force, calculated as a weighted sum of the four forces defining the force field. That is, a part of the Decoder's task was to output the four coefficients corresponding to the contribution of each of the four forces to the resulting force. The decoding scheme we used, rather than using the maximal of the four forces, calculates the resultant force to be applied to the dynamical system as a combination of the four force components of the force field. With this implementation, in a future set-up, the animal's voluntary control of the four forces, and/or additional, combinatorial stimuli provided by the Encoder could contribute to the computation of the final force. In a correctly performed decoding, recordings acquired when the device was in each of the four regions should cause an average force maximally similar to the desired force field within that region. We approached this task by combining the constraints of a multi-class classification task with additional constraints that account for the BMI-specific requirements related to the simultaneous contribution of all four classes to each decoded force.

5.4.2 Designing the silicon neuronal network

We designed a feed-forward spiking neural network on the ROLLS that employs the spike-timing dependent plasticity of the chip's LTP synapses to learn to decode the contributions of the four forces to the resulting force when presented with a recording of cortical activity. Each of the output neurons of the network was trained to act as a binary classifier by re-weighting the features of its input that were distributed across its synapses, so as to ultimately yield, via its activation function, a higher output spike rate for one, positive class of input compared to the other three, negative classes. Neurons were grouped into four ensembles, each corresponding to one of the four stimuli. The spike counts output by the four ensembles during the presentation of the recordings to the network were directly used as the coefficients that weight the contributions of the four component forces acting on the BMI's end effector.

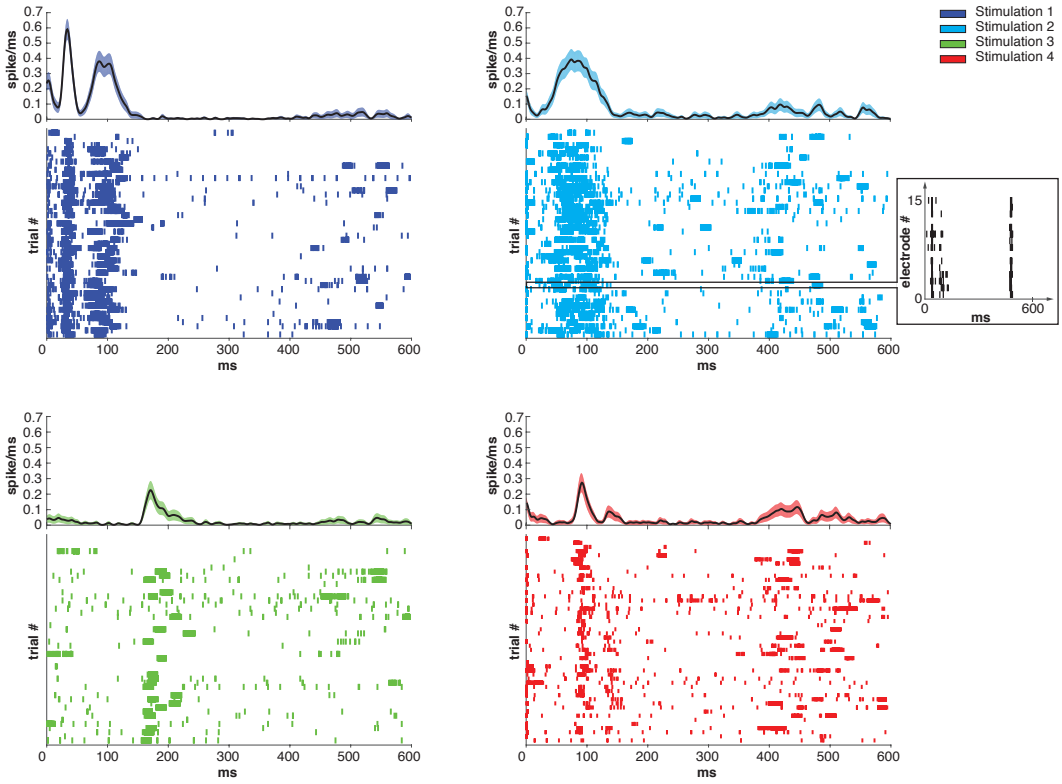

Fig. 5.5: *Raster plots and post-stimulus time histograms (PSTH) of the neural activity evoked by 4 different stimulation patterns. Each short vertical line in the raster plots represents a* 1 *ms time bin during which at least one spike was detected on the recording array. The related PSTHs are plotted above each raster. For each stimulus we report the mean evoked activity (black line) and its standard error (colored area) computed on all trials. In the inset we report the neural activity recorded on each individual electrode of the microwire array in a single trial.*

5.4.3 Inputting the recordings to the ROLLS network

The spiking neurons' instantaneous activation depends on the distribution of past input spike intervals that are primarily characterized by the input's mean spike rate and that are recent relative to the neuron's time constant. That is, the specific timing of the input to the output neurons with respect to a given distant past time point cannot be used to differentiate between classes of input patterns. However, we found that, in the motocortical data we recorded, the principal feature that is common between patterns of one class and different between classes is the timing of the recorded spikes with respect to the offset of the sensory-cortical micro-stimulation (Fig. 5.5), implying that a transformation of the input into an array of firing rates is required before it reaches the output layer. Furthermore, the number of non-redundant features of the input to the output neurons needs to be sufficiently high to support the number of classes to be discriminated. We found that the

recorded activity was very similar across all recording channels (see Fig. 5.5, inset). Therefore, there is likely no synaptic weight configuration that a single-layer feed-forward network can use to classify the recordings based on features corresponding directly to the recording channels.

To reconcile these characteristics of the data with the silicon single-layer feed-forward neural network, the requirements that are entailed are two. Firstly, to make use of the time sequence of the recorded spikes as the principal differentiating feature, while addressing the redundancy of the dimensions of the recording that correspond to recording channels, different synapses of the output neurons of the network need to receive input that encodes uncorrelated sub-samples of the spike sequence. Secondly, this encoding of the input needs to be rate-based because rate is the input's attribute that mostly governs post-synaptic firing. To implement this, the recorded spike trains were binned in time bins of one ms (Fig. 5.6 B) and each bin was associated with one input synapse of each neuron of the network (Fig. 5.6 C). A high mean-rate ($100\,Hz$) Poisson spike train was provided for $400\,ms$ to the learning synapses corresponding to time bins that did contain recorded spikes, while no input was provided to the rest of the synapses (Fig. 5.6 C). We reached the decision of one-ms bins after the following analysis.

Under the constraint of a finite number (256) of available synapses per neuron, there was a trade-off among, firstly, the amount of spatial information in the recordings, i.e. the number of recording channels, secondly, the duration of the recording patterns that were used, and thirdly, the temporal precision, i.e. the number of time bins. To settle this trade-off, we visually analyzed samples of the recorded data. This analysis revealed that the first $200\,ms$ - $300\,ms$ of each recorded pattern included significant differences across the four different classes, that would potentially be sufficient for the classifier to discriminate between them (Fig. 5.5). This, together with the observation that the distributions of spike timings were very similar across different recording channels, led us to merge the 15 recording channels into a single spike train and to use the first $256\,ms$ of the recordings, thus acquiring a temporal precision of one ms per time bin. We additionally confirmed that longer recording duration, with a two-millisecond or lower precision, diminished decoding performance.

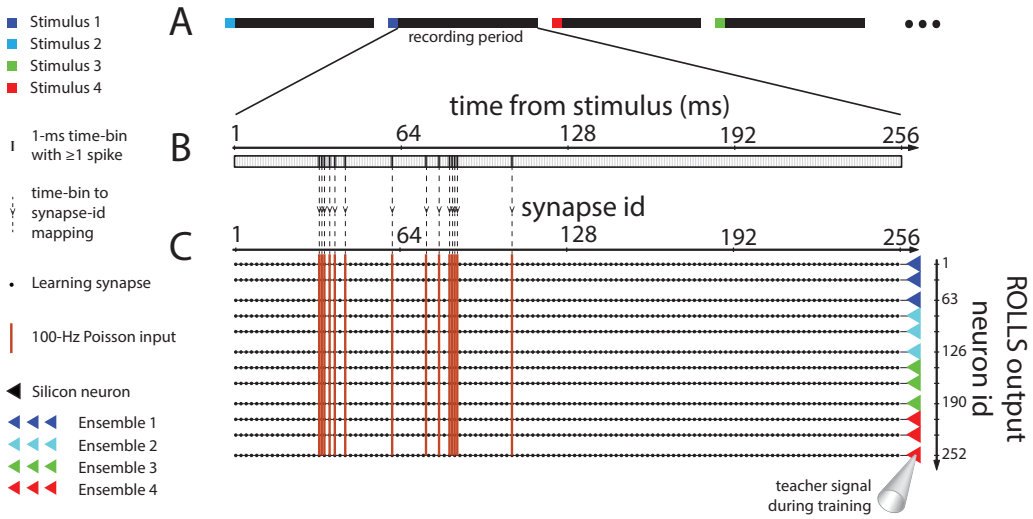

Fig. 5.6: ***Input, training, and use of the neuromorphic Decoder.*** *(A) To train the Decoder, four different stimuli were provided to the rat's sensory cortex. Stimuli were provided in random order, 40 times each, and the activity in the motor cortex was recorded during the session. (B) The activity in the first* $256\,ms$ *after the end of each stimulus was used with the Decoder. The recording was binned in 1-ms time bins, and bins where at least one action potential was detected across any of the recording channels were marked. (C) Each time bin was mapped to a column of 252 learning synapses on the ROLLS, whereby each synapse belonged to a different post-synaptic neuron on the chip. Synapses corresponding to time bins in the recording that included detected spikes received a Poisson spike train with a mean rate of* $100\,Hz$*. Synapses corresponding to empty time bins received no input. In addition, the silicon neurons were stimulated by a teacher signal, as follows. The 252 post-synaptic neurons were separated in four ensembles of 63, and we associated each ensemble with one of the four stimuli provided to the rat's sensory cortex. During the presentation of each recording to the chip, the ensemble corresponding to the preceding cortical stimulus was stimulated by a Poisson spike train of* $75\,Hz$ *as a teacher signal, while the other three neuronal ensembles received a teacher signal of* $25\,Hz$*. After training, the ROLLS received no teacher signal, and each recording was decoded into a force applied to the end effector, by weighting four force components by the number of spikes output by each of the four ensembles.*

5.4.4 The decoding task as more than classification

The aim of the BMI is to best approximate the desired force field over the duration of the experimental session, through weighting the four force components. To achieve this aim, there are two criteria based on which the Decoder has to simultaneously optimize its learning. Firstly, it needs to learn to classify the patterns, i.e. to correctly output the single class to which each presented recording truly belongs, as expressed by the "winning" (i.e. the most firing) ensemble of output neurons. Secondly, the Decoder also needs to prevent the other three "losing" ensembles from biasing the force field towards particular directions on average over the trajectory of the end effector. That is, it needs to classify the recordings under the constraint of learning to equalize the average outputs of "losing" ensembles. Thus, despite the similarities to a classifier, classification of individual recordings is only partly the Decoder's task.

5.4.5 Biased similarities and differences between classes of recordings

The Decoder had to address certain additional characteristics of the recordings to achieve its goal of approximating the desired force field over the experiment's course. Specifically, firstly, we found that different classes of recordings differed in number of recorded spikes on average (Fig. 5.5), and this difference in the input energy could be reflected as a bias in the chip's output and consequently in the direction of the decoded force in each trial. Moreover, even though spike timing was the principal difference between recordings of different classes, some spike timings were common between classes. This increased the difficulty in distinguishing between different classes. That is, the different classes had a certain level of overlap between their features, which could increase classification errors. Additionally, this overlap was not of the same extent for all pairs of classes, i.e. some classes were more similar to some than to others in terms of common spike timings (Fig. 5.5). This asymmetry could result in additional biases in the weighting of the force components by the Decoder, thus misshaping the resulting force field in certain parts of the working space.

5.4.6 Using heterosynaptic competition, and inter-synaptic and inter-neuronal variability to learn the decoding task

To address these points, we used the "stop learning" feature of the ROLLS chip, which prohibits potentiation of synapses when the post-synaptic firing rate exceeds a threshold. When a certain number of synapses that correspond to a neuron's positive class are potentiated, the increased excitation from the input causes the neuron to

stop learning. This introduces heterosynaptic competition [Royer and Paré, 2003] to the chip's output neurons, which serves (a) to normalize the network's output in response to different classes, (b) to make potentiated synapses a scarce resource hence biasing potentiation towards non-overlapping features, and (c) to equalize the output of "losing" ensembles. In addition, combined with device mismatch on the neuromorphic circuits, it biases different members of each ensemble to learn a slightly different decision boundary. This is similar to boosting techniques employed in machine learning and improves the classification performance by allowing for non-linear decision boundaries for the ensemble through the aggregation of the multiple linear boundaries defined by the ensemble's member neurons.

5.4.7 Training the neuromorphic Decoder

To train the neuromorphic Decoder, we used an experimental session composed of 40 repetitions of each stimulation pattern (i.e. 160 evoked recordings). During the training procedure for each class we presented to the ROLLS processor the 40 training trials randomly interleaved (Fig. 5.6 A) along with a teacher signal representing the label of the presented example, i.e. the type of sensory-cortical microstimulation that produced the recorded motocortical response. 63 output neurons were assigned to each class (Fig. 5.6 C, right). The teacher signal biased each neuron to be tuned to one class, by causing it to fire with a rate that maximized the probability that the neuron's synapses got potentiated when an example of that class was presented, and depressed when an example of the other classes was presented. The mean rate of the Poisson spike train that would act as a teacher signal with these properties, as well as the analog parameters of the silicon neurons and synapses of the ROLLS processor were configured to match the characteristics of the input data with the requirements of the learning and of the decoding task.

5.4.8 Decoding results

We evaluated the performance of the Decoder by using a testing dataset acquired by 10 repetitions of each stimulation pattern (i.e. 40 evoked recordings), which were previously unseen by the Decoder. For each decoded pattern, the output spikes produced by each neuronal ensemble (Fig. 5.10A) were counted.

Given a stimulus, the average spike count of the ensemble of silicon neurons corresponding to that stimulus was higher than the other three (Fig. 5.10B).

In addition, as a result of the introduction of "stop learning" to the silicon neurons (see 5.4.6) average spike counts were relatively uniform across the other three ensembles despite the biases in pairwise similarities between input classes, and despite the unbalanced energy of recording classes (Fig. 5.5). For instance, spike timings

characterizing motocortical responses to Stimulus 4, also characterized Stimulus 2, but less so Stimuli 1 and 3 (Fig. 5.5). Nevertheless, the chip learned to suppress this bias, as evidenced by the fact that the average output of the chip's neuronal ensemble 2 in response to recordings acquired after Stimulus 4 was not larger than the output of ensembles 1 and 3. In addition, Consequently, decoded resultant forces for each stimulus were, as originally intended, most similar to one of the four forces used during the calibration phase (colored thick arrows shown in Fig. 5.9B).

While the task of the Decoder was not a classification task and it was not optimized to perform as a classifier, we also evaluated its performance in correctly classifying the recordings, as expressed by the maximally firing ensemble of neurons. For 20 different random splits between the training and the testing sets, the classification performance on the testing set ranged between 50% and 70% correct, when the performance level of a random guess would be 25%.

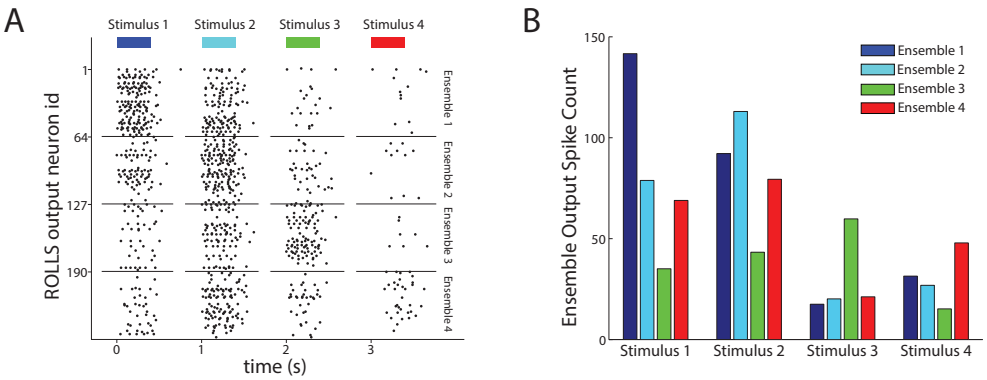

Fig. 5.7: ***Output of the trained Decoder.*** *(A) Raster plot of the output spikes of the trained ROLLS chip during presentation of four example test recordings each resulting from a different type of stimulus. The length of the bars on top shows the 400-ms long presentation of the input. During presentation of the four examples, the most active ensemble of output neurons corresponds to the true stimulus that caused the input recording. The spike count of the output each of the four neuronal ensembles was directly used to weight each of the four components of the force field to result in the motor command, i.e. force, that acted on the controlled object. The chip's neurons maintained some activity till shortly after the input stopped, mainly due to excitatory current leaking between the firing neuronal electronic circuits. (B) Average output spike count for each ensemble of neurons, for each type of stimulus that caused the decoded recording. For each stimulus, its corresponding ensemble fires on average more than the other three, demonstrating the classification aspect of the Decoder's task. In addition, the Decoder learned for each stimulus to partially equalize the response amplitudes of the three non-corresponding ensembles, compared to the extent of the differences between input classes (cf. Fig. 5.5 and see subsection 5.4.8).*

5.4.9 BMI performance

Once the decoding and encoding interfaces were properly calibrated, we run the BMI by decoding from each neural trial a bidimensional force and by associating to each position of the controlled object an ICMS pattern. In order to test the BMI capabilities, we selected 8 different equispaced and equidistant positions as starting conditions in which the dynamical system was initialized (see Fig. 5.8A). Every second a random test trial was picked up from the test set and sent to the Decoder that returns a force to be applied to the controlled device. With the purpose of quantifying the system performance, we run the BMI 100 times, starting from each initial position, both with the Encoder interface turned ON and OFF. This means that in the Encoder-ON test trials were kept in according to dynamical system current position. In the Encoder-OFF case each test trial was randomly selected among all the available entries. What is expected is that the bmBMI overall performance are good just in the case in which the encoder is turned ON demonstrating the fact that the desired behavior is not random but due to a well trained decoding/encoding interface.

Initially we run the BMI for a constant predefined amount of time and in Fig. 5.8A we report in red and in blue the coordinates of the closest points of the performed trajectories respectively when Encoder was set ON and OFF. The distributions of the two sets of points (Fig. 5.8B) are statistically different (independent samples t-test, $p < 0.001$) showing a decrease of 99% and demonstrating that closing the loop in the proposed BMI is crucial in order to correctly drive the dynamical system towards a predefined target.

To evaluate the repeatability, the speed and the optimality of the generated trajectories we measured the mean *within-trajectories variance* (abbreviated to *wtv*) and the number of steps required to converge to the target. We obtained the mean *wtv* by averaging the *wtv* computed for each set of trajectories starting from one initial location. In particular for each trajectory set its *wtv* is defined as $\sqrt{C_x^2 + C_y^2}$, where C_x and C_y are respectively the covariance computed along the x and y axes. In the Encoder-ON case the mean *wtv* and the steps needed to reach the target significantly decrease (respectively 92% and 80%) with respect to the Encoder-OFF case (Fig. 5.8C and 5.8D). Finally, for each force produced by the decoding process, we measured the magnitude of two components: the component of the force that points towards the target named *Directed to the target - DT* and the component orthogonal to it named *Orthogonal to the target - OT*. The mean of the DT-component is strongly positive (directed to the target) in the case of Encoder-ON and slightly negative (divergent from the target) when the Encoder is turned OFF (Fig. 5.8E shows an increase of 69%). In both conditions (ON and OFF), the mean OT-components are almost null compared to the mean DT obtained with the Encoder-ON (respectively

90% and 97% less). In the OFF condition, this can be attributed to the randomness of the motion. In the ON condition, combined with the increased DT force, this is an indication of the successful decoding strategies.

Fig. 5.9A shows the trajectories performed during the testing phase with the Encoder turned ON. Two distinct behaviors are distinguishable: if the pathway from the starting position to the target lies inside the same sensory regions we obtained an almost straight trajectory. On the other hand, when the controlled device crosses the border of one region, the systems oscillates along the border of the two adjacent regions. This particular behavior does not represent a decoding error but rather reflects the limitation of having only four different stimulation patterns encoding the information about the region in which the device is, disregarding the precise position inside it [Romo et al., 1998b], [Tehovnik, 1996].

The BMI converges to the target with 100% success, and it does so in a very stable and straight path because the decoded forces obtained in response to the same stimulation pattern are very similar to each other, both in terms of direction and magnitude. This is demonstrated in the compass plots in Fig. 5.9B showing that the decoded forces when the controlled object was in each region, used during the testing phase (black arrows) are almost overlapping. In order to further assess the neuromorphic decoding capabilities we also report the forces used to calibrate the BMI motor interface (colored thick arrows in Fig. 5.9B) that, especially in terms of direction, are almost equal to most of the related forces decoded during the BMI run.

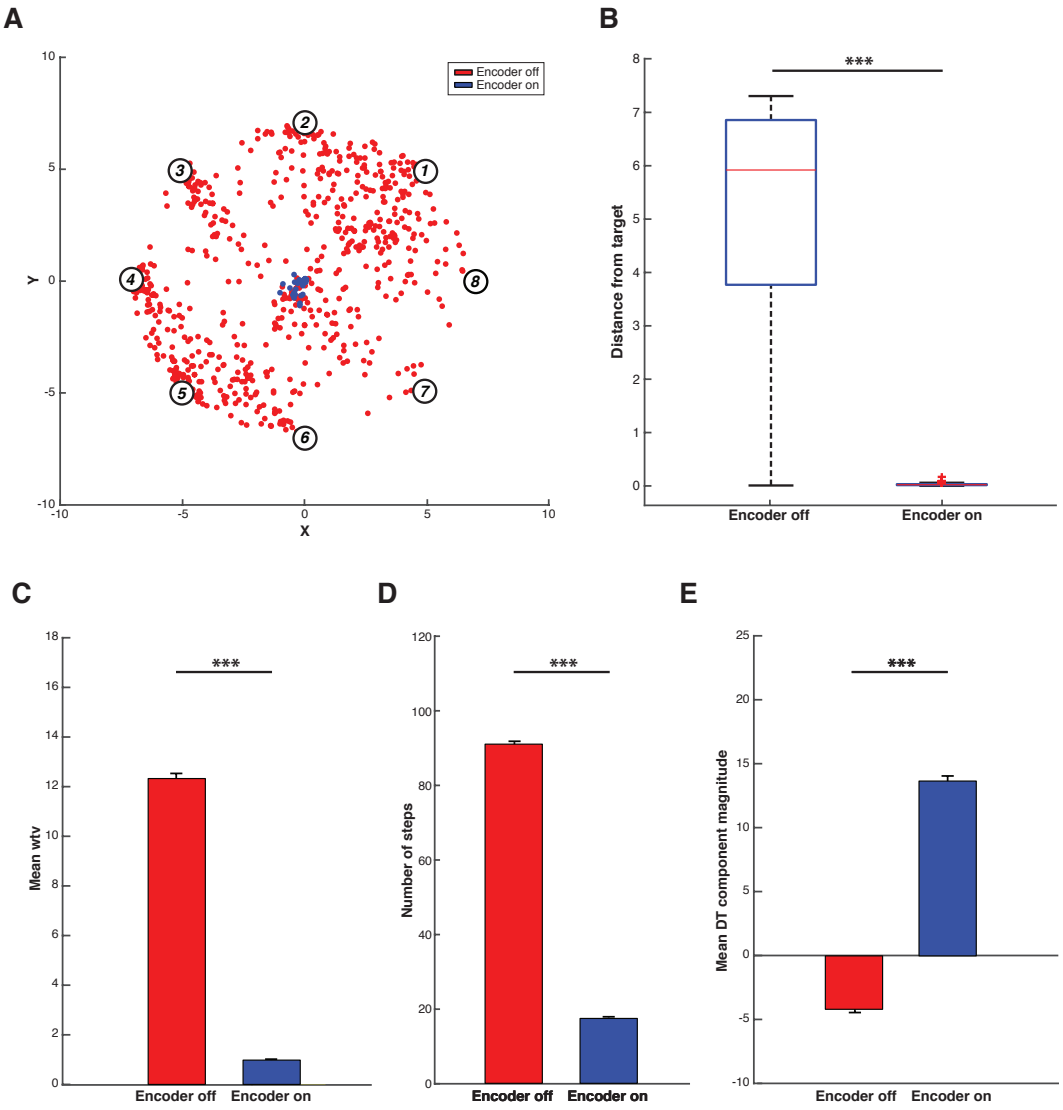

Fig. 5.8: *A. Trajectories' closest points to the target. Red dots indicate the closest points to the target with the Encoder switched OFF while blue are with the Encoder ON. Data were collected by running the BMI 100 times initializing it from each of the 8 predefined initial positions (indicated by the numbered colored circles) both with the Encoder turned ON and OFF. B. Box plots of the trajectories closest points distributions with the encoder ON and OFF. C. Mean wtv ± SEM of all the 800 trajectories recorded both with the Encoder turned ON (blue bar) and OFF (red bar). D. Mean number of steps to convergence ± SEM. The red bar, obtained with the Encoder turned OFF, is quite close to the maximum step allowed (100 steps) while when the Encoder is active the steps number necessary to reach the target region is significantly lower. E. Mean DT component magnitude ± SEM. Each decoded force has been split into Directed to the target - DT (magnitude of the force that points towards the target) and Orthogonal to the target - OT one (part of the force perpendicular to the directive component). The mean magnitude of the DT component obtained from forces generated with the Encoder turned off (red bar)is much higher than when the Encoder activated (blue bar). (two sample t-test, $^{***}p < 0.001$)*

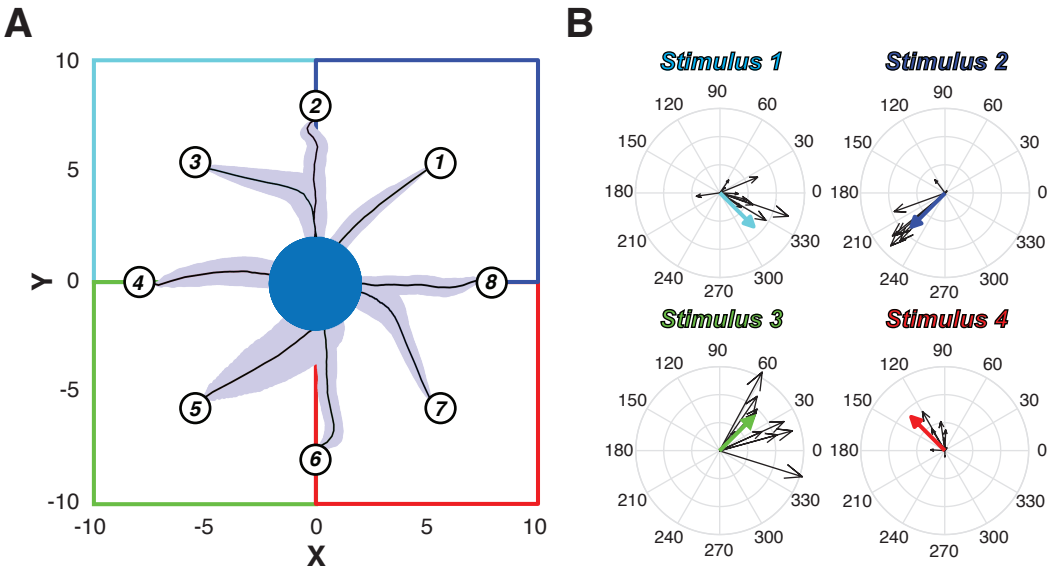

Fig. 5.9: *A. Mean trajectories plot. Paths resulting from the average of all the performed trajectories. Light blue areas represent the covariance of the trajectories along different trials. The workspace is subdivided into four sensory regions, one per each stimulation, highlighted by four different colors B. Decoded forces computed during the BMI test phase. Forces are grouped on the basis of the stimulus that generates them.*

5.5 Alternative decoding with an off-chip computational layer

The addition of "stop learning" on the ROLLS' neural network, allowed the use of the chip's output with no post-processing of its activity. Prior to this, an alternative method of decoding the recorded brain activity was developed and tested. In this method, the patterns were decoded partly by the chip, and partly, at a second stage off the chip. The network on the chip itself and the protocol for training was the same as the purely on-chip decoding method, differing only in the parameters of the synaptic and neuronal circuits mainly resulting in the absence of a strong "stop learning" property subsection 5.4.6.

The transformation that yields, from the chip's output, the resultant force that acts on the end effector was found in three steps:

1. Finding the transformation of the chip's spiking output to forces

   To find the resultant force F_k associated with a decoded motocortical recording k, we weighted the four component forces f_i by the probability P_{ki} that the recording was caused by each of the four associated stimuli S_i.

   $$F_k = \sum_{i=1}^{4} (P_{ki} \cdot f_i) \tag{5.1}$$

   To translate the spiking output of the ROLLS into these probabilities P_{ki}, we found the probability coefficients p_{jki} associated with each perceptron j and averaged over all $N = 252$ output neurons. Each output neuron is trained and used similarly to a perceptron, so we refer to them as "perceptrons" in the following paragraphs.

   $$P_{ki} = \frac{\sum_{j=1}^{N} p_{jki}}{N} \tag{5.2}$$

   We found these four probabilities for each decoded pattern k from each perceptron j as a function of the number of spikes R output by the perceptron in response to the pattern. We approximated this function by use of the training dataset: for each class i at every level of output spike count R, we found the number of training patterns ${}_{tr}M_i^R$ that caused this spike count and simultaneously belonged to class i, as a fraction of all the training patterns ${}_{tr}M^R$ that caused this spike count.

   $$p_{jki}(R) = \frac{{}_{tr}M_i^R}{{}_{tr}M^R} \tag{5.3}$$

2. Mapping forces to stimuli

   Among the different possible one-to-one mappings of component forces f_j to

stimuli i ($4! = 24$ possible mappings), we selected the mapping $f_j \mapsto S_i$ that minimizes the difference of the resultant force $E[F_i]$ expected to be decoded after stimulus S_i, from the component force f_j that is mapped to the stimulus.

$$f_j \mapsto S_i : i = \underset{j \in [1,4]}{\arg\min} \left(E[F_j] - f_j \right) \tag{5.4}$$

For each stimulus S_i we calculate $E[F_i]$, by using the training set:

$$E[F_i] = \frac{\sum_{k_i=1}^{{}_{tr}M_i} \left({}_{tr}F_{k_i} \right)}{{}_{tr}M_i} \tag{5.5}$$

where patterns k_i are the training patterns that are caused by stimulus S_i, ${}_{tr}M_i$ is their number, and F_{k_i} is the decoded force.

3. Transforming the target force field to best match the recorded activity

   The four component forces of the desired field are so far orthogonal, while the four classes of motocortical recordings are not necessarily so. Therefore, to best match the recorded activity with the force field, we reshaped the force field. Specifically, we associated a new component force g_i with stimulus S_i such that it equals the expected force:

$$g_i = E[F_i] \tag{5.6}$$

   Thus, ultimately, by replacing f_i with g_i in equation (5.1), the resultant force G_k associated with a decoded motocortical recording k becomes:

$$G_k = \sum_{i=1}^{4} \left(P_{ki} \cdot g_i \right) \tag{5.7}$$

5.5.1 Testing the system

The output Perceptron behaves as a binary classifier, i.e. it votes on whether the presented pattern is of the class of data it was trained to represent. In our case, we had a total of four classes, and the Perceptron recognizes the pattern as belonging to its corresponding class if its output is higher than a threshold θ.

The output of an *ensemble* of binary classifiers is commonly taken as the class that receives the majority of positive votes. The threshold θ is therefore important for minimizing the error rate of the ensemble of classifiers. In our experiments we determined this threshold by minimizing the number of false positives and maximizing the number of true positives in the responses by use of each perceptron's Receiver-Operator Characteristic (ROC) curve. We performed this characterization

on a subset of the training dataset to preserve cross-validation standards.

We modified the standard perceptron ensemble voting technique based on the following realizations:

(a) A spiking perceptron's activation function is not binary, but real-valued. A perceptron's output firing rate is an expression of its degree of confidence on its positive or negative verdict.

(b) A perceptron intended to be trained to vote positively on a particular class, is collaterally trained to vote and does vote also on the other ones, positively or negatively depending on the degree of overlap of the features of different classes.

(c) A perceptron trained and voting on a particular segmentation of the data space is voting collaterally also on all other possible segmentations. For example, suppose a perceptron trained to represent the first of the four classes of neural activity patterns. A negative verdict with respect to its corresponding class upon the presentation of an example signifies a collateral positive verdict for the superclass that contains the other three classes.

(d) Combining (c) with (b) above, a perceptron's positive or negative vote concerning a collateral class respectively deducts or adds confidence to the perceptron's unary vote on its own class, thus yielding an aggregate confidence on this class. Symmetrically, the perceptron expresses an aggregate confidence on the rest of the classes too.

Addressing point (a), we defined the degree of confidence ${}^{P}C_i^k$ on a perceptron's i^{th} verdict on a pattern p concerning a class k as a function of the firing rate FR as the proportion of correct verdicts given during the second phase of training at this firing rate, with a negative sign for negative verdicts:

$${}^{P}C_i^k(FR) = \frac{N_{True\_Positives}(FR) - N_{True\_Negatives}(FR)}{N_{Total}(FR)}$$

Addressing point (b), we found this firing rate-confidence function for all four classes of patterns for each perceptron. Addressing points (c) and (d), we defined aggregate confidence ${}^{P}q_i^k$ of a perceptron i for a pattern p concerning a class k as a function of the perceptron's unary confidences concerning all N classes j as:

$${}^{P}q_i^k = \frac{\sum_{j=1}^{N}[(2 \cdot \delta_{jk} - 1) \cdot {}^{P}C_i^j]}{\sum_{j=1}^{N} \left| {}^{P}C_i^j \right|}$$

where the denominator is for normalizing purposes and $\delta_{jk} = \begin{cases} 1 & \text{if } j = k \\ 0 & \text{if } j \neq k. \end{cases}$

5.5.2 Classification results

While *all four* component forces contributed to the decoding, we evaluated the classifier by measuring its performance in correctly outputting the *single* stimulus class that caused each of the presented recording patterns. This was the class that corresponded to the ensemble of output neurons that output the most spikes during the presentation of the input pattern, selected from the four ensembles of neurons. The evaluation was performed by use of a set of 10 recordings per class, that were not included in the training set. By training and testing the decoder 30 times, each with a random segregation between the training and the testing set, we obtained a classification performance on the testing set of up to 80% correct (average 69% correct). Example raster plots of the chip's output and the confusion matrix of the classification are shown in Figure 5.10.

Using the maximally active ensemble of output neurons to classify the patterns, without the additional processing, yielded performances of 40% to 60% correct, indicating a significant improvement in performance by the added computational layer.

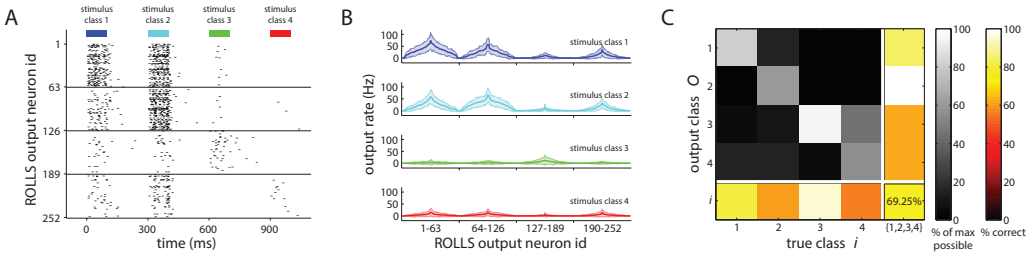

Fig. 5.10: ***Classification results.*** *(A) Raster plot of the output of the ROLLS chip during presentation of four example recordings each resulting from a different type of stimulus. It is visible that during presentation of the three examples belonging to classes 1, 2, and 4, the most active group of output neurons corresponds to the true class of the input. During presentation of the example that belongs to class 2, the maximally active output group alone does not give a clear result, as groups 1-63 and 64-126 both respond strongly. Nevertheless, the distribution of output spikes across all neurons is visibly different between any two of the four examples. (B) Output spike rate for all input recordings, for each output neuron. Each coloured graph shows output for one input class. Average and standard deviation are shown. In the figure, output neurons (horizontal axis) are sorted within each 63-neuron group according to their average response to the group's corresponding class. The output rate either of single neurons or of ensembles of 63 similarly-trained neurons largely overlaps between inputs of different classes. The distribution of output rates across all 252 neurons has comparatively less overlap between the different input classes. This is because all neurons were trained on the same input space, albeit different segmentations thereof, due to different teaching signals and device mismatch. Therefore each of the 252 neurons provides additional information about each point in the input space. Hence, the ensemble of all 252 neurons was used as a classifier. (C) Confusion matrix, for results averaged over 20 different partitionings of the recording dataset into training and testing subsets. The rows correspond to the class output by the classifier, and the columns show the true class. In grayscale colour-coding, the diagonal cells show for what percentage of the examples the classifier correctly estimates the class of the input recording, while the off-diagonal cells show where the classifier has made mistakes. In heat colour-scale, the far-right column shows the accuracy for each output class, while the row at the bottom shows the accuracy for each true class. The cell in the bottom right shows the overall accuracy, which in average was 69.25%, with maximum achieved performance of 85%, contrasted to chance-level classification performance at 25% for four equinumerous classes.*

5.5.3 Discussing the off-chip computations

In this method we attempted to determine what exploitable information is contained in the output of the neural network's first layer and what computations the layers thereafter should do to exploit the information and express it in an interpretable way, in a task of assigning probabilities to potential classes to which a classified pattern may belong. These points are essentially the following.

(1) The most firing unit (argmax) of a last layer with n units needs to be the one that corresponds to the class with the maximum probability to be true. For this to be the case, several conditions need to be met:

   (a) The activation functions of the n units need to be increasing functions of the probability of the unit's corresponding class,

   (b) The n activation functions need to be the same, and

   (c) The inputs to this layer (outputs from the first layer) need to be normalized (i.e. not of unequal energies among the classes).

(2) The output of each of the neurons in the first layer contains information concerning all of the classes and not just one of them, and this information can be exploited.

(3) The information that only one class can be true for each pattern should also be taken into consideration.

One added layer with three perceptrons could take care of point (2), by connecting each of the output neurons in layer one to all of the n perceptrons in layer two. However, the rest of the requirements make a neuromorphic implementation of such a decoding scheme non-trivial. Specifically, point (1a) requires a neural activation function that is dependent on the data; point (1b) would need elimination of mismatch between neurons; (1c) could be implemented by recurrent inhibition to normalize the first layer's output; and point (3) could be implemented by a third layer of three perceptrons where each of them would be excited by one of the second layer's perceptrons and inhibited by the other two, or, alternatively, a winner-take-all type of competition in a recurrent implementation.

So, theoretically, a neural implementation of these computations is possible, even though not with a two-layer feed-forward network, not with neurons that cannot learn their own activation function, and not with significant device mismatch in the electronic elements of the neuromorphic circuits.

5.6 Discussion

5.6.1 Recapitulation of the BMI's neuromorphic aspect

This BMI implementation demonstrates the applicability of neuromorphic hardware in BMIs, in the first demonstration of this kind. In particular, the Decoder module of the BMI was implemented by a spiking neural network on a mixed analog-digital neuromorphic processor, the ROLLS, that learned on line to decode the neural recordings into commands addressing the brain-controlled device. The analog neuromorphic circuits of the ROLLS neuromorphic processor emulate functions of biological neurons and synapses by replacing biophysical properties with analogous properties of the sub-threshold physics of transistors. The resulting spiking neural networks operate on a power-efficient and compact system for applications of pattern recognition such as a BMI Decoder's task. On the other hand, because of these underlying principles of operation, analog neuromorphic circuits like the ones found on the ROLLS are imprecise and variable, similar to biological neural elements, in sharp contrast to simulations of spiking neurons and synapses on digital neuromorphic or general-purpose processors. The neuromorphic decoding task was further complicated by the recorded data. The to-be-decoded motor activity was highly variable, sparse, and with strong similarities between the to-be-discriminated classes. Further difficulty arose by the fact that the Decoder's task was not a standard classification task, as the BMI required the Decoder to output a contribution of all potential classes of recorded activity simultaneously, while preventing the average chip output from being biased towards any pair of classes, even though the pair-wise similarities between classes were biased.

Despite these particularities, the spiking network we designed successfully learned to perform the decoding task, enabling the BMI to perform at similar levels of a previous non-neuromorphic version of the bidirectional BMI. This was achieved by exploiting two key characteristics of the ROLLS chip: variability between silicon synapses and neurons deployed into an ensemble learning technique that aggregated multiple weak classifiers into a powerful one, and the heterosynaptic competition through the "stop-learning" feature of synapses on the ROLLS chip, which enabled the network to focus on the discriminative features of the input, thus both improving classification performance and reducing the reflection of biased similarities in the input onto the output of the trained network. A key feature of the Decoder is that the spiking output of the neuromorphic chip is directly used to compute the force controlling the end-effector. The components of the force were weighted by the spike counts of the chip's output, an important step towards using neuromorphic hardware not only as a Decoder, but also a prosthetics controller.

5.6.2 Strengths of the presented neuromorphic Decoder

Our set-up is not only a proof of concept with regards to future applications of neuromorphic hardware, but also demonstrates and reaffirms what is possible here at present on a single neuromorphic chip. First, it shows that integration of neuromorphic hardware in set-ups characterized by the intricacy of a bidirectional BMI is technically possible. Second, even though the time-varying aspect of the recorded patterns was transformed into a spatial representation, the BMI set-up did demonstrate that a neuromorphic chip can recognize multi-dimensional input patterns. Third, our work demonstrates that neuromorphic hardware can perform a pattern recognition task while satisfying abstract, high-level constraints. This is demonstrated in our set-up by the fact that even though forces decoded from individual recordings could strongly deviate from the target (Fig. 5.9 B) due to the contributions of all four force components combined with unbalanced inputs (Fig. 5.5), average forces over the controlled object's trajectory did not (Fig. 5.9 A) as the chip was able to balance the average contributions of the forces in the long term (Fig. 5.4.8 of kept largely unbiased during the trajectories (see also subsection 5.4.8). Fourth, our work demonstrates that these computationally demanding tasks can be *learned* by the neuromorphic hardware itself as opposed to learning off the chip and subsequently configuring the network's connectivity. Fifth, the ROLLS chip shows that neuromorphic hardware needs not be fabricated *ad hoc* for a particular application, but can instead be configurable to match the particularities of multiple applications. Sixth, the fact that in our set-up the spike counts of our neuromorphic Decoder's output are directly used to weight the force coefficients, demonstrates that a single neuromorphic chip can be a multi-purpose element, simultaneously acting both as a Decoder and as a controller of an appropriately interfaced prosthetic device. Sixth, the chip decodes the brain activity on line in the BMI's loop, within one time step of the dynamical system's operation, whose bottleneck is determined not by the Decoder, but by the inter-stimulus interval. Seventh, the chip operates on very low power consumption, of the order of $4\,mW$, much lower than a general-purpose computer running pattern recognition software. Last but not least, its size of $51.4\,mm^2$ makes it much smaller than a conventional computer. It is worth noting however, that in the current set-up the neuromorphic chip is interfaced through additional devices that allow high configurability of the chip, and multiple readouts for debugging, but consumes additional relatively high power and area, as it is not optimized for power consumption and size.

5.6.3 Limitations of the system and proposed future additions

The simplicity of the single-layer feed-forward network of only 252 neurons that was employed for this particular application demonstrates the computational power of spiking neural networks and suggests that further development of analog neuromorphic hardware and spike-based algorithms may yield a computationally powerful, yet low-power consuming alternative to software and conventional processors for a broad spectrum of tasks. With respect to the neuromorphic BMI Decoder in particular, further work could enable two specific improvements and additions.

Firstly, the present implementation addresses the complex temporal dynamics of the recordings with a processing step between the neural recording and the output layer of the neural network performed off-chip. In the future it could be implemented by one or more layers of silicon neurons. In this way, the chip could directly receive the recorded spike train, and operate on it with no need for an intermediate off-chip storage step. This would be possible because of the ROLLS' real-time operation, with time constants that match those of real neurons.

Secondly, the fact that the network learns on line could be used to allow the Decoder to adapt to changes in the neural responses with time. Specifically, in the current implementation, the Decoder updates itself incrementally after the presentation of each training pattern. Training inputs are combined with a teacher signal that biases different neurons to strengthen or weaken their connections to different features of the input, through imposing different levels of output firing during the presentation of different input classes. After training, we use the chip to decode new recordings of brain activity. In a future implementation, learning could continue during the chip's use as a trained Decoder. As the trained silicon neurons respond with high firing rates to their corresponding input classes, and with lower rates to the other classes, the neurons could bias themselves to continue correctly adapting their synapses to the input patterns in the absence of an externally provided teacher signal. This would be made possible after tuning the parameters of STDP synaptic dynamics of the ROLLS to enable potentiation and depression in the ranges of firing rate that the trained neurons maintain.

On a separate but related note, here we framed the input patterns between specific time points that define the patterns' beginning and end. However, the chip itself does not have an internal clock that has to be synchronized with those time points. It rather recognizes inputs in which time represents itself in the spike train's statistics. This implies that the chip could be used to decode recordings in future BMI set-ups that operate continuously, rather than in discrete time steps. To this end, removing any off-chip transformation that intermediates the input as discussed above would be essential.

In this chapter we described the testing of the BMI by modifying a well-established

experimental set-up with the goal of exploring the impact of inserting a neuromorphic Decoder in such a closed-loop system. This experimental configuration with anesthetized rats is not using any volitional input from the subjects. However, the current BMI is designed for future experiments with behaving subjects controlling the movements of a small mobile cart connected to a water or food dispenser. The unique characteristics of the neuromorphic Decoder could allow our bidirectional BMI to integrate the volitional component of brain activity in the decoding scheme, allowing a behaving rat to control the movements of the dynamical system.

Chapter 6

Discussion

In summary, the work presented in this thesis was concerned with the study of interactions between cognitive and automatic components of sensory-motor systems.

In particular, in chapter 2, we simulated a system consisting of a musculoskeletal joint equipped with proprioceptive sensors, moved initially by a source of tightly constrained motor commands, and later by a separate source of goal-directed motor commands. The later source was equipped with two forms of learning; firstly, a classification of sensory feedback from the joint's movements, from which goals for the commands were selected; and, secondly, an error-based learning of the sensory-motor transformations yielding the motor commands from the sensory goals. From these properties of the simulated early and late motor controllers which are akin to properties of the spinal cord and the cerebral cortex, a mechanism emerged that allowed the early simulated spinal reflexes to influence the types of movements learned by the cortex. In addition, lesioning the system by deactivating the early spinal reflexes, hindered the sensory-motor learning of the cortex in both accuracy and speed.

In chapter 3, we used an experimental set-up, whereby human subjects were instructed to inhibit their endogenous, spontaneous eye blinks for varying periods of time. EMG recordings allowed us to detect and time their blinks. The analysis of the post-inhibition blink latency distributions gave us access to the mechanism through which voluntary inhibition acts on the automatic eye blink generator. Specifically, the experiment revealed that the blink generator is turned off and reset by the voluntary inhibition, resulting in a post-inhibition excitatory effect expressed as a blink.

In chapter 4, volunteers reacted to unpredictably provided tactile stimuli to the fingertip by clicking a mouse button. By again timing eye-blinks through EMG, and by comparing stimulus-to-blink latency distributions to theoretical ones generated based on inter-stimulus and inter-blink intervals, we conclude that the reaction task influences eye-blinks, specifically by introducing a trigger to individual blinks.

Finally, in chapter 5, we configured a neuromorphic chip to learn to decode the

spiking activity recorded in the motor cortex of a rat so as to successfully control an object in a closed-loop bidirectional brain-machine interface.

The implications of our results are multiple. For instance, the fact that the cortex recruits spinal circuits to implement its motor commands, makes it commonly thought of as hierarchically higher than the spinal cord. However, mechanisms similar to our "reflex-tutored cortical motor control" presented in chapter 2 may provide a means for the developmentally and evolutionarily faster to mature levels of the neuraxis, like the spinal cord, to oversee the development of later ones, like the cortex, thus creating a parallel, inverse hierarchy.

In addition, while here the artificial, simulated system was used to enable us to flexibly study the biological system, the results reveal that the mechanism is beneficial to the system, and that the early-active controller can provide guidance to the types of movements that the later one learns to generate. This implies that an artificial system equipped with sensors, and a controller capable of learning, could benefit from a pre-programmed automatic controller, which could seed the learning-capable controller with sensations that describe the controlled body in its environment. Ultimately, this could be helpful for robotic controllers that could be attachable to different bodies or different environments and be able to quickly learn to properly control the bodies in the different conditions.

Our result in chapter 3 implies that voluntary inhibition may be able to completely shut off certain automatic motor processes, as opposed to pausing the automatic controllers or issuing commands to countermand the automatic commands after their generation. This may be indicative of how cognitive motor processes in the brain cooperate with or exploit automatic ones to achieve their own purpose.

The fact that a voluntary reaction task leads to the triggering of an automatic action, as was revealed in chapter 4, may imply that the generation of an anticipated action increases the excitability of the rest of the motor system, and while it is evidently expressed in eye blinking, it could be detectable in other tasks as well. The fact that the two controllers were functionally linked despite the lack of any apparent relationship between them, arguably even in terms of shared cognitive load given the automaticity of eye-blinks has additional significance. Specifically, it implies that, in certain multitasking paradigms, there may be yet unknown mechanisms influencing the decision whether and when to act.

The integration of a neuromorphic chip in a closed-loop sensory-motor system in chapter 5 demonstrates that in a hybrid system, the artificial counterpart can be the cognitive one. In the future, artificial neural hardware may permit the brain to off-load or augment its function.

The "reflex-tutoring" mechanism proposed and studied here through computational modelling and simulations emerges from biologically plausible ingredients.

However, future work should include attempts for validation through biological data. These data could originate for instance from the comparisons of adult movements between species or individuals with different reflexes. Alternatively, evidence for such a mechanism could potentially be uncovered by experimentally studying the effects of lesioning or modifying the circuits controlling developmentally early movements onto the properties and the learning of later movements. An interesting paradigm could involve the study of motor adaptation of adult individuals in a novel environment, after a period of exposure to sensory experiences provided by reflexes in that environment. All these potential sources of relevant biological data have inherent difficulties arising from the fact that the early and late motor controllers, e.g. spinal cord and cortex, are in a hierarchical relationship. As a consequence, any potential influences on the high-level motor control and learning in these paradigms, could be attributed to the recruitment of the changed low-level circuits instead of the tutoring of the high level by these low-level circuits. Our computational model did allow us to dissociate these alternatives, but in a future biological set-up, the experiment would have to be very cautiously designed to achieve the same.

In conclusion, our results propose possible design strategies for artificial and hybrid systems, while suggesting that automatic controllers could furnish new reductionistic experimental paradigms revealing of general principles of biological sensory-motor function.

References

Rick A Adams, Stewart Shipp, and Karl J Friston. Predictions not commands: active inference in the motor system. *Brain Structure and Function*, 218(3):611–643, 2013. ISSN 1863-2661. doi: 10.1007/s00429-012-0475-5. URL http://dx.doi.org/10.1007/s00429-012-0475-5.

Rocco Agostino, Matteo Bologna, Loredana Dinapoli, Bruno Gregori, Giovanni Fabbrini, Neri Accornero, and Alfredo Berardelli. Voluntary, spontaneous, and reflex blinking in Parkinson's disease. *Movement Disorders*, 23(5):669–675, 2008. ISSN 08853185. doi: 10.1002/mds.21887.

Hossein Ahmadzadeh and Ellips Masehian. Modular robotic systems: Methods and algorithms for abstraction, planning, control, and synchronization. *Artificial Intelligence*, 223:27–64, 2015. ISSN 00043702. doi: 10.1016/j.artint.2015.02.004.

Robert Ajemian, Alessandro D'Ausilio, Helene Moorman, and Emilio Bizzi. Why Professional Athletes Need a Prolonged Period of Warm-Up and Other Peculiarities of Human Motor Learning. *Journal of Motor Behavior*, 42(6):381–388, 2010. doi: 10.1080/00222895.2010.528262. URL http://dx.doi.org/10.1080/00222895.2010.528262.

K Akazawa, J W Aldridge, J D Steeves, and R B Stein. Modulation of stretch reflexes during locomotion in the mesencephalic cat. *The Journal of physiology*, 329:553–67, 1982. ISSN 0022-3751. doi: 10.1113/jphysiol.1982.sp014319. URL http://www.ncbi.nlm.nih.gov/pubmed/7143259{%}5Cnhttp://www.pubmedcentral.nih.gov/articlerender.fcgi?artid=PMC1224796.

Michael A Arbib. From Mirror Neurons to Complex Imitation in the Evolution of Language and Tool Use*. *Annual Review of Anthropology*, 40(1):257–273, 2011. doi: doi:10.1146/annurev-anthro-081309-145722. URL http://www.annualreviews.org/doi/abs/10.1146/annurev-anthro-081309-145722.

Amy F T Arnsten and Katya Rubia. Neurobiological circuits regulating attention, cognitive control, motivation, and emotion: Disruptions in neurodevelopmental psychiatric disorders, 2012. ISSN 08908567.

Friedemann Awiszus. Chapter 2 TMS and threshold hunting. In F Tergau M A Nitsche J G Rothwell U Ziemann W. Paulus and M Hallett, editors, *Supplements to Clinical Neurophysiology*, volume Volume 56, pages 13–23. Elsevier, 2003. ISBN 1567-424X. doi: http://dx.doi.org/10.1016/S1567-424X(09)70205-3. URL `http://www.sciencedirect.com/science/article/pii/S1567424X09702053`.

Paul Bach-y Rita and Stephen W. Kercel. Sensory substitution and the human-machine interface, 2003. ISSN 13646613.

Alan Baddeley. Working memory: theories, models, and controversies. *Annual review of psychology*, 63:1–29, 2012. ISSN 1545-2085. doi: 10.1146/annurev-psych-120710-100422. URL `http://www.ncbi.nlm.nih.gov/pubmed/21961947`.

Yoseph Bar-cohen and Cynthia Breazeal. Biologically Inspired Intelligent Robotics. In *Electroactive Polymer Actuators and Devices (EAPAD)*, volume 5051, pages 14–20, 2003. doi: 10.1117/12.484379.

Sliman J Bensmaia and Lee E Miller. Restoring sensorimotor function through intracortical interfaces: progress and looming challenges. *Nat Rev Neurosci*, 15 (5):313–325, may 2014. ISSN 1471-003X. URL `http://dx.doi.org/10.1038/nrn3724http://10.0.4.14/nrn3724`.

Brian D. Berman, Silvina G. Horovitz, Brent Morel, and Mark Hallett. Neural correlates of blink suppression and the buildup of a natural bodily urge. *NeuroImage*, 59(2):1441–1450, 2012. ISSN 10538119. doi: 10.1016/j.neuroimage.2011.08.050.

V Biousse, B C Skibell, R L Watts, D N Loupe, C Drews-Botsch, and N J Newman. Ophthalmologic features of Parkinson's disease. *Neurology*, 62(2):177–180, 2004. ISSN 0028-3878. doi: 10.1212/WNL.63.5.940.

N Birbaumer, N Ghanayim, T Hinterberger, I Iversen, B Kotchoubey, A Kübler, J Perelmouter, E Taub, and H Flor. A spelling device for the paralysed. *Nature*, 398(6725):297–298, 1999. ISSN 0028-0836. doi: 10.1038/18581. URL `http://www.nature.com/doifinder/10.1038/18581`.

Ambra Bisio, Natale Stucchi, Marco Jacono, Luciano Fadiga, and Thierry Pozzo. Automatic versus voluntary motor imitation: Effect of visual context and stimulus velocity. *PLoS ONE*, 5(10), 2010. ISSN 19326203. doi: 10.1371/journal.pone.0013506.

Clayton Blehm, Seema Vishnu, Ashbala Khattak, Shrabanee Mitra, and Richard W Yee. Computer vision syndrome: a review. *Survey of ophthalmology*, 50(3):253–262, 2005.

Mark S Blumberg. Developing Sensorimotor Systems in Our Sleep. *Current Directions in Psychological Science*, 24(1):32–37, 2015. doi: 10.1177/0963721414551362. URL http://cdp.sagepub.com/content/24/1/32.abstract.

Mark S. Blumberg, Hugo Gravato Marques, and Fumiya Iida. Twitching in sensorimotor development from sleeping rats to robots, 2013. ISSN 09609822.

I Bodis-Wollner, S F Bucher, and K C Seelos. Cortical activation patterns during voluntary blinks and voluntary saccades. *Neurology*, 53(8):1800–5, 1999. ISSN 0028-3878. doi: 10.1212/WNL.53.8.1800. URL http://www.ncbi.nlm.nih.gov/pubmed/10563631.

Boi, F. and Moraitis, T., V.D. Feo, F. Diotalevi, C. Bartolozzi, G. Indiveri, and A. Vato. A bidirectional brain-machine interface featuring a neuromorphic hardware decoder. *Frontiers in Neuroscience*, 10, 2016. ISSN 1662453X 16624548. doi: 10.3389/fnins.2016.00563.

J Borg, Lennart Grimby, and Jan Hannerz. Motor neuron firing range, axonal conduction velocity, and muscle fiber histochemistry in neuromuscular diseases. *Muscle & nerve*, 2(6):423–430, 1979.

Claude Bouchard and Robert M Malina. GENETICS OF PHYSIOLOGICAL FITNESS AND MOTOR PERFORMANCE. *Exercise and Sport Sciences Reviews*, 11(1), 1983. ISSN 0091-6331. URL http://journals.lww.com/acsm-essr/Fulltext/1983/01000/GENETICS{_}OF{_}PHYSIOLOGICAL{_}FITNESS{_}AND{_}MOTOR.11.aspx.

J Brader, W Senn, and S Fusi. Learning real world stimuli in a neural network with spike-driven synaptic dynamics. *Neural Computation*, 19:2881–2912, 2007.

Michael S Brainard and Allison J Doupe. What songbirds teach us about learning. *Nature*, 417(6886):351–358, 2002. URL http://dx.doi.org/10.1038/417351a.

Marcel Brass and Patrick Haggard. To do or not to do: the neural signature of self-control. *The Journal of neuroscience : the official journal of the Society for Neuroscience*, 27(34):9141–9145, 2007. ISSN 0270-6474. doi: 10.1523/JNEUROSCI.0924-07.2007. URL http://www.ncbi.nlm.nih.gov/sites/entrez?Db=pubmed{&}DbFrom=pubmed{&}Cmd=Link{&}LinkName=pubmed{_}pubmed{&}LinkReadableName=RelatedArticles{&}IdsFromResult=

17715350{&}ordinalpos=3{&}itool=EntrezSystem2.PEntrez.Pubmed.Pubmed{_}ResultsPanel.Pubmed{_}RVDocSum.

Marcel Brass and Patrick Haggard. The what, when, whether model of intentional action. *The Neuroscientist : a review journal bringing neurobiology, neurology and psychiatry*, 14(4):319–325, 2008. ISSN 1073-8584. doi: 10.1177/1073858408317417.

P R Burgess and F J Clark. Characteristics of knee joint receptors in the cat. *J Physiol*, 203(2):317–335, 1969. URL http://jp.physoc.org/content/203/2/317.abstract.

P A Burrough, P F M van Gaans, and R A MacMillan. High-resolution landform classification using fuzzy k-means. *Fuzzy Sets and Systems*, 113(1):37–52, 2000. doi: http://dx.doi.org/10.1016/S0165-0114(99)00011-1. URL http://www.sciencedirect.com/science/article/pii/S0165011499000111.

Blair Calancie, Belinda Needham-shropshire, Patrick Jacobs, Keith Willer, Gregory Zych, and Barth A. Green. Involuntary stepping after chronic spinal cord injury: Evidence for a central rhythm generator for locomotion in man. *Brain*, 117(5):1143–1159, 1994. ISSN 00068950. doi: 10.1093/brain/117.5.1143.

C Capaday and R B Stein. Amplitude modulation of the soleus H-reflex in the human during walking and standing. *The Journal of neuroscience : the official journal of the Society for Neuroscience*, 6(5):1308–1313, 1986. ISSN 0270-6474.

Maria D Caramia, Paola Cicinelli, Claudio Paradiso, Roberto Mariorenzi, Flora Zarola, Giorgio Bernardi, and Paolo M Rossini. 'Excitability' changes of muscular responses to magnetic brain stimulation in patients with central motor disorders. *Electroencephalography and Clinical Neurophysiology/Evoked Potentials Section*, 81(4):243–250, 1991. doi: http://dx.doi.org/10.1016/0168-5597(91)90009-M. URL http://www.sciencedirect.com/science/article/pii/016855979190009M.

R H S Carpenter. Oculomotor procrastination. *Eye movements: Cognition and visual perception*, pages 237–246, 1981.

Jorge G Cham, Sean A Bailey, Jonathan E Clark, Robert J Full, and Mark R Cutkosky. Fast and Robust: Hexapedal Robots via Shape Deposition Manufacturing. *The International Journal of Robotics Research*, 21(10):869–882, 2002. ISSN 0278-3649. doi: 10.1177/027836490202101083 7. URL http://ijr.sagepub.com/cgi/doi/10.1177/027836490202101083 7.

Anand R Chandrasekaran, Daniel T Plas, Ernesto Gonzalez, and Michael C Crair. Evidence for an Instructive Role of Retinal Activity in Retinotopic Map Re-

finement in the Superior Colliculus of the Mouse. *The Journal of Neuroscience*, 25(29):6929–6938, 2005. doi: 10.1523/jneurosci.1470-05.2005. URL `http://www.jneurosci.org/content/25/29/6929.abstract`.

J K Chapin, K A Moxon, R S Markowitz, and M A L Nicolelis. Real-time control of a robot arm using simultaneously recorded neurons in the motor cortex. *Nature Neuroscience*, 2(7):664–670, 1999. ISSN 1097-6256. doi: 10.1038/10223.

W J Chen and R E Poppele. Small-signal analysis of response of mammalian muscle spindles with fusimotor stimulation and a comparison with large-signal responses. *J Neurophysiol*, 41(1):15–27, 1978. URL `http://jn.physiology.org/content/41/1/15.abstract`.

Yi Chen, Enyi Yao, and Arindam Basu. A 128-Channel Extreme Learning Machine-Based Neural Decoder for Brain Machine Interfaces. *IEEE Transactions on Biomedical Circuits and Systems*, 10(3):679–692, 2016. ISSN 19324545. doi: 10.1109/TBCAS.2015.2483618.

Elisabetta Chicca, Fabio Stefanini, Chiara Bartolozzi, and Giacomo Indiveri. Neuromorphic electronic circuits for building autonomous cognitive systems. *Proceedings of the IEEE*, 102(9):1367–1388, sep 2014. ISSN 0018-9219. doi: 10.1109/JPROC.2014.2313954.

Jun Young Chung, Hyo Woon Yoon, Myung Sung Song, and HyunWook Park. Event related fMRI studies of voluntary and inhibited eye blinking using a time marker of EOG. *Neuroscience Letters*, 395(3):196–200, 2006. ISSN 03043940. doi: 10.1016/j.neulet.2005.10.094.

B. Clancy, R. B. Darlington, and B. L. Finlay. Translating developmental time across mammalian species. *Neuroscience*, 105(1):7–17, 2001. ISSN 03064522. doi: 10.1016/S0306-4522(01)00171-3.

Andy Clark and Rick Grush. Towards a Cognitive Robotics. *Adaptive Behavior*, 7 (1):5–16, 1999. ISSN 1059-7123. doi: 10.1177/105971239900700101.

Avis H Cohen, Serge Rossignol, Sten Grillner, et al. *Neural control of rhythmic movements in vertebrates*. Wiley, 1988.

D. K. Cong, M. Sharikadze, G. Staude, H. Deubel, and W. Wolf. Spontaneous eye blinks are entrained by finger tapping. *Human Movement Science*, 29(1):1–18, 2010. ISSN 01679457. doi: 10.1016/j.humov.2009.08.003.

Noah J Cowan, Emily J Ma, Mark Cutkosky, and Robert J Full. A Biologically Inspired Passive Antenna for Steering Control of a Running Robot. *Star*, pages 541– 550, 2005. ISSN 16107438.

Richard Stephen Creed, Derek Denny-Brown, John Carew Eccles, Edward George Tandy Liddell, and Charles Scott Sherrington. Reflex activity of the spinal cord. 1932.

Holk Cruse. The evolution of cognition—a hypothesis. *Cognitive Science*, 27(1): 135–155, 2003. ISSN 03640213. doi: 10.1016/S0364-0213(02)00110-6. URL http://doi.wiley.com/10.1016/S0364-0213(02)00110-6.

Antonio a V Cruz, Denny M Garcia, Carolina T Pinto, and Sheila P Cechetti. Spontaneous eyeblink activity. *The ocular surface*, 9(1):29–41, 2011. ISSN 15420124. doi: 10.1016/S1542-0124(11)70007-6. URL http://dx.doi.org/10.1016/S1542-0124(11)70007-6.

Antoine Cully, Jeff Clune, Danesh Tarapore, and J.-B. Mouret. Robots that can adapt like animals. *Nature*, pages 1–26, 2015. ISSN 0028-0836. doi: 10.1038/nature14422. URL http://arxiv.org/abs/1407.3501.

S Dangi, S Gowda, R Heliot, and Jose M Carmena. Adaptive Kalman Filtering for Closed-Loop Brain-Machine Interface Systems. In *5th International IEEE EMBS Conference on Neural Engineering*, pages 609–612, 2011.

Antonia F de C. Hamilton and Scott T. Grafton. The motor hierarchy: from kinematics to goals and intentions. *Sensorimotor foundations of higher cognition*, page pp. 381, 2007. ISSN 10752846. doi: DOI:10.1093/acprof:oso/9780199231447.003.0018. URL http://books.google.com/books?hl=en{&}lr={&}id=FfKIf{_}VZw{_}EC{&}oi=fnd{&}pg=PA381{&}dq=The+motor+hierarchy:+from+kinematics+to+goals+and+intentions{&}ots=OPntRO2gEm{&}sig=2VeV6{_}4Uyy4NzS{_}G1uOVQQAfBoI.

Jack De Havas, Arko Ghosh, Hiroaki Gomi, and Patrick Haggard. Voluntary motor commands reveal awareness and control of involuntary movement. *Cognition*, 155: 155–167, 2016.

Aymar de Rugy, Gerald E Loeb, and Timothy J Carroll. Muscle Coordination Is Habitual Rather than Optimal. *The Journal of Neuroscience*, 32(21):7384–7391, 2012. doi: 10.1523/jneurosci.5792-11.2012. URL http://www.jneurosci.org/content/32/21/7384.abstract.

Michel Desmurget, Nathalie Richard, Sylvain Harquel, Pierre Baraduc, Alexandru Szathmari, Carmine Mottolese, and Angela Sirigu. Neural representations of ethologically relevant hand/mouth synergies in the human precentral gyrus. *Proceedings of the National Academy of Sciences of the United States of America*,

111(15):5718–22, 2014. ISSN 1091-6490. doi: 10.1073/pnas.1321909111. URL http://www.ncbi.nlm.nih.gov/pubmed/24706796.

T E Dick, Y Oku, J R Romaniuk, and N S Cherniack. Interaction between central pattern generators for breathing and swallowing in the cat., 1993. ISSN 0022-3751.

M G Doane. Dynamics of the Human Blink. In Wolfgang Jaeger, editor, *Plastische Chirurgie der Lider und Chirurgie der Tr{ä}nenwege*, pages 13–17. J.F. Bergmann-Verlag, Munich, 1980. ISBN 978-3-642-87882-4. doi: 10.1007/978-3-642-87882-4_2. URL http://dx.doi.org/10.1007/978-3-642-87882-4{_}2.

Tobias H. Donner and Markus Siegel. A framework for local cortical oscillation patterns, 2011. ISSN 13646613.

John P Donoghue. Connecting cortex to machines: recent advances in brain interfaces. *Nature neuroscience*, 5 Suppl:1085–8, 2002. ISSN 1097-6256. doi: 10.1038/nn947. URL http://www.ncbi.nlm.nih.gov/pubmed/12403992.

Michael J. Doughty. Consideration of three types of spontaneous eyeblink activity in normal humans: during reading and video display terminal use, in primary gaze, and while in conversation. *Optometry and vision science : official publication of the American Academy of Optometry*, 78(October):712–725, 2001. ISSN 1040-5488. doi: 10.1097/00006324-200110000-00011. URL http://www.ncbi.nlm.nih.gov/pubmed/11700965.

M Doyle and R Walker. Curved saccade trajectories: voluntary and reflexive saccades curve away from irrelevant distractors. *Experimental brain research. Experimentelle Hirnforschung. Experimentation cerebrale*, 139(3):333–344, 2001. ISSN 00144819. doi: 10.1007/s002210100742.

George Charles Drew. Variations in reflex blink-rate during visual-motor tasks. *Quarterly Journal of Experimental Psychology*, 3(2):73–88, 1951.

Florin Dzeladini, Jesse van den Kieboom, and Auke Ijspeert. The contribution of a central pattern generator in a reflex-based neuromuscular model. *Frontiers in Human Neuroscience*, 8(June):1–18, 2014. ISSN 1662-5161. doi: 10.3389/fnhum.2014.00371. URL http://www.frontiersin.org/Human{_}Neuroscience/10.3389/fnhum.2014.00371/abstract.

Benoni B Edin. Cutaneous afferents provide information about knee joint movements in humans. *J Physiol*, 531(1):289–297, 2001. doi: 10.1111/j.1469-7793.2001.0289j.x. URL http://dx.doi.org/10.1111/j.1469-7793.2001.0289j.x.

T. Eggert, U. Sailer, J. Ditterich, and A. Straube. Differential effect of a distractor on primary saccades and perceptual localization. *Vision Research*, 42(28):2969–2984, 2002. ISSN 00426989. doi: 10.1016/S0042-6989(02)00392-9.

Irenäus Eibl-Eibesfeldt. The expressive behavior of the deaf-and-blind born. In *Social Comm. and Mov., Ed. I.*, pages 163–193. Academic Press, 1973.

C. Evinger, K. A. Manning, and P. A. Sibony. Eyelid movements: Mechanisms and normal data. *Investigative Ophthalmology and Visual Science*, 32(2):387–400, 1991. ISSN 01460404.

J A Eyre, J P Taylor, F Villagra, M Smith, and S Miller. Evidence of activity-dependent withdrawal of corticospinal projections during human development. *Neurology*, 57(9):1543–1554, 2001.

E. E. Fetz. Operant conditioning of cortical unit activity. *Science (New York, N.Y.)*, 163(3870):955–8, 1969. ISSN 0036-8075. doi: 10.1126/science.174.4007.431. URL `http://www.sciencemag.org/content/174/4007/431.abstract{%}5Cnhttp://www.ncbi.nlm.nih.gov/pubmed/4974291`.

Elisa Filevich, Simone Kühn, and Patrick Haggard. Neuroscience and Biobehavioral Reviews Intentional inhibition in human action : The power of ' no '. *Neuroscience and Biobehavioral Reviews*, 36(4):1107–1118, 2012a. ISSN 0149-7634. doi: 10.1016/j.neubiorev.2012.01.006. URL `http://dx.doi.org/10.1016/j.neubiorev.2012.01.006`.

Elisa Filevich, Simone Kühn, and Patrick Haggard. Negative motor phenomena in cortical stimulation: Implications for inhibitory control of human action, 2012b. ISSN 00109452.

Rico Fischer and Franziska Plessow. Efficient multitasking: parallel versus serial processing of multiple tasks. *Frontiers in psychology*, 6:1366, 2015. ISSN 1664-1078. doi: 10.3389/fpsyg.2015.01366. URL `http://www.pubmedcentral.nih.gov/articlerender.fcgi?artid=4561751{&}tool=pmcentrez{&}rendertype=abstract`.

Tamar Flash and Binyamin Hochner. Motor primitives in vertebrates and invertebrates, 2005. ISSN 09594388.

P W Fox, S L Hershberger, and T J Bouchard. Genetic and environmental contributions to the acquisition of a motor skill. *Nature*, 384(6607):356–358, 1996. ISSN 0028-0836. doi: 10.1038/384356a0. URL `http://www.nature.com/doifinder/10.1038/384356a0{%}5Cnpapers2://publication/doi/10.1038/384356a0`.

Gene Y. Fridman, Hugh T. Blair, Aaron P. Blaisdell, and Jack W. Judy. Perceived intensity of somatosensory cortical electrical stimulation. *Experimental Brain Research*, 203(3):499–515, 2010. ISSN 00144819. doi: 10.1007/s00221-010-2254-y.

Karl Friston. What is optimal about motor control? *Neuron*, 72(3):488–498, 2011.

A J Fuglevand, D A Winter, and A E Patla. Models of recruitment and rate coding organization in motor-unit pools. *J Neurophysiol*, 70(6):2470–2488, 1993. URL http://jn.physiology.org/content/70/6/2470.abstract.

Kentaro Fujita. On Conceptualizing Self-Control as More Than the Effortful Inhibition of Impulses. *Personality and Social Psychology Review*, 15(4):352–366, 2011. ISSN 1088-8683. doi: 10.1177/1088868311411165.

Kyosuke Fukuda. Analysis of eyeblink activity during discriminative tasks. *Perceptual and motor skills*, 79(3f):1599–608, 1994. ISSN 0031-5125. doi: 10.2466/pms.1994.79.3f.1599. URL http://www.ncbi.nlm.nih.gov/pubmed/7870552{%}5Cnhttp://www.amsciepub.com/doi/abs/10.2466/pms.1994.79.3f.1599.

Zoubin Ghahramani, Daniel M Wolpert, and Jordan Michale I. Computational models of sensorimotor integration. In Morasso Pietro and Sanguineti Vittorio, editors, *Advances in Psychology*, volume Volume 119, pages 117–147. North-Holland, 1997. ISBN 0166-4115. doi: 10.1016/s0166-4115(97)80006-4. URL http://www.sciencedirect.com/science/article/pii/S0166411597800064.

Joshua I. Gold and Michael N. Shadlen. The Neural Basis of Decision Making. *Annual Review of Neuroscience*, 30(1):535–574, 2007. ISSN 0147-006X. doi: 10.1146/annurev.neuro.29.051605.113038. URL http://www.annualreviews.org/doi/abs/10.1146/annurev.neuro.29.051605.113038.

Dale Goldhaber. *The Nature-nurture Debates: Bridging the Gap*. Cambridge University Press, 2012. ISBN 0521148790.

Robert Goldstein, Larry C. Walrath, John A Stern, and Barbara D. Strock. Blink activity in a discrimination task as a function of stimulus modality and schedule of presentation. *Psychophysiology*, 22(6):629–635, 1985. ISSN 0048-5772.

I. Greenhouse, a. Sias, L. Labruna, and R. B. Ivry. Nonspecific Inhibition of the Motor System during Response Preparation. *Journal of Neuroscience*, 35(30):10675–10684, 2015. ISSN 0270-6474. doi: 10.1523/JNEUROSCI.1436-15.2015. URL http://www.jneurosci.org/content/35/30/10675.abstract?etoc.

Anthony G Greenwald and Harvey G Shulman. On doing two things at once: II. Elimination of the psychological refractory period effect. *Journal of Experimental Psychology*, 101(1):70–76, 1973. ISSN 0022-1015. doi: 10.1037/h0035451. URL http://psycnet.apa.org/journals/xge/101/1/70/.

Patrick Haggard. Human volition: towards a neuroscience of will. *Nature reviews. Neuroscience*, 9(12):934–46, 2008. ISSN 1471-0048. doi: 10.1038/nrn2497. URL http://www.ncbi.nlm.nih.gov/pubmed/19020512.

Richard H R Hahnloser and Andreas Kotowicz. Auditory representations and memory in birdsong learning. *Current opinion in neurobiology*, 20(3):332–339, 2010. doi: http://dx.doi.org/10.1016/j.conb.2010.02.011. URL http://www.sciencedirect.com/science/article/pii/S0959438810000334.

Arthur Hall. The origin and purposes of blinking. *The British journal of ophthalmology*, 29(9):445, 1945.

Mark Hallett. Volitional control of movement: The physiology of free will, 2007. ISSN 13882457.

Eliot Hazeltine, Donald Teague, and Richard B. Ivry. Simultaneous dual-task performance reveals parallel response selection after practice. *Journal of Experimental Psychology: Human Perception and Performance*, 28(3):527–545, 2002. ISSN 1939-1277(Electronic);0096-1523(Print). doi: 10.1037/0096-1523.28.3.527. URL http://psycnet.apa.org/journals/xhp/28/3/527.pdf.

Leigh R Hochberg, Mijail D Serruya, Gerhard M Friehs, Jon A Mukand, Maryam Saleh, Abraham H Caplan, Almut Branner, David Chen, Richard D Penn, and John P Donoghue. Neuronal ensemble control of prosthetic devices by a human with tetraplegia. *Nature*, 442(7099):164–71, 2006. ISSN 1476-4687. doi: 10.1038/nature04970. URL http://www.ncbi.nlm.nih.gov/pubmed/16838014.

Leigh R. Hochberg, Daniel Bacher, Beata Jarosiewicz, Nicolas Y. Masse, John D. Simeral, Joern Vogel, Sami Haddadin, Jie Liu, Sydney S. Cash, Patrick van der Smagt, and John P. Donoghue. Reach and grasp by people with tetraplegia using a neurally controlled robotic arm. *Nature*, 485(7398):372–375, 2012. ISSN 0028-0836. doi: 10.1038/nature11076. URL http://dx.doi.org/10.1038/nature11076.

Bradley J. Holinski, Kevin A. Mazurek, Dirk G. Everaert, Richard B. Stein, and Vivian K. Mushahwar. Restoring stepping after spinal cord injury using intraspinal microstimulation and novel control strategies. In *Proceedings of the Annual International Conference of the IEEE Engineering in Medicine and*

Biology Society, EMBS, pages 5798–5801, 2011. ISBN 9781424441211. doi: 10.1109/IEMBS.2011.6091435.

K Hoshino. Ornstein-Uhlenbeck first-passage-time models for spontaneous eye blinking. In *Engineering in Medicine and Biology Society, 1996. Bridging Disciplines for Biomedicine. Proceedings of the 18th Annual International Conference of the IEEE*, volume 5, pages 1784–1785 vol.5, 1996. doi: 10.1109/IEMBS.1996.646254.

J Houk and W Simon. Responses of Golgi tendon organs to forces applied to muscle tendon. *J Neurophysiol*, 30(6):1466–1481, 1967. URL `http://jn.physiology.org/content/30/6/1466.short`.

James C. Houk and Steven P. Wise. Feature article: Distributed modular architectures linking basal ganglia, cerebellum, and cerebral cortex: Their role in planning and controlling action. *Cerebral Cortex*, 5(2):95–110, 1995. ISSN 10473211. doi: 10.1093/cercor/5.2.95.

Andrew D Huberman, Colenso M Speer, and Barbara Chapman. Spontaneous Retinal Activity Mediates Development of Ocular Dominance Columns and Binocular Receptive Fields in V1. *Neuron*, 52(2):247–254, 2006. doi: http://dx.doi.org/10.1016/j.neuron.2006.07.028. URL `http://www.sciencedirect.com/science/article/pii/S0896627306006258`.

Fumiya Iida and Auke Jan Ijspeert. Biologically Inspired Robotics. In *Springer Handbook of Robotics*, pages 2015–2034. Springer, 2016.

Auke Jan Ijspeert. Central pattern generators for locomotion control in animals and robots: A review. *Neural Networks*, 21(4):642–653, 2008. ISSN 08936080. doi: 10.1016/j.neunet.2008.03.014.

Yuri P Ivanenko, Richard E Poppele, and Francesco Lacquaniti. Motor Control Programs and Walking. *The Neuroscientist*, 12(4):339–348, 2006. doi: 10.1177/1073858406287987. URL `http://nro.sagepub.com/content/12/4/339.abstract`.

Robert a. Jacobs, Michael I. Jordan, Steven J. Nowlan, and Geoffrey E. Hinton. Adaptive Mixtures of Local Experts. *Neural Computation*, 3(1):79–87, 1991. ISSN 0899-7667. doi: 10.1162/neco.1991.3.1.79.

Beata Jarosiewicz, Steven M Chase, George W Fraser, Meel Velliste, Robert E Kass, and Andrew B Schwartz. Functional network reorganization during learning in a brain-computer interface paradigm. *Proceedings of the National Academy of Sciences*, 105(49):19486–19491, 2008.

Daniel Kahneman. *Attention and Effort*, volume 88. 1973. ISBN 0130505188. doi: 10.2307/1421603. URL http://www.jstor.org/stable/1421603?origin=crossref{%}5Cnhttp://www.citeulike.org/group/7631/article/4299238.

Nir Kalisman, Gilad Silberberg, and Henry Markram. The neocortical microcircuit as a tabula rasa. *Proceedings of the National Academy of Sciences of the United States of America*, 102(3):880–885, 2005. doi: 10.1073/pnas.0407088102. URL http://www.pnas.org/content/102/3/880.abstract.

Jaime Kaminer, Alice S Powers, Kyle G. Horn, Channing Hui, and Craig Evinger. Characterizing the spontaneous blink generator: an animal model. *Journal of Neuroscience*, 31(31):11256–11267, 2011. ISSN 0270-6474. doi: 10.1523/JNEUROSCI.6218-10.2011.

C N Karson. Spontaneous eye-blink rates and dopaminergic systems. *Brain : a journal of neurology*, 106 (Pt 3):643–653, 1983. ISSN 0006-8950. doi: 10.1093/brain/106.3.643.

C N Karson, R a Dykman, and S R Paige. Blink rates in schizophrenia. *Schizophrenia bulletin*, 16(2):345–354, 1990. ISSN 0586-7614. doi: 10.1002/ana.410120614.

Rustem Khazipov and Heiko J. Luhmann. Early patterns of electrical activity in the developing cerebral cortex of humans and rodents, 2006. ISSN 01662236.

Rustem Khazipov, Anton Sirota, Xavier Leinekugel, Gregory L Holmes, Yehezkel Ben-Ari, and Gyorgy Buzsaki. Early motor activity drives spindle bursts in the developing somatosensory cortex. *Nature*, 432(7018):758–761, 2004. doi: http://www.nature.com/nature/journal/v432/n7018/suppinfo/nature03132_S1.html. URL http://dx.doi.org/10.1038/nature03132.

Jens Kober, J Andrew Bagnell, and Jan Peters. Reinforcement learning in robotics: A survey. *The International Journal of Robotics Research*, 32(11):1238–1274, aug 2013. ISSN 0278-3649. doi: 10.1177/0278364913495721. URL http://journals.sagepub.com/doi/abs/10.1177/0278364913495721.

Kurt Konolige, Motilal Agrawal, Robert Bolles, Cregg Cowan, Martin Fischler, and Brian Gerkey. Outdoor Mapping and Navigation Using Stereo Vision. *Experimental Robotics*, 39:179–190, 2008. doi: 10.1007/978-3-540-77457-0_17.

Donald R Korb, David F Baron, John P Herman, Victor M Finnemore, Joan M Exford, Jeannette Londono Hermosa, Charles D Leahy, Thomas Glonek, and Jack V Greiner. Tear film lipid layer thickness as a function of blinking. *Cornea*, 13(4):354–359, 1994.

Konrad P Körding and Daniel M Wolpert. Bayesian decision theory in sensorimotor control. *Trends in Cognitive Sciences*, 10(7):319–326, 2006. doi: http://dx.doi.org/10.1016/j.tics.2006.05.003. URL `http://www.sciencedirect.com/science/article/pii/S1364661306001276`.

Simone Kühn, Patrick Haggard, and Marcel Brass. Intentional inhibition: How the "veto-area" exerts control. *Human Brain Mapping*, 30(9):2834–2843, 2009. ISSN 10659471. doi: 10.1002/hbm.20711.

A Kurjak, N Vecek, T Hafner, T Bozek, B Funduk-Kurjak, and B Ujevic. Prenatal diagnosis: what does four-dimensional ultrasound add?, 2002. URL `http://www.degruyter.com/view/j/jpme.2002.30.issue-1/jpm.2002.008/jpm.2002.008.xml`.

Mikhail A Lebedev and Miguel A L Nicolelis. Brain-machine interfaces: past, present and future. *TRENDS in Neurosciences*, 29(9):536–546, 2006.

Roger N Lemon. Descending pathways in motor control. *Annual review of neuroscience*, 31(Cm):195–218, 2008. ISSN 0147-006X. doi: 10.1146/annurev.neuro.31.060407.125547. URL `http://www.ncbi.nlm.nih.gov/pubmed/18558853`.

Alicja Lerner, Anto Bagic, Takashi Hanakawa, Eilis A. Boudreau, Fernando Pagan, Zoltan Mari, William Bara-Jimenez, Murat Aksu, Susumu Sato, Dennis L. Murphy, and Mark Hallett. Involvement of insula and cingulate cortices in control and suppression of natural urges. *Cerebral Cortex*, 19(1):218–223, 2009. ISSN 10473211. doi: 10.1093/cercor/bhn074.

J Levy and H Pashler. Is dual-task slowing instruction dependent? *Journal of experimental psychology. Human perception and performance*, 27(4):862–869, 2001. ISSN 0096-1523. doi: 10.1037/0096-1523.27.4.862.

M. Anthony Lewis, Ralph Etienne-Cummings, Mitra J. Hartmann, Zi Rong Xu, and Avis H. Cohen. An in silico central pattern generator: Silicon oscillator, coupling, entrainment, and physical computation. *Biological Cybernetics*, 88(2):137–151, 2003. ISSN 03401200. doi: 10.1007/s00422-002-0365-7.

Mei-Ching Lien and Robert W Proctor. Stimulus-response compatibility and psychological refractory period effects: Implications for response selection. *Psychonomic Bulletin & Review*, 9(2):212–238, 2002. ISSN 1069-9384. doi: 10.3758/BF03196277.

Dan Liu and Emanuel Todorov. Evidence for the Flexible Sensorimotor Strategies Predicted by Optimal Feedback Control. *The Journal of Neuroscience*, 27

(35):9354–9368, 2007. doi: 10.1523/jneurosci.1110-06.2007. URL http://www.jneurosci.org/content/27/35/9354.abstract.

Brian M. London, Luke R. Jordan, Christopher R. Jackson, and Lee E. Miller. Electrical stimulation of the proprioceptive cortex (area 3a) used to instruct a behaving monkey. *IEEE Transactions on Neural Systems and Rehabilitation Engineering*, 16(1):32–36, 2008. ISSN 15344320. doi: 10.1109/TNSRE.2007.907544.

Sarah E London and David F Clayton. Functional identification of sensory mechanisms required for developmental song learning. *Nat Neurosci*, 11(5):579–586, 2008. doi: http://www.nature.com/neuro/journal/v11/n5/suppinfo/nn.2103_S1.html. URL http://dx.doi.org/10.1038/nn.2103.

Arthur Mackert, Charles Woyth, Klaus Malte Flechtner, and Hans Peter Volz. Increased blink rate in drug-naive acute schizophrenic patients. *Biological Psychiatry*, 27(11):1197–1202, 1990. ISSN 00063223. doi: 10.1016/0006-3223(90)90417-Z.

Arthur Mackert, Klaus Malte Flechtner, Charles Woyth, and Konrad Frick. Increased blink rates in schizophrenics. influences of neuroleptics and psychopathology. *Schizophrenia Research*, 4(1):41–47, 1991. ISSN 09209964. doi: 10.1016/0920-9964(91)90008-F.

J. H. Mackintosh, R. Kumar, and T. Kitamura. Blink rate in psychiatric illness. *British Journal of Psychiatry*, 143(1):55–57, 1983. ISSN 00071250. doi: 10.1192/bjp.143.1.55.

Karen A Manning, Lorrin A Riggs, and Julieane K Komenda. Reflex eyeblinks and visual suppression. *Perception & psychophysics*, 34(3):250–256, 1983.

N. T. Markov, M. M. Ercsey-Ravasz, A. R. Ribeiro Gomes, C. Lamy, L. Magrou, J. Vezoli, P. Misery, A. Falchier, R. Quilodran, M. A. Gariel, J. Sallet, R. Gamanut, C. Huissoud, S. Clavagnier, P. Giroud, D. Sappey-Marinier, P. Barone, C. Dehay, Z. Toroczkai, K. Knoblauch, D. C. Van Essen, and H. Kennedy. A weighted and directed interareal connectivity matrix for macaque cerebral cortex. *Cerebral Cortex*, 24(1):17–36, 2014. ISSN 10473211. doi: 10.1093/cercor/bhs270.

Hugo Gravato Marques, Farhan Imtiaz, Fumiya Iida, and Rolf Pfeifer. Self-organization of reflexive behavior from spontaneous motor activity. *Biological Cybernetics*, 107(1):25–37, 2013. doi: 10.1007/s00422-012-0521-7. URL http://dx.doi.org/10.1007/s00422-012-0521-7.

Sébastien Marti, Jean Rémi King, and Stanislas Dehaene. Time-Resolved Decoding of Two Processing Chains during Dual-Task Interference. *Neuron*, 88(6):1297–1307, 2015. ISSN 10974199. doi: 10.1016/j.neuron.2015.10.040.

John H Martin. The corticospinal system: from development to motor control. *The Neuroscientist*, 11(2):161–173, 2005. doi: 10.1177/1073858404270843. URL http://nro.sagepub.com/content/11/2/161.abstract.

K A Mazurek, B J Holinski, D G Everaert, R B Stein, R Etienne-Cummings, and V K Mushahwar. Feed forward and feedback control for over-ground locomotion in anaesthetized cats. *Journal of Neural Engineering*, 9(2):026003, 2012. ISSN 1741-2560. doi: 10.1088/1741-2560/9/2/026003. URL http://www.pubmedcentral.nih.gov/articlerender.fcgi?artid=3314725{&}tool=pmcentrez{&}rendertype=abstract.

Glenda McCartney and Peter Hepper. Development of lateralized behaviour in the human fetus from 12 to 27 weeks'gestation. *Developmental Medicine & Child Neurology*, 41(2):83–86, 1999. doi: 10.1111/j.1469-8749.1999.tb00559.x. URL http://dx.doi.org/10.1111/j.1469-8749.1999.tb00559.x.

Todd McLaughlin, Christine L Torborg, Marla B Feller, and Dennis D M O'Leary. Retinotopic Map Refinement Requires Spontaneous Retinal Waves during a Brief Critical Period of Development. *Neuron*, 40(6):1147–1160, 2003. doi: http://dx.doi.org/10.1016/S0896-6273(03)00790-6. URL http://www.sciencedirect.com/science/article/pii/S0896627303007906.

David A McVea, Majid H Mohajerani, and Timothy H Murphy. Voltage-Sensitive Dye Imaging Reveals Dynamic Spatiotemporal Properties of Cortical Activity after Spontaneous Muscle Twitches in the Newborn Rat. *The Journal of Neuroscience*, 32(32):10982–10994, 2012. doi: 10.1523/jneurosci.1322-12.2012. URL http://www.jneurosci.org/content/32/32/10982.abstract.

Andrew N Meltzoff and M Keith Moore. Newborn infants imitate adult facial gestures. *Child development*, pages 702–709, 1983.

Zhuo Meng and John H Martin. Postnatal development of corticospinal postsynaptic action. *Journal of Neurophysiology*, 90(2):683–692, 2003.

Julia Missitzi, Nickos Geladas, and Vassilis Klissouras. Heritability in Neuromuscular Coordination: Implications for Motor Control Strategies. *Medicine and Science in Sports and Exercise*, 36(2):233–240, 2004. ISSN 01959131. doi: 10.1249/01.MSS.0000113479.98631.C4.

Julia Missitzi, Reinhard Gentner, Angelica Misitzi, Nickos Geladas, Panagiotis Politis, Vassilis Klissouras, and Joseph Classen. Heritability of motor control and motor learning. *Physiological reports*, 1(7):e00188, 2013. ISSN 2051-817X. doi:

10.1002/phy2.188. URL http://www.pubmedcentral.nih.gov/articlerender.fcgi?artid=3970744{&}tool=pmcentrez{&}rendertype=abstract.

Srinjoy Mitra, Stefano Fusi, and Giacomo Indiveri. Real-time classification of complex patterns using spike-based learning in neuromorphic VLSI. *Biomedical Circuits and Systems, IEEE Transactions on*, 3(1):32–42, 2009.

Richard Mooney. Neural mechanisms for learned birdsong. *Learning & Memory*, 16(11):655–669, 2009. doi: 10.1101/lm.1065209. URL http://learnmem.cshlp.org/content/16/11/655.abstract.

Timoleon Moraitis and Arko Ghosh. Withdrawal of voluntary inhibition unravels the off state of the spontaneous blink generator. *Neuropsychologia*, 65:279–286, 2014.

Hesham Mostafa, Federico Corradi, Fabio Stefanini, and Giacomo Indiveri. A hybrid analog/digital Spike-Timing Dependent Plasticity learning circuit for neuromorphic VLSI multi-neuron architectures. In *Proceedings - IEEE International Symposium on Circuits and Systems*, pages 854–857. IEEE, 2014. ISBN 9781479934324. doi: 10.1109/ISCAS.2014.6865270.

V K Mushahwar, D F Collins, and A Prochazka. Spinal cord microstimulation generates functional limb movements in chronically implanted cats. *Experimental neurology*, 163(2):422–9, 2000. ISSN 0014-4886. doi: 10.1006/exnr.2000.7381. URL http://www.ncbi.nlm.nih.gov/pubmed/10833317.

F. A. Mussa-Ivaldi and E. Bizzi. Motor learning through the combination of primitives. *Philosophical Transactions of the Royal Society B: Biological Sciences*, 355 (1404):1755–1769, 2000. ISSN 0962-8436. doi: 10.1098/rstb.2000.0733. URL http://rstb.royalsocietypublishing.org/cgi/doi/10.1098/rstb.2000.0733.

F. A. Mussa-Ivaldi, S. F. Giszter, and E. Bizzi. Linear combinations of primitives in vertebrate motor control. *Proceedings of the National Academy of Sciences*, 91(16):7534–7538, 1994. ISSN 0027-8424. doi: 10.1073/pnas.91.16.7534. URL http://www.pnas.org/cgi/doi/10.1073/pnas.91.16.7534.

Ferdinando A. Mussa-Ivaldi. Modular features of motor control and learning, 1999. ISSN 09594388.

Taher Naase, Michael J. Doughty, and Norman F. Button. An assessment of the pattern of spontaneous eyeblink activity under the influence of topical ocular anaesthesia. *Graefe's Archive for Clinical and Experimental Ophthalmology*, 243(4): 306–312, 2005. ISSN 0721832X. doi: 10.1007/s00417-004-0990-z.

K Nakamori, M Odawara, T Nakajima, T Mizutani, and K Tsubota. Blinking is controlled primarily by ocular surface conditions. *American journal of ophthalmology*, 124(1):24–30, 1997. ISSN 0002-9394. URL http://www.ncbi.nlm.nih.gov/pubmed/9222228.

Tamami Nakano, Yoshiharu Yamamoto, Keiichi Kitajo, Toshimitsu Takahashi, and Shigeru Kitazawa. Synchronization of spontaneous eyeblinks while viewing video stories. *Proceedings. Biological sciences / The Royal Society*, 276(1673):3635–44, 2009. ISSN 0962-8452. doi: 10.1098/rspb.2009.0828. URL http://www.pubmedcentral.nih.gov/articlerender.fcgi?artid=2817301{&}tool=pmcentrez{&}rendertype=abstract.

Tamami Nakano, Makoto Kato, Yusuke Morito, Seishi Itoi, and Shigeru Kitazawa. Blink-related momentary activation of the default mode network while viewing videos. *Proceedings of the National Academy of Sciences*, 110(2):702–706, 2013. ISSN 0027-8424. doi: 10.1073/pnas.1214804110. URL http://www.pubmedcentral.nih.gov/articlerender.fcgi?artid=3545766{&}tool=pmcentrez{&}rendertype=abstract{%}5Cnhttp://www.pnas.org/cgi/doi/10.1073/pnas.1214804110.

Emre Neftci, Jonathan Binas, Ueli Rutishauser, Elisabetta Chicca, Giacomo Indiveri, and Rodney J Douglas. Synthesizing cognition in neuromorphic electronic systems. *Proceedings of the National Academy of Sciences of the United States of America*, 110(37):E3468—-76, 2013. ISSN 1091-6490. doi: 10.1073/pnas.1212083110. URL http://www.pnas.org/cgi/content/long/110/37/E3468.

Miguel A. L. Nicolelis. Brain-machine Interfaces to Restore Motor Function and Probe Neural Circuits. *Nature Reviews Neuroscience*, 4(May):417–422, 2003. ISSN 1471-003X. doi: 10.1016/j.conb.2011.07.004.Specificity. URL http://www.ncbi.nlm.nih.gov/pubmed/21222154.

Imran Noorani and R. H.S. Carpenter. The LATER model of reaction time and decision, 2016. ISSN 18737528.

Donald A. Norman and Tim Shallice. Attention to Action. *Consciousness & Self-Regulation*, 4:1–18, 1986. ISSN 0962-8436. doi: 10.1007/978-1-4757-0629-1_1. URL http://link.springer.com/chapter/10.1007/978-1-4757-0629-1{_}1{%}5Cnhttp://dx.doi.org/10.1007/978-1-4757-0629-1{_}1{%}5Cnhttp://scholar.google.com/scholar?hl=en{&}btnG=Search{&}q=intitle:Attention+to+Action:+Willed+and+Automatic+Control+of+Behaviour{#}1{%}5Cnhttp://scholar.goo.

Joseph E. O'Doherty. A brain-machine interface instructed by direct intracortical microstimulation. *Frontiers in Integrative Neuroscience*, 3, 2009. ISSN 16625145. doi: 10.3389/neuro.07.020.2009. URL `http://journal.frontiersin.org/article/10.3389/neuro.07.020.2009/abstract`.

Joseph E. O'Doherty, Mikhail A. Lebedev, Peter J. Ifft, Katie Z. Zhuang, Solaiman Shokur, Hannes Bleuler, and Miguel A. L. Nicolelis. Active tactile exploration using a brain-machine-brain interface. *Nature*, 479(7372):228–231, 2011a. ISSN 0028-0836. doi: 10.1038/nature10489. URL `http://www.nature.com/nature/journal/v479/n7372/full/nature10489.html{%}5Cnhttp://www.nature.com/nature/journal/v479/n7372/pdf/nature10489.pdf`.

Joseph E O'Doherty, Mikhail A Lebedev, Peter J Ifft, Katie Z Zhuang, Solaiman Shokur, Hannes Bleuler, Miguel A L Nicolelis, Joseph E O'Doherty, Mikhail A Lebedev, Peter J Ifft, Katie Z Zhuang, Solaiman Shokur, Hannes Bleuler, and Miguel A L Nicolelis. Active tactile exploration using a brain-machine-brain interface. *Nature*, 479(7372):228–231, 2011b.

Lois N. Orchard and John A. Stern. Blinks as an index of cognitive activity during reading. *Integrative Physiological and Behavioral Science*, 26(2):108–116, 1991. ISSN 1053881X. doi: 10.1007/BF02691032.

Amy L Orsborn, Helene G Moorman, Simon A Overduin, Maryam M Shanechi, Dragan F Dimitrov, and Jose M Carmena. Closed-Loop Decoder Adaptation Shapes Neural Plasticity for Skillful Neuroprosthetic Control. *Neuron*, 82:1380–1393, 2014.

Erhan Oztop, Mitsuo Kawato, and Michael A. Arbib. Mirror neurons: Functions, mechanisms and models, 2013. ISSN 03043940.

Harold Pashler. Dual-task interference in simple tasks: Data and theory. *Psychological Bulletin*, 116(2):220–244, 1994. ISSN 0033-2909. doi: 10.1037/0033-2909.116.2.220.

Harold Pashler and James C. Johnston. Chronometric evidence for central postponement in temporally overlapping tasks. *The Quarterly Journal of Experimental Psychology Section A*, 41(1):19–45, 1989. ISSN 0272-4987. doi: 10.1080/14640748908402351.

K G Pearson. Common principles of motor control in vertebrates and invertebrates. *Annual Review of Neuroscience*, 16(1):265–297, 1993.

Wilder Penfield and Edwin Boldrey. Somatic motor and sensory representation in the cerebral cortex of man as studied by electrical stimulation. *Brain*, 60(4):389–443, 1937. ISSN 00068950. doi: 10.1093/brain/60.4.389.

Anna A Penn, Patricio A Riquelme, Marla B Feller, and Carla J Shatz. Competition in Retinogeniculate Patterning Driven by Spontaneous Activity. *Science*, 279(5359):2108–2112, 1998. doi: 10.1126/science.279.5359.2108. URL `http://www.sciencemag.org/content/279/5359/2108.abstract`.

Per Petersson, Alexandra Waldenström, Christer Fåhraeus, and Jens Schouenborg. Spontaneous muscle twitches during sleep guide spinal self-organization. *Nature*, 424(6944):72–75, 2003. ISSN 00280836. doi: 10.1038/nature01719.

Rolf Pfeifer, Max Lungarella, and Fumiya Iida. Self-organization, embodiment, and biologically inspired robotics. *Science (New York, N.Y.)*, 318(5853):1088–93, 2007. ISSN 1095-9203. doi: 10.1126/science.1145803. URL `http://www.ncbi.nlm.nih.gov/pubmed/18006736`.

Jean Piaget. Play, dreams and imitation in childhood. *Journal of Consulting Psychology*, 16(5):413–414, 1952.

Jean Piaget and Margaret Trans Cook. The origins of intelligence in children. 1952.

Eric Ponder and W P Kennedy. On the act of blinking. *Experimental Physiology*, 18 (2):89, 1927. ISSN 03702901. doi: 10.1113/expphysiol.1927.sp000433.

Arthur Prochazka. Proprioceptive Feedback and Movement Regulation. In *Comprehensive Physiology*. John Wiley & Sons, Inc., 2010. ISBN 9780470650714. doi: 10.1002/cphy.cp120103. URL `http://dx.doi.org/10.1002/cphy.cp120103`.

Arthur Prochazka and Sergiy Yakovenko. The neuromechanical tuning hypothesis, 2007. ISSN 00796123.

M J Prud'homme, D A Cohen, and J F Kalaska. Tactile activity in primate primary somatosensory cortex during active arm movements: cytoarchitectonic distribution. *J Neurophysiol*, 71(1):173–181, 1994. URL `http://jn.physiology.org/content/71/1/173.abstract`.

N Qiao, H Mostafa, F Corradi, M Osswald, F Stefanini, D Sumislawska, and G Indiveri. A re-configurable on-line learning spiking neuromorphic processor. *Frontiers in Neuroscience (submitted)*, 2015.

G. Rizzolatti, G. Luppino, and M. Matelli. The organization of the cortical motor system: New concepts, 1998. ISSN 00134694.

Giacomo Rizzolatti and Laila Craighero. THE MIRROR-NEURON SYSTEM. *Annual Review of Neuroscience*, 27(1):169–192, 2004. doi: doi:10.1146/annurev.neuro.27.070203.144230. URL http://www.annualreviews.org/doi/abs/10.1146/annurev.neuro.27.070203.144230.

Edwin M Robertson, Alvaro Pascual-Leone, C. Chris Miall, and R Chris Miall. Current Concepts in procedural consolidation. *Nature reviews. Neuroscience*, 5(7): 1–7, 2004. ISSN 1471-003X. doi: 10.1038/nrn1426.

Scott R. Robinson, Mark S. Blumberg, Maura S. Lane, and Lisa A S. Kreber. Spontaneous Motor Activity in Fetal and Infant Rats Is Organized Into Discrete Multilimb Bouts. *Behavioral Neuroscience*, 114(2):328–336, 2000. ISSN 0735-7044. doi: 10.1037//0735-7044.114.2.328. URL http://doi.apa.org/getdoi.cfm?doi=10.1037/0735-7044.114.2.328.

George John Romanes and Charles Darwin. *Mental evolution in animals*. D. Appleton, 1884.

Ranulfo Romo, Adrián Hernández, Anótonio Zainos, and Emilio Salinas. Somatosensory discrimination based on cortical microstimulation. *Nature*, 392 (6674):387–390, 1998a. ISSN 0028-0836. doi: 10.1038/32891. URL http://www.nature.com/nature/journal/v392/n6674/full/392387a0.html{%}5Cnhttp://www.nature.com/nature/journal/v392/n6674/pdf/392387a0.pdf.

Ranulfo Romo, Adrián Hernández, Anótonio Zainos, and Emilio Salinas. Somatosensory discrimination based on cortical microstimulation. *Nature*, 392(6674):387–390, 1998b.

Serge Rossignol, Réjean Dubuc, Jean-Pierre Gossard, and Jean Dubuc. Dynamic Sensorimotor Interactions in Locomotion. *Physiological Reviews*, 86:89–154, 2006. ISSN 0031-9333. doi: 10.1152/physrev.00028.2005.

Sébastien Royer and Denis Paré. Conservation of total synaptic weight through balanced synaptic depression and potentiation. *Nature*, 422(6931):518–522, 2003. ISSN 0028-0836. doi: 10.1038/nature01530.

Michael Rubenstein, Alejandro Cornejo, and Radhika Nagpal. Programmable self-assembly in a thousand-robot swarm. *Science*, 345(6198):795–799, 2014. ISSN 0036-8075, 1095-9203. doi: 10.1126/science.1254295. URL http://www.sciencemag.org/cgi/doi/10.1126/science.1254295{%}5Cnpapers3://publication/doi/10.1126/science.1254295.

Rajiv Saigal, Costantino Renzi, and Vivian K. Mushahwar. Intraspinal microstimulation generates functional movements after spinal-cord injury. *IEEE Transactions*

on Neural Systems and Rehabilitation Engineering, 12(4):430–440, 2004. ISSN 15344320. doi: 10.1109/TNSRE.2004.837754.

Sergio Della Sala, Alan Baddeley, Costanza Papagno, and Hans Spinnler. Dual-task paradigm: a means to examine the central executive. *Annals of the New York Academy of Sciences*, 769(1):161–172, 1995.

C F Sambo, M Liang, G Cruccu, and G D Iannetti. Defensive peripersonal space: the blink reflex evoked by hand stimulation is increased when the hand is near the face. *Journal of neurophysiology*, 107(3):880–9, 2012. ISSN 1522-1598. doi: 10.1152/jn.00731.2011. URL `http://www.ncbi.nlm.nih.gov/pubmed/22090460`.

Uluc Saranli, Martin Buehler, and Daniel E Koditschek. RHex: A Simple and Highly Mobile Hexapod Robot. *The International Journal of Robotics Research*, 20(July): 616–631, 2001. ISSN 0278-3649. doi: 10.1177/02783640122067570.

K Sathian, J Buxbaum, G Cohen, W Krakauer, E Lang, Maurizio Corbetta, and M Fitzpatrick. Neurological Principles and Rehabilitation of Action Disorders: Common Clinical Deficits. *Neurorehabilitation & Neural Repair*, 25:21S—-NaN, 2011. ISSN 15459683. doi: 25/5_suppl/21S[pii]\r10.1177/1545968311410941.

Stefan Schaal. Is imitation learning the route to humanoid robots? *Trends in Cognitive Sciences*, 3(6):233–242, 1999. URL `http://linkinghub.elsevier.com/retrieve/pii/S1364661399013273`.

Stefan Schaal, Auke Ijspeert, and Aude Billard. Computational approaches to motor learning by imitation. *Philosophical Transactions of the Royal Society of London. Series B: Biological Sciences*, 358(1431):537–547, 2003. doi: 10.1098/rstb.2002.1258. URL `http://rstb.royalsocietypublishing.org/content/358/1431/537.abstract`.

Stefan Schaal, Peyman Mohajerian, and Auke Ijspeert. Dynamics systems vs. optimal control — a unifying view. In Trevor Drew Paul Cisek and F Kalaska John, editors, *Progress in Brain Research*, volume Volume 165, pages 425–445. Elsevier, 2007. ISBN 0079-6123. doi: http://dx.doi.org/10.1016/S0079-6123(06)65027-9. URL `http://www.sciencedirect.com/science/article/pii/S0079612306650279`.

Margot A Schel, Simone Kühn, Marcel Brass, Patrick Haggard, K Richard Ridderinkhof, and Eveline A Crone. Neural correlates of intentional and stimulus-driven inhibition: a comparison. *Frontiers in human neuroscience*, 8(February):27, 2014. ISSN 1662-5161. doi: 10.3389/fnhum.2014.

00027. URL http://www.pubmedcentral.nih.gov/articlerender.fcgi?artid=3913912{&}tool=pmcentrez{&}rendertype=abstract.

E M Schmidt. Single neuron recording from motor cortex as a possible source of signals for control of external devices. *Annals of biomedical engineering*, 8(4-6): 339–349, 1980. ISSN 0090-6964. doi: 10.1007/BF02363437.

E. H. Schumacher, T. L. Seymour, J. M. Glass, D. E. Fencsik, E. J. Lauber, D. E. Kieras, and D. E. Meyer. Virtually Perfect Time Sharing in Dual-Task Performance: Uncorking the Central Cognitive Bottleneck. *Psychological Science*, 12(2):101–108, 2001. ISSN 0956-7976. doi: 10.1111/1467-9280.00318. URL http://pss.sagepub.com/content/12/2/101.short.

Marianna Semprini, Lorenzo Bennicelli, and Alessandro Vato. A parametric study of intracortical microstimulation in behaving rats for the development of artificial sensory channels. In *Proceedings of the Annual International Conference of the IEEE Engineering in Medicine and Biology Society, EMBS*, pages 799–802, 2012. ISBN 9781424441198. doi: 10.1109/EMBC.2012.6346052.

Mijail D. Serruya, Nicholas G. Hatsopoulos, Liam Paninski, Matthew R Fellows, and John P Donoghue. Instant neural control of a movement signal. *Nature*, 416(6877):141–2, 2002. ISSN 0028-0836. doi: 10.1038/416141a. URL http://www.nature.com/doifinder/10.1038/416141a{%}5Cnhttp://www.ncbi.nlm.nih.gov/pubmed/11894084.

R Shadmehr and S Wise. A simple muscle model. *Supplement to (Shadmehr and Wise, 2005a). Online at http://www.shadmehrlab.org/book/musclemodel.pdf*, 2005.

Reza Shadmehr, Maurice A Smith, and John W Krakauer. Error correction, sensory prediction, and adaptation in motor control. *Annual Review of Neuroscience*, 33: 89–108, 2010.

Liwei Shi, Maki K. Habib, Nan Xiao, and Huosheng Hu. Biologically Inspired Robotics. *Journal of Robotics*, 2015, 2015. ISSN 16879619. doi: 10.1155/2015/894394.

Hiroshi Shibasaki. Cortical activities associated with voluntary movements and involuntary movements, 2012. ISSN 13882457.

Yun Kyoung Shin, Yang Seok Cho, Mei Ching Lien, and Robert W. Proctor. Is the psychological refractory period effect for ideomotor compatible tasks eliminated by speed-stress instructions? *Psychological Research*, 71(5):553–567, 2007. ISSN 03400727. doi: 10.1007/s00426-006-0066-2.

Mariano Sigman and Stanislas Dehaene. Parsing a cognitive task: A characterization of the mind's bottleneck. *PLoS Biology*, 3(2):0334–0349, 2005. ISSN 15449173. doi: 10.1371/journal.pbio.0030037.

J C Smith, H H Ellenberger, K Ballanyi, D W Richter, and J L Feldman. Pre-Bötzinger complex: a brainstem region that may generate respiratory rhythm in mammals. *Science*, 254(5032):726–9, 1991. ISSN 0036-8075. doi: 10.1126/science.1683005. URL `http://www.pubmedcentral.nih.gov/articlerender.fcgi?artid=3209964{&}tool=pmcentrez{&}rendertype=abstract`.

W R Softky and C Koch. The highly irregular firing of cortical cells is inconsistent with temporal integration of random EPSPs. *The Journal of Neuroscience*, 13(1): 334–350, 1993. URL `http://www.jneurosci.org/content/13/1/334.abstract`.

Greta Sokoloff, Alan M Plumeau, Didhiti Mukherjee, and Mark S Blumberg. Twitch-related and rhythmic activation of the developing cerebellar cortex. *Journal of Neurophysiology*, 114(3):1746–1756, 2015. doi: 10.1152/jn.00284.2015. URL `http://jn.physiology.org/content/jn/114/3/1746.full.pdf`.

J C Spagna, D I Goldman, P-C Lin, D E Koditschek, and R J Full. Distributed mechanical feedback in arthropods and robots simplifies control of rapid running on challenging terrain. *Bioinspiration & biomimetics*, 2(1):9–18, 2007. ISSN 1748-3182. doi: 10.1088/1748-3182/2/1/002.

Fabio Stefanini, Emre O Neftci, Sadique Sheik, and Giacomo Indiveri. PyNCS: a microkernel for high-level definition and configuration of neuromorphic electronic systems. *Frontiers in neuroinformatics*, 8:73, 2014.

P. S G Stein. Neuronal control of turtle hindlimb motor rhythms, 2005. ISSN 03407594.

Paul SG Stein. Motor systems, with specific reference to the control of locomotion. *Annual review of neuroscience*, 1(1):61–81, 1978.

Richard B. Stein and Charles Capaday. The modulation of human reflexes during functional motor tasks, 1988. ISSN 01662236.

D Stellwagen and C J Shatz. An Instructive Role for Retinal Waves in the Development of Retinogeniculate Connectivity. *Neuron*, 33(3):357–367, 2002. doi: http://dx.doi.org/10.1016/S0896-6273(02)00577-9. URL `http://www.sciencedirect.com/science/article/pii/S0896627302005779`.

Diane Swick, Victoria Ashley, and U. Turken. Are the neural correlates of stopping and not going identical? Quantitative meta-analysis of two response in-

hibition tasks. *NeuroImage*, 56(3):1655–1665, 2011. ISSN 10538119. doi: 10.1016/j.neuroimage.2011.02.070.

Gregg A. Tabot, John F. Dammann, Joshua A. Berg, Francesco V. Tenore, Jessica L. Boback, R. Jacob Vogelstein, and Sliman J. Bensmaia. Restoring the sense of touch with a prosthetic hand through a brain interface. *Proceedings of the National Academy of Sciences of the United States of America*, 110 (45):18279–84, 2013. ISSN 1091-6490. doi: 10.1073/pnas.1221113110. URL http://www.pnas.org/cgi/doi/10.1073/pnas.1221113110{%}5Cnhttp://www.ncbi.nlm.nih.gov/pubmed/24127595{%}5Cnhttp://www.pubmedcentral.nih.gov/articlerender.fcgi?artid=PMC3831459.

Gentaro Taga. A model of the neuro-musculo-skeletal system for human locomotion - I. Emergence of basic gait. *Biological Cybernetics*, 73(2):97–111, 1995. ISSN 03401200. doi: 10.1007/BF00204048.

Sanjiv K. Talwar, Shaohua Xu, Emerson S. Hawley, Shennan A. Weiss, Karen A. Moxon, and John K. Chapi. Rat navigation guided by remote control. *Nature*, 417 (May):37–38, 2002. ISSN 0028-0836. doi: 10.1038/417037a. URL http://www.nature.com/nature/journal/v417/n6884/full/417037a.html.

Dawn M Taylor, Stephen I Helms Tillery, and Andrew B Schwartz. Direct Cortical Control of 3D Neuroprosthetic Devices. *Science*, 296(5574):1829–1832, 2002. ISSN 0036-8075. doi: 10.1126/science.1070291. URL http://science.sciencemag.org/content/296/5574/1829.

Edward J Tehovnik. Electrical stimulation of neural tissue to evoke behavioral responses. *Journal of neuroscience methods*, 65(1):1–17, 1996.

Esther Thelen. Developmental origins of motor coordination: Leg movements in human infants. *Developmental Psychobiology*, 18(1):1–22, 1985. doi: 10.1002/dev.420180102. URL http://dx.doi.org/10.1002/dev.420180102.

Esther Thelen, Gary Bradshaw, and Jerry Ann Ward. Spontaneous kicking in month-old infants: Manifestation of a human central locomotor program. *Behavioral and Neural Biology*, 32(1):45–53, 1981. doi: 10.1016/s0163-1047(81)90257-0. URL http://www.sciencedirect.com/science/article/pii/S0163104781902570.

Esther Thelen, J A Scott Kelso, and Alan Fogel. Self-organizing systems and infant motor development. *Developmental Review*, 7(1):39–65, 1987. doi: 10.1016/0273-2297(87)90004-9. URL http://www.sciencedirect.com/science/article/pii/0273229787900049.

Esther Thelen, Daniela Corbetta, and John P Spencer. Development of reaching during the first year: role of movement speed. *Journal of Experimental Psychology: Human Perception and Performance*, 22(5):1059, 1996.

Michael Tomasello, Sue Savage-Rumbaugh, and Ann Cale Kruger. Imitative Learning of Actions on Objects by Children, Chimpanzees, and Enculturated Chimpanzees. *Child Development*, 64(6):1688–1705, 1993. ISSN 0009-3920. doi: 10.1111/j.1467-8624.1993.tb04207.x. URL `http://search.ebscohost.com/login.aspx?direct=true{&}db=aph{&}AN=9406130028{&}site=ehost-live`.

Michael Tombu and Pierre Jolicœur. A central capacity sharing model of dual-task performance. *Journal of Experimental Psychology: Human Perception and Performance*, 29(1):3–18, 2003. ISSN 0096-1523. doi: 10.1037/0096-1523.29.1.3.

Michael Tombu and Pierre Jolicoeur. Virtually no evidence for virtually perfect time-sharing. *Journal of experimental psychology. Human perception and performance*, 30(5):795–810, 2004. ISSN 0096-1523. doi: 10.1037/0096-1523.30.5.795.

K Tsubota, K K Kwong, T Y Lee, J Nakamura, and H M Cheng. Functional MRI of brain activation by eye blinking. *Experimental eye research*, 69(1):1–7, 1999. ISSN 0014-4835. doi: 10.1006/exer.1999.0660. URL `http://www.ncbi.nlm.nih.gov/pubmed/10375444`.

Sebo Uithol, Iris van Rooij, Harold Bekkering, Pim Haselager, Iris Van Rooij, Harold Bekkering, and Pim Haselager. Hierarchies in action and motor control. *Journal of cognitive neuroscience*, 24(5):1077–86, 2012. ISSN 1530-8898. doi: 10.1162/jocn_a_00204. URL `http://www.ncbi.nlm.nih.gov/pubmed/22288396`.

James S Uleman and John A Bargh. *Unintended thought*. Guilford Press, 1989.

David C. Van Essen and John H R Maunsell. Hierarchical organization and functional streams in the visual cortex, 1983. ISSN 01662236.

Wieske van Zoest, Mieke Donk, and Jan Theeuwes. The Role of Stimulus-Driven and Goal-Driven Control in Saccadic Visual Selection. *Journal of Experimental Psychology: Human Perception and Performance*, 30 (4):746–759, 2004. ISSN 0096-1523. doi: 10.1037/0096-1523.30.4.749. URL `http://psycnet.apa.org/journals/xhp/30/4/746.html{%}5Cnpapers3://publication/doi/10.1037/0096-1523.30.4.749`.

A Vato, M Semprini, E Maggiolini, F D Szymanski, L Fadiga, S Panzeri, and F A Mussa-Ivaldi. Shaping the dynamics of a bidirectional neural interface. *PLoS computational biology*, 8(7), 2012.

A Vato, F D Szymanski, M Semprini, F A Mussa-Ivaldi, and S Panzeri. A bidirectional brain-machine interface algorithm that approximates arbitrary force-fields. *PLoS One*, 9(3), 2014.

Meel Velliste, Sagi Perel, M Chance Spalding, Andrew S Whitford, and Andrew B Schwartz. Cortical control of a prosthetic arm for self-feeding. *Nature*, 453(7198): 1098–1101, 2008.

R. Jacob Vogelstein, Francesco V G Tenore, Lisa Guevremont, Ralp Etienne-Cummings, and Vivian K. Mushahwar. A silicon central pattern generator controls locomotion in Vivo. In *IEEE Transactions on Biomedical Circuits and Systems*, volume 2, pages 212–222, 2008. ISBN 1932-4545. doi: 10.1109/TBCAS.2008.2001867.

Steve Vucic and Matthew C Kiernan. Novel threshold tracking techniques suggest that cortical hyperexcitability is an early feature of motor neuron disease. *Brain*, 129(9):2436–2446, 2006.

Tom Wadden and Örjan Ekeberg. A neuro-mechanical model of legged locomotion: single leg control. *Biological Cybernetics*, 79(2):161–173, 1998. ISSN 0340-1200. doi: 10.1007/s004220050468. URL `http://link.springer.com/10.1007/s004220050468`.

Alan Traviss Welford. The 'psychological refractory period'and the timing of high-speed performance—a review and a theory. *British Journal of Psychology. General Section*, 43(1):2–19, 1952.

Johan Wessberg and Miguel a L Nicolelis. Optimizing a linear algorithm for real-time robotic control using chronic cortical ensemble recordings in monkeys. *Journal of cognitive neuroscience*, 16(6):1022–1035, 2004. ISSN 0898-929X. doi: 10.1162/0898929041502652.

Heather Williams, Kerry Kilander, and Mary Lou Sotanski. Untutored song, reproductive success and song learning. *Animal Behaviour*, 45(4):695–705, 1993. doi: http://dx.doi.org/10.1006/anbe.1993.1084. URL `http://www.sciencedirect.com/science/article/pii/S0003347283710845`.

L R Williams and J B Gross. Heritability of motor skill. *Acta Genet.Med Gemellol.(Roma.)*, 29(2):127, 1980. ISSN 00015660.

H R Wilson and J D Cowan. Excitatory and inhibitory interactions in localized populations of model neurons. *Biophysical journal*, 12(1):1–24, 1972. ISSN 0006-3495. doi: 10.1016/S0006-3495(72)86068-5. URL `http://www.sciencedirect.com/science/article/pii/S0006349572860685`.

D. M. Wolpert and M. Kawato. Multiple paired forward and inverse models for motor control, 1998. ISSN 08936080.

Daniel M Wolpert and Zoubin Ghahramani. Computational principles of movement neuroscience. *Nat Neurosci*, 2000.

Daniel M Wolpert, Zoubin Ghahramani, and J Randall Flanagan. Perspectives and problems in motor learning. *Trends in Cognitive Sciences*, 5(11):487–494, 2001. doi: 10.1016/s1364-6613(00)01773-3. URL `http://www.sciencedirect.com/science/article/pii/S1364661300017733`.

Daniel M Wolpert, Jörn Diedrichsen, and J Randall Flanagan. Principles of sensorimotor learning. *Nat Rev Neurosci*, 12(12):739–751, 2011. URL `http://dx.doi.org/10.1038/nrn3112`.

Sergiy Yakovenko, Vivian Mushahwar, Veronique VanderHorst, Gert Holstege, and Arthur Prochazka. Spatiotemporal activation of lumbosacral motoneurons in the locomotor step cycle. *Journal of neurophysiology*, 87(3):1542–1553, 2002. ISSN 0022-3077. doi: DOI10.1152/jn.00479.2001.

Motonori Yamaguchi, Gordon D. Logan, and Patrick G. Bissett. Stopping while going! Response inhibition does not suffer dual-task interference. *Journal of Experimental Psychology: Human Perception and Performance*, 38(1):123–134, 2012. ISSN 0096-1523. doi: 10.1037/a0023918.

Hyo Woon Yoon, Jun Young Chung, Myung Sung Song, and HyunWook Park. Neural correlates of eye blinking; improved by simultaneous fMRI and EOG measurement. *Neuroscience Letters*, 381(1-2):26–30, 2005. ISSN 03043940. doi: 10.1016/j.neulet.2005.01.077.

Boubker Zaaimi, Ricardo Ruiz-Torres, Sara A Solla, and Lee E Miller. Multi-electrode stimulation in somatosensory cortex increases probability of detection. *Journal of Neural Engineering*, 10(5):056013, 2013. ISSN 1741-2560. doi: 10.1088/1741-2560/10/5/056013. URL `http://stacks.iop.org/1741-2552/10/i=5/a=056013?key=crossref.41bc91ebb733d5dabce5b1d804f59b68`.

F E Zajac. Muscle and tendon: properties, models, scaling, and application to biomechanics and motor control. *Critical reviews in biomedical engineering*, 17(4):359–411, 1989. URL `http://ukpmc.ac.uk/abstract/MED/2676342`.

Laura Zapparoli, Silvia Seghezzi, and Eraldo Paulesu. The what, the when and the whether of intentional action in the brain: a meta-analytical review. *Front. Hum. Neurosci.*, 2017.

E. Paul Zehr and Richard B. Stein. What functions do reflexes serve during human locomotion? *Progress in Neurobiology*, 58(2):185–205, 1999. ISSN 03010082. doi: 10.1016/S0301-0082(98)00081-1.

Stefania Zoia, Laura Blason, Giuseppina D'Ottavio, Maria Bulgheroni, Eva Pezzetta, Aldo Scabar, and Umberto Castiello. Evidence of early development of action planning in the human foetus: A kinematic study. *Experimental Brain Research*, 176(2):217–226, 2007. ISSN 00144819. doi: 10.1007/s00221-006-0607-3.